

Discovery of ERD-3111 as a Potent and Orally Efficacious Estrogen Receptor PROTAC Degradator with Strong Antitumor Activity

Zhixiang Chen,[#] Biao Hu,[#] Rohan Kalyan Rej,[#] Dimin Wu,[#] Ranjan Kumar Acharyya,[#] Mingliang Wang,[#] Tianfeng Xu,[#] Jianfeng Lu, Hoda Metwally, Yu Wang, Donna McEachern, Longchuan Bai, Christina L. Gersch, Meilin Wang, Wenjing Zhang, Qiuxia Li, Bo Wen, Duxin Sun, James M. Rae, and Shaomeng Wang*



Cite This: <https://doi.org/10.1021/acs.jmedchem.3c01186>



Read Online

ACCESS |



Metrics & More



Article Recommendations



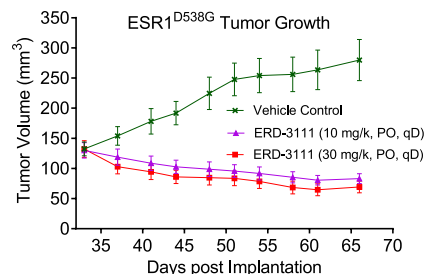
Supporting Information



ERD-3111

$DC_{50} = 0.5$ nM and $D_{max} = 91\%$;

A highly potent and orally efficacious PROTAC ER α degrader



ABSTRACT: Estrogen receptor α (ER α) is a prime target for the treatment of ER-positive (ER+) breast cancer. Despite the development of several effective therapies targeting ER α signaling, clinical resistance remains a major challenge. In this study, we report the discovery of a new class of potent and orally bioavailable ER α degraders using the PROTAC technology, with ERD-3111 being the most promising compound. ERD-3111 exhibits potent in vitro degradation activity against ER α and demonstrates high oral bioavailability in mice, rats, and dogs. Oral administration of ERD-3111 effectively reduces the levels of wild-type and mutated ER α proteins in tumor tissues. ERD-3111 achieves tumor regression or complete tumor growth inhibition in the parental MCF-7 xenograft model with wild-type ER and two clinically relevant ESR1 mutated models in mice. ERD-3111 is a promising ER α degrader for further extensive evaluations for the treatment of ER+ breast cancer.

INTRODUCTION

Breast cancer is the most common invasive cancer diagnosed in women worldwide, with approximately 2.3 million new cases each year.¹ In the United States alone, there are over 300,000 new cases expected annually.² Breast cancer accounts for 24.5% of all cancer cases in women and causes nearly 685,000 deaths each year.¹ Approximately 70% of newly diagnosed breast cancers will express the estrogen receptor, a nuclear hormone transcription factor that plays a central role in the development and progression of breast cancer.^{3–6}

To treat ER α -positive (ER+) breast cancer, blocking the signaling of ER α using endocrine therapy (ET) is a well-established strategy for both early and advanced stages of the disease.⁷ The current standard of care therapies for ER α -positive breast cancer includes the following.^{7,8} (1) The third generation aromatase inhibitors (AIs) letrozole, anastrozole, and exemestane, which prevent the conversion of androgens to estrogen, thereby reducing the circulating estrogens in the body. (2) Selective estrogen receptor modulators (SERMs), which block ER signaling by competing with estrogen for receptor binding in breast cancer cells with tamoxifen being the most commonly

used SERM. (3) Selective estrogen receptor degraders (SERDs) with fulvestrant as a prime example that not only blocks ER α by functioning as a pure antagonist but also induces ER α degradation through the ubiquitin–proteasome system (UPS). (4) Cyclin-dependent kinase 4 and 6 (CDK4/6) inhibitors, such as palbociclib, ribociclib, and abemaciclib, which are often used in combination with AIs or fulvestrant to enhance the effectiveness of ET, particularly for advanced or metastatic breast cancer.

While SERMs, SERDs and AIs have been the mainstay of ET for ER+ breast cancer for over 30 years, de novo and acquired resistance to all of these therapies is a major clinical problem leading to cancer recurrences, metastasis and mortality.^{9–12} One major mechanism of resistance is the acquisition of mutations in

Received: June 29, 2023

ESR1, the gene encoding $ER\alpha$.¹³ Two most common mutations, known as Y537S and D538G, occur in the ligand binding domain (LBD) of $ER\alpha$ and account for more than 70% of *ESR1* mutations.¹⁰ Preclinical studies have shown that while these *ESR1* mutations do not prevent ligand binding, they do confer constitutive ER signaling activity in the absence of estrogen.¹¹ Therefore, breast cancer cells harboring these mutations still rely on $ER\alpha$ for their growth and survival, making continuous targeting of $ER\alpha$ an effective therapeutic strategy.¹⁴

In contrast to the SERM tamoxifen which acts as a partial ER agonist, SERDs not only antagonize $ER\alpha$ through direct binding but also promote $ER\alpha$ degradation, leading to a more comprehensive blockade of the $ER\alpha$ signaling pathway. Fulvestrant is the first SERD that was approved by FDA in 2002 and has demonstrated efficacy in patients who have progressed on prior treatment with tamoxifen¹⁵ or AIs.¹⁶ However, its clinical use and efficacy are limited due to its low solubility and poor oral bioavailability.¹⁷ Fulvestrant is currently administered via intramuscular injection.

Significant efforts have been made to develop orally effective SERDs for the treatment of human breast cancer.^{9,17–39} Indeed, many oral SERDs have been identified, and more than 10 SERD molecules have been progressed into different stages of clinical development.^{40–43} Some representative examples of these oral SERDs are shown in Figure 1. One notable advancement in the

(PFS) compared to fulvestrant, suggesting that AZD9833 may be superior to fulvestrant in treating $ER+$ breast cancer.⁴⁵

In addition to oral SERDs, another promising therapeutic strategy to overcome endocrine resistance in $ER+$ breast cancer is the development of ER degraders using the proteolysis-targeting chimera (PROTAC) technology.^{46–53} ER PROTACs are heterobifunctional molecules that consist of an $ER\alpha$ binder and a ligand for an E3 ubiquitin ligase or an E3 ubiquitin ligase complex, connected by a linker. These molecules work by directly recruiting an E3 ligase or an E3 ligase complex to the proximity of $ER\alpha$, leading to ubiquitination and subsequent degradation of $ER\alpha$ protein by the cellular proteasome.^{49,53} This approach provides an alternative mechanism for inducing $ER\alpha$ degradation and represents a promising new therapeutic approach for the treatment of $ER+$ breast cancer.

Because of their high molecular weights and often poor physicochemical properties, the development of highly potent and orally bioavailable ER PROTACs has been challenging.^{54–60} However, extensive research has led to the discovery of ARV-471 as an orally bioavailable ER PROTAC degrader.⁶¹ In preclinical *in vivo* studies, ARV-471 demonstrated superior anti-tumor activity compared to fulvestrant.⁶¹ Importantly, ARV-471 has shown promising responses in patients who were previously treated with at least one prior CDK 4/6 inhibitor and at least 2 prior endocrine therapies in a phase I clinical study,⁶² indicating its potential use for treating patients who have progressed on prior standard of care therapy.⁷ These preclinical and initial clinical data for ARV-471 suggested that oral $ER\alpha$ PROTACs may have a promising therapeutic potential for the treatment of $ER+$ human breast cancer.

In the present study, we describe the design, synthesis, and biological evaluation of new classes of $ER\alpha$ PROTACs based on a new cereblon ligand^{63,64} and three classes of ER ligands. This work led to the discovery of ERD-3111 as a potent, orally bioavailable, and highly efficacious $ER\alpha$ PROTAC that effectively inhibits the *in vivo* growth of breast cancers with either wild-type or mutated ER in mice.

RESULTS AND DISCUSSION

Design of PROTAC ER Degradors Using a New Cereblon (CRBN) Ligand TX-16. In recent years, there have been tremendous efforts in the development of PROTAC degraders for the treatment of human diseases, particularly human cancer.⁵⁰ Currently, there are 18 PROTAC molecules in different stages of clinical development in the United States, and 12 of them are orally administered.⁶⁵ It is worth noting that all of the oral PROTAC degraders in clinical development with disclosed chemical structures are exclusively designed based on CRBN ligands, which are generally considered superior in achieving oral bioavailability compared to other known E3 ligands.⁶⁶ Therefore, we focused on identification of an optimized CRBN ligand with a good binding affinity and importantly favorable absorption, distribution, metabolism, and excretion (ADME) properties toward achieving superior oral bioavailability with the resulting PROTAC degraders. Our efforts in the design of new CRBN ligands have resulted in the discovery of TX-16,^{63,64} which exhibits a binding affinity comparable to thalidomide and lenalidomide and with excellent ADME properties such as high permeability, low plasma protein binding, and good pharmacokinetic (PK) parameters in rats (Table 1). We decided to employ TX-16 for the design of oral ER PROTAC degraders using different ER ligands (Figure 2).

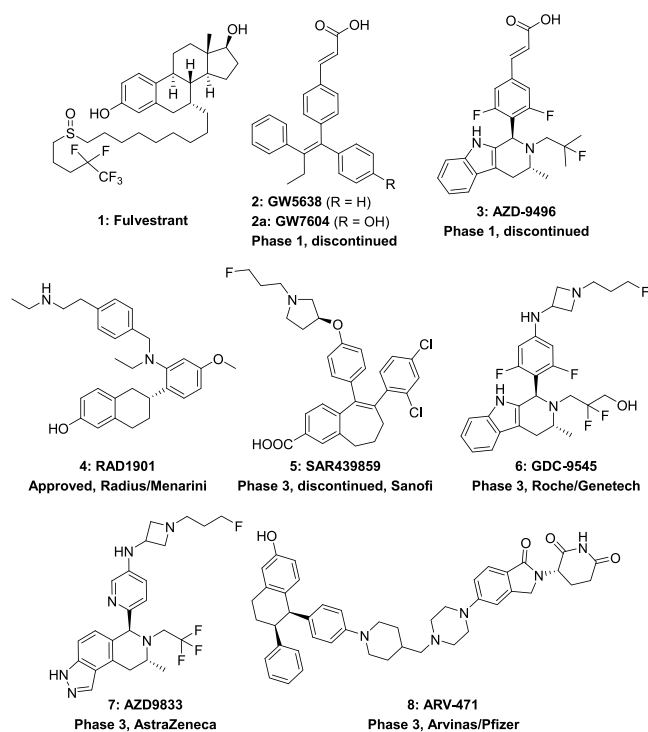
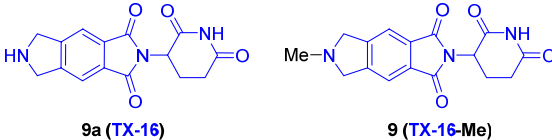


Figure 1. Representative SERDs and ER PROTAC.

development of oral SERD molecules is the recent approval of RAD1901 by the FDA for the treatment of *ESR1*-mutated advanced or metastatic $ER+$ breast cancer in patients who have experienced progression on at least one line of ET.⁴⁴ Other oral SERDs that have shown promise include GDC-9545²⁶ from Roche/Genentech and AZD9833²⁷ from AstraZeneca, both of which are currently in phase III clinical trials. In recently published phase II clinical data from the SERENA-2 trial, AZD9833 demonstrated improved progression-free survival

Table 1. Profiling of New CRBN Ligand TX-16 and Its Analogue 9 (TX-16-Me)^c


CRBN binding affinity IC ₅₀ (μM)			Caco-2 permeability of compound 9		plasma protein binding of compound 9 (%)	
TX16 (9a)	lenalidomide	thalidomide	P _{app} ^a (10 ⁻⁶ cm/s)	ER ^b	human/dog/monkey/rat/mouse	
2.6	3.6	2.9	7.4	1.1	12.5/17.0/14.4/36.5/26.3	
rat pharmacokinetic profile of compound 9 ^c						
IV/PO (mg/kg)	V _{ss} ^d (L/kg)	Cl ^d (mL/min/kg)	T _{1/2} ^e (h)	C _{max} ^e (ng/mL)	AUC ^e (h*ng/mL)	F (%)
1/3	5.0	29.2	1.8	228.4	1147	70

^aApparent permeability coefficient (P_{app}), the rate of permeation across the Caco-2 cell monolayer from the apical (A) to the basolateral (B) side. ^bEfflux ratio (ER) = P_{app} (B to A)/P_{app} (A to B). ^cThe definitions are as follows: IV, intravenous administration; T_{1/2}, elimination half-life; AUC, area-under-the-curve; V_{ss}, volume of distribution at steady state; Cl, clearance; PO, oral administration; C_{max}, maximum drug concentration; F, oral bioavailability. ^dIV. ^ePO.

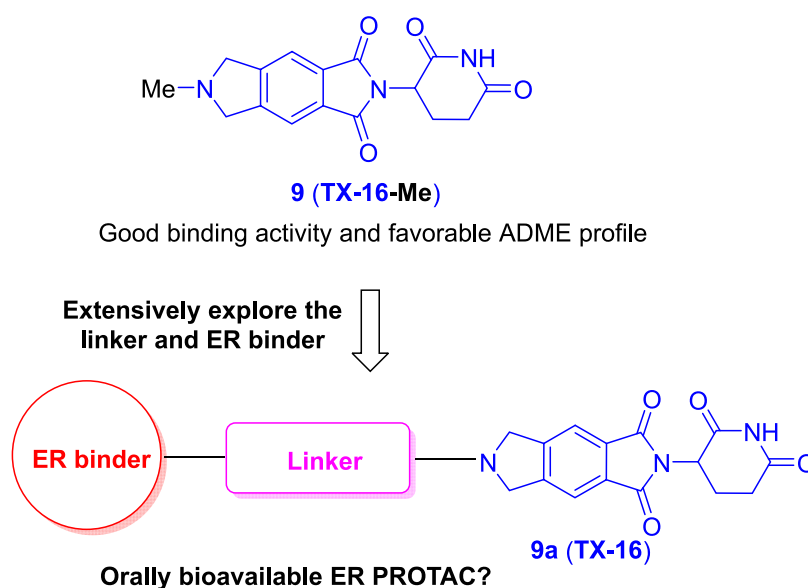


Figure 2. Design of new classes of oral ER PROTACs based on CRBN ligand TX-16 and different classes of ER ligands.

Design of ER PROTAC Degraders Using Lasofoxifene and TX-16. Lasofoxifene is a highly potent ER antagonist and has been extensively evaluated in human clinical trials. In addition, lasofoxifene has been utilized for the design of ARV-471, an orally bioavailable ER PROTAC degrader in clinical development. Therefore, we decided to first employ the ER ligand in lasofoxifene as the ER binder and TX-16 as the CRBN ligand for the design of orally bioavailable ER PROTAC degraders.

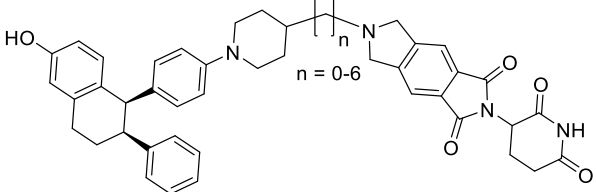
We first synthesized a series of potential ER PROTAC degraders (compounds 10–16) using linear and flexible linkers with different lengths. In order to determine the degradation potency (DC₅₀ value) and efficiency (D_{max} value) of our designed ER PROTAC degraders more quantitatively, we developed and optimized an in-cell western (ICW) assay in the estrogen receptor-positive and estrogen-dependent MCF-7 breast cancer cell line. In our ICW experiments, we included fulvestrant and ARV-471 as controls. The degradation data for compounds 10–16, fulvestrant and ARV-471 are summarized in Table 2.

Compound 10 (*n* = 0) and 12 (*n* = 2) displayed weak degradation potencies (DC₅₀ > 1 μM) and poor degradation

efficiencies (D_{max} = 32 and 50%, respectively, at 1 μM). Interestingly, compound 11, which has only one methylene group in the linker, exhibited a better potency (DC₅₀ = 415 nM) and degradation efficiency (D_{max} = 65%) than compounds 10 and 12. Increasing the linker length to *n* = 3 (compound 13) significantly improved the degradation potency (DC₅₀ = 171 nM) and efficiency (D_{max} = 79%) over compounds 10–12. However, further elongating the linker to *n* = 4 (compound 14) did not enhance degradation and instead caused a slight decrease in D_{max} (67%). Notably, a remarkable improvement in both degradation potency and efficiency was observed when using a linker with a length of *n* = 5 (compound 15), which has DC₅₀ = 31 nM and D_{max} = 106%. The addition of one more methylene group to the linker of compound 15, giving compound 16, resulted in a 3–4 times reduction in potency (DC₅₀ = 129 nM) but maintained the same high degradation efficiency (D_{max} = 101%). Our data on compounds 10–16 showed that the linkers play a critical role in ER degradation potency and efficiency.

Our previous studies have shown that employing conformationally rigid linkers in PROTAC degraders improves not only degradation potency and efficiency but also oral bioavail-

Table 2. Determination of Optimal Linker Lengths in PROTAC Degraders Designed Based on the ER Binder in ARV-471 and TX-16



compound	linker length (<i>n</i>)	ER α degradation ^a	
		DC ₅₀ (nM) ^b	D _{max} (%) ^c
fulvestrant	N.A.	0.9 ± 0.2	100 ± 3
ARV-471	N.A.	0.4 ± 0.04	89 ± 1
10 (ERD-838)	0	>1000	32 ± 5
11 (ERD-821)	1	415 ± 75	65 ± 8
12 (ERD-839)	2	>1000	50 ± 4
13 (ERD-840)	3	171 ± 48	79 ± 12
14 (ERD-841)	4	236 ± 40	67 ± 6
15 (ERD-842)	5	31 ± 4	106 ± 4
16 (ERD-843)	6	129 ± 15	101 ± 6

^aER α degradation potency was tested in the MCF-7 cell line using ICW assay. The data were collected based on triplicate experiments. The maximum level of ER α degradation achieved by fulvestrant was set as 100%. The data were provided as mean ± SEM. ^bThe concentration needed to reduce ER α protein by 50%. ^cMaximal ER α degradation relative to that (100%) achieved by fulvestrant.

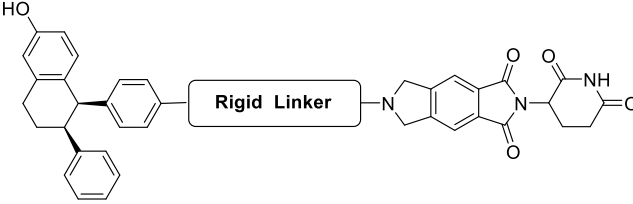
ability.^{67,68} We next synthesized a series of compounds (**17–21**) using conformationally rigid linkers with their degradation data summarized in **Table 3**.

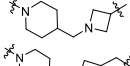
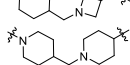
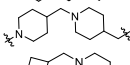
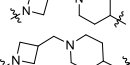
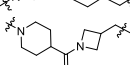
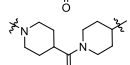
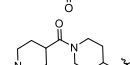
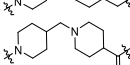
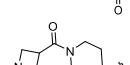
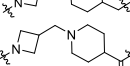
Compound **17**, with the linker conformation restricted by an azetidine ring, displayed poor ER degradation. Inserting one more methylene group at the right side of the linker in **17** resulted in compound **18**, which showed a dramatic enhancement of degradation potency (DC₅₀ = 21 nM) but only moderate efficiency (D_{max} = 59%). Substituting the 3-methylazetidine moiety of compound **18** with a piperidine ring (compound **19**) led to a substantial improvement in both degradation potency (DC₅₀ = 2.3 nM) and efficiency (D_{max} = 84%). Inserting one more methylene group at the right side of the linker of compound **19** yielded compound **20**, which is slightly less potent and effective than compound **19**. Changing the piperidine ring close to the ER ligand in compounds **19** and **20** with an azetidine ring led to compounds **21** and **22**, which are much less potent and effective than compounds **19** and **20** in inducing ER degradation.

Because compounds **19** and **20** are fairly potent and effective ER degraders, we evaluated their pharmacokinetics in rats. Both compounds were found to have a moderate clearance and good oral bioavailability of 30–36% (**Table 4**). Consistent with their chemical structures, which contain two positively charged amino groups, compounds **19** and **20** have high volumes of distribution of 8.8 and 55.4 L/kg, respectively. Further evaluation of the PK profile of compound **19** in mice showed that it has a moderate clearance, a high volume of distribution (16.2 L/kg), and a good oral bioavailability (58%).

Encouraged by their good degradation potency and efficiency, and importantly excellent oral bioavailability of compounds **19** and **20**, we next performed further optimization of their linker, with the resulting compounds **23–28** and degradation data summarized in **Table 3**.

Table 3. Rigidification of the Linker to Enhance Potency



Compound	Linker	ER α degradation ^a	
		DC ₅₀ (nM) ^b	D _{max} (%) ^c
17 (ERD-2218)		989 ± 237	50 ± 2
18 (ERD-9038)		21 ± 7	59 ± 3
19 (ERD-2217)		2.3 ± 0.7	84 ± 5
20 (ERD-9033)		4.3 ± 1.0	79 ± 3
21 (ERD-2141)		295 ± 94	57 ± 2
22 (ERD-2142)		19 ± 7	64 ± 5
23 (ERD-849)		6.0 ± 1.4	84 ± 4
24 (ERD-9115)		1.6 ± 0.3	95 ± 4
25 (ERD-10108)		13 ± 3.2	76 ± 4
26 (ERD-846)		9.7 ± 3.4	63 ± 4
27 (ERD-9096)		32 ± 6.3	87 ± 5
28 (ERD-2270)		>1000	40 ± 8

^{a,b,c}Same legends as in **Table 2**.

Introduction of a carbonyl group adjacent to the middle basic nitrogen of the linker in compounds **18** and **19** resulted in compounds **23** and **24**, respectively, which have a similar degradation potency but an improved degradation efficiency, as compared to compound **18** and **19**. Converting either amine group into an amide in compound **20** resulted in compounds **25** and **26**, respectively, which are less potent and effective than compound **20**. Similarly, converting either amine group to an amide in compound **22** resulted in compounds **27** and **28**, respectively. While compound **27** has a similar potency and a decreased efficacy compared to compound **22**, compound **28** is much weaker and less effective than compound **22** in inducing ER degradation.

Since compound **24** showed the best potency and degradation efficiency among the series of compounds shown in **Table 3**, we evaluated its PK profile in rats (**Table 4**). As compared to compounds **19** and **20**, compound **24** has a much reduced volume of distribution (V_{ss} = 2.0 L/kg), consistent with their chemical structures. Compound **24** exhibits moderate clearance but only has 10% of oral bioavailability.

In our design of orally bioavailable AR degraders, we have shown that incorporation of rigid spiro-ring-containing linkers produces degraders with high degradation potency and efficiency and excellent PK profiles, including high oral bioavailability.⁶⁹ We considered spiro-ring-containing linkers as privileged structures due to their high conformational rigidity,

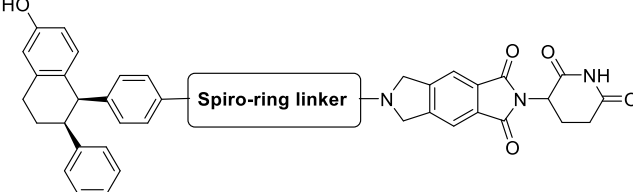
Table 4. PK Profiles for Compounds 19, 20, 24, and 36 and ARV-471 in Rats and/or Mice^a

compound	species	IV/PO (mg/kg)	V_{ss}^b (L/kg)	Cl^b (mL/min/kg)	$T_{1/2}^c$ (h)	C_{max}^c (ng/mL)	AUC ^c (h*ng/mL)	F^c (%)
19 (ERD-2217)	rat	1/3	8.8	25.7	4.0	54.6	552	30
	mouse	1/3	16.2	14.2	9.8	93.3	1482	58
20 (ERD-9033)	rat	1/3	55.4	17.0	16.0	24.9	399	36
24 (ERD-9115)	rat	1/3	2.0	23.1	2.7	40.6	206	10
36 (ERD-1173)	rat	1/3	1.6	20.0	2.5	69.5	328	13
	mouse	1/3	2.2	31	3.1	146	550	35
ARV-471	rat	1/3	2.4	18.6	4.0	46.5	244	10
	mouse	1/3	1.8	21.9	2.5	156.3	684	31

^aThe definitions are as follows: IV, intravenous administration; $T_{1/2}$, elimination half-life; AUC, area-under-the-curve; V_{ss} , volume of distribution at steady state; Cl, clearance; PO, oral administration; C_{max} , maximum drug concentration; F , oral bioavailability. ^bIV. ^cPO.

low polar surface area, and exclusive sp^3 atoms, which are particularly suited for the design of orally bioavailable PROTAC degraders. We next designed and synthesized a series of ER PROTAC degraders (29–38) using rigid spiro-ring-containing linkers, with the data summarized in Table 5.

Table 5. Improvement of the PK Profiles by Employing More Rigid Spiro-Ring-Containing Linkers



Compound	Spiro-ring Linker	ERα degradation ^a	
		DC ₅₀ (nM) ^b	D _{max} (%) ^c
29 (ERD-853)		11 ± 3.4	65 ± 3
30 (ERD-854)		>1000	23 ± 21
31 (ERD-855)		4.0 ± 1.5	63 ± 3
32 (ERD-856)		1.8 ± 0.6	68 ± 3
33 (ERD-1152)		2.8 ± 0.9	71 ± 3
34 (ERD-857)		18 ± 6.3	58 ± 2
35 (ERD-851)		4.6 ± 1.2	75 ± 3
36 (ERD-1173)		5.5 ± 1.2	90 ± 4
37 (ERD-852)		393 ± 165	58 ± 8
38 (ERD-858)		>1000	16 ± 8

^{a,b,c}Same legend as in Table 2.

ER degraders containing a spiro-ring system displayed a wide range of degradation potencies and efficiencies. Compound 36 containing a 6,6-spiro ring linker has the best degradation potency ($DC_{50} = 5.5$ nM) and efficiency ($D_{max} = 90\%$). Interestingly, changing the position of the amide in the linker in compound 36 resulted in compound 38, which is a very weak and ineffective ER degrader. These data further highlight the

importance of the linker in determining degradation potencies and efficiencies of PROTAC degrader molecules.

Consequently, compound 36 was selected for PK studies in rats with the data summarized in Table 4. Compound 36 has a moderate volume of distribution ($V_{ss} = 1.6$ L/kg) and a moderate clearance (20 mL/kg/min). As compared to compound 24, compound 36 has an improved overall exposure based upon their C_{max} and AUC values and displays an oral bioavailability (F) value of 13%.

We further evaluated compound 36 for its PK in mice with the data shown in Table 4. As compared to its PK parameters in rats, compound 36 has a higher oral exposure in mice and achieves an oral bioavailability of 35%.

While compound 36 has reasonable degradation potency and efficiency and PK parameters in mice and rats, it is 10 times less potent than ARV-471 and fulvestrant. We decided to perform further optimization of compound 36 with the objectives to further improve its potency and PK profile.

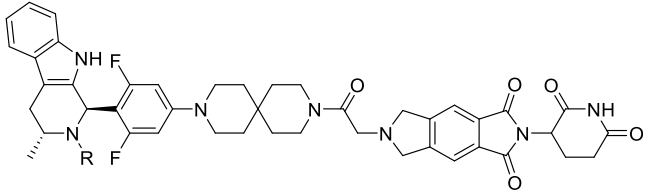
Further Optimization of Compound 36. We sought to replace the ER ligand in compound 36 with other ER ligands. In recent years, extensive research efforts have resulted in the identification of different classes of orally bioavailable SERD molecules. Among them, the tricyclic indole and tricyclic indazole scaffolds have been used for the design of highly promising oral SERD molecules,^{21,24–28,31,39} exemplified by GDC-9545, which contains a tricyclic indole, and AZD-9833, which contains a tricyclic indazole. GDC-9545 and AZD-9833 exhibit high ER binding affinities and favorable drug metabolism and pharmacokinetic (DMPK) profiles^{26,27} and importantly demonstrate clinical efficacy and acceptable safety profiles in human breast cancer patients. We decided to replace the ER core in compound 36 with a tricyclic indole or indazole core, toward improving potency and/or PK profile.

Substituting the ER core of compound 36 with the core of GDC-9545 resulted in compound 39, which is a highly potent and effective ER degrader, with $DC_{50} = 0.1$ nM and $D_{max} = 97\%$ (Table 6). Further modifications of the side chain in compound 39 led to compounds 40 and 41. While compounds 40 and 41 are 8 times less potent than compound 39, they are still 6 times more potent than compound 36 based upon their DC_{50} values.

We evaluated the oral exposures of compounds 39–41 in rats with limited time-points (Table 6). To our disappointment, our PK data showed that these three highly potent ER degraders all have very poor oral bioavailability in rats.

We next explored the use of the tricyclic indazole ER ligand for the design of potent and orally bioavailable PROTAC ER degraders with the data summarized in Table 7. We synthesized and evaluated compound 42, which contains the ER ligand core of AZD-9833. Compound 42 is a potent and highly effective ER

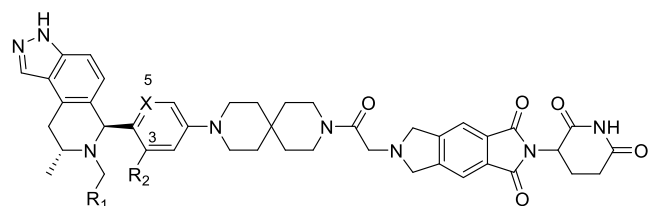
Table 6. Replacing the ER Core of Compound 36 with Tricyclic Indole Cores



Compound	R	ER α degradation ^a		Oral plasma exposure in rat ^d (Drug concentration, ng/mL)			
		DC ₅₀ (nM) ^b	D _{max} (%) ^c	1 h	3 h	6 h	24 h
39 (ERD-876)		0.1 ± 0.02	97 ± 3	9.3 ± 4.1	6.6 ± 3.2	3.0 ± 1.0	N/A
40 (ERD-2279)		0.8 ± 0.18	83 ± 3	7.9 ± 4.3	8.2 ± 3.4	8.3 ± 3.5	4.0 ± 0.2
41 (ERD-1099)		0.8 ± 0.11	106 ± 2	8.3 ± 0.4 ^e	14.0 ± 1.5 ^e	10.3 ± 4.9 ^e	

^{a,b,c}Same legend as in Table 2. ^dDose (3 mg/kg); the plasma drug concentration data for each compound was independently collected from 3 rats and provided as the mean ± SD. ^eDose (5 mg/kg).

Table 7. Replacing the ER Core of Compound 36 with Tricyclic Indazole Cores



compound	X	R ₁	R ₂	ER α degradation ^a	
				DC ₅₀ (nM) ^a	D _{max} (%) ^a
42 (ERD-3327)	N	CF ₃	H	3.8 ± 0.6	107 ± 4
43 (ERD-809)	C–F	CF ₃	F	2.0 ± 0.3	88 ± 2
44 ^b (ERD-3111)	C–F	CHF ₂	F	0.5 ± 0.04	91 ± 1
45 (ERD-576)	N	CHF ₂	H	14 ± 3.0	112 ± 6
46 (ERD-570)	C–H	CHF ₂	OMe	1.4 ± 0.3	82 ± 3
ARV-471 ^c				0.4 ± 0.04	89 ± 1

^aSame legend as in Table 2. ^b_n = 21 experiments. ^c_n = 16 experiments.

degrader with DC₅₀ = 3.8 nM and D_{max} = 107%. We evaluated the PK profile of compound 42 in rats (Table 8), and our data showed that it has a similar PK profile as compared to that of compound 36.

Based upon the promising degradation and PK data for compound 42, we next performed further modifications of the pyridine group and the R₁ substitution in compound 42, which yielded compounds 43–46. Compound 43 containing a 3,5-di-

F phenyl group exhibited a slightly improved potency but a decreased degradation efficiency (D_{max} = 88%) compared to compound 42. Replacement of the CF₃ group (R₁) in compound 43 by a CHF₂ group which yielded compound 44 (ERD-3111), increased the potency by 4-fold (DC₅₀ = 0.5 nM) compared to compound 43, while maintaining a high degradation efficiency (D_{max} = 91%). Changing the 3,5-di-F phenyl group in compound 44 back to the pyridine group (compound 45) reduced its potency (DC₅₀ = 14 nM). Replacing the 3,5-di-F substituents in compound 44 with a 3-OMe substituent resulted in compound 46, which is weaker and less effective than compound 44. Overall, compound 44 (ERD-3111) exhibited a similarly high degradation potency and efficiency as compared to ARV-471 (Table 7) and was evaluated for its PK profiles in rats, mice, and dogs.

Our PK data (Table 8) showed that ERD-3111 demonstrates an attractive PK profile in rats, characterized by a low clearance (7.4 mL/min/kg), a relatively long T_{1/2} (4.0 h), an excellent oral exposure with C_{max} = 141 ng/mL and AUC = 1317 h*ng/mL at 3 mg/kg of PO dosing. ERD-3111 has a moderate oral bioavailability of 20% in rats, which is improved over ARV-471 (10%) and compound 36 (13%). ERD-3111 achieves 3 times higher C_{max} and 5.4 times higher AUC than ARV-471 with the same 3 mg/kg oral dose in rats.

In mice, ERD-3111 shows a favorable V_{ss} of 3.2 L/kg, a low clearance of 5.7 mL/min/kg, an extended T_{1/2} of 6.4 h, an excellent oral plasma exposure with C_{max} of 260 ng/mL and AUC of 3366 h*ng/mL at 3 mg/kg of oral dosing and an overall oral bioavailability of 42%. In dogs, ERD-3111 demonstrates a

Table 8. Summary of the PK Profiles for Compounds 42, ERD-3111, and ARV-471^a

compound	species	IV/PO (mg/kg)	V _{ss} ^a (L/kg)	Cl ^a (mL/min/kg)	T _{1/2} ^a (h)	C _{max} ^a (ng/mL)	AUC ^a (h*ng/mL)	F (%)
42 (ERD-3237)	rat	1/3	3.7	27.0	2.3	51.8	243	14
44 (ERD-3111)	rat	1/3	1.3	7.4	4.0	141.1	1317	20
	mouse	1/3	3.2	5.7	6.4	260	3366	42
	dog	0.5/1	5.2	11.0	7.9	87	937	66
ARV-471	rat	1/3	2.4	18.6	4.0	46.5	244	10
	mouse	1/3	1.8	21.9	2.5	156.3	684	31

^aSame legend as in Table 4.

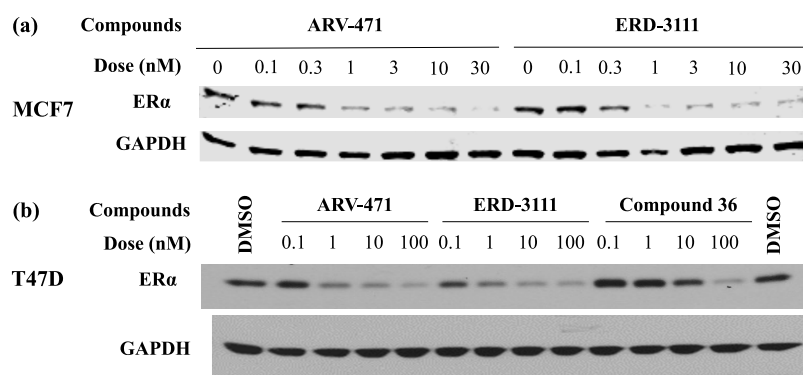
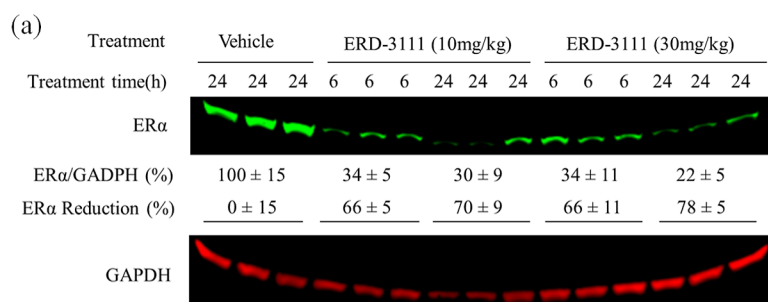


Figure 3. Western blot analysis of the concentration-dependent ER α degradation by ERD-3111 and ARV-471 in the MCF-7 cell line (a) and by ERD-3111, ARV-471 and compound 36 in the T47D cell line (b).

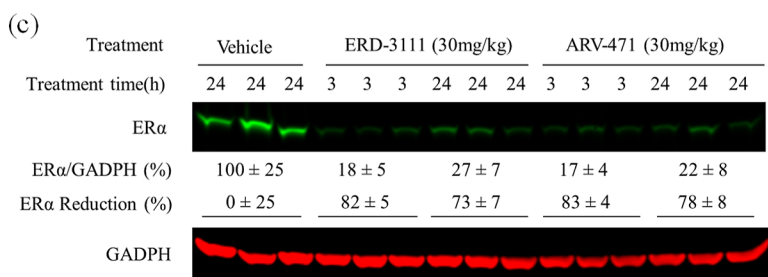
Table 9. Metabolic Stability and Safety Profiling of ERD-3111

liver microsomal stability $T_{1/2}$ (min)		hERG inhibition		CYP inhibition IC_{50} (μ M)	
human	rat	IC_{50} (μ M)	1A2/2C8/2C9/2C19/2D6	3A4 (midazolam)	3A4 (testosterone)
>60	>60	>30	>10	>10	>10



(b). Drug concentrations in plasma and tumor

Drug (Dose)	Time point (h)	Plasma Concentration (ng/mL)	Tumor Concentration (ng/mL)
ERD-3111 (10 mg/ kg)	6	433 \pm 116	385 \pm 61
	24	18 \pm 5	162 \pm 50
ERD-3111 (30 mg/ kg)	6	1437 \pm 330	1466 \pm 313
	24	80 \pm 16	413 \pm 84



(d). Drug concentrations in plasma and tumor

Drug (Dose)	Time point (h)	Plasma Concentration (ng/mL)	Tumor Concentration (ng/mL)
ERD-3111 (30 mg/ kg)	3	1977 \pm 827	1407 \pm 153
	24	167 \pm 118	449 \pm 269
ARV-471 (30 mg/ kg)	3	921 \pm 254	1708 \pm 458
	24	56 \pm 63	709 \pm 512

Figure 4. PD study and drug concentrations of ERD-3111 and ARV-471 in wide-type ER α MCF7 tumor bearing mice. Mice were treated with once-daily oral dose for three days with either vehicle, ERD-3111 or ARV-471 and plasma and tumors were collected after the last dose at indicated time points. (a,c) Western blotting analysis of the levels of ER α protein in the MCF7 tumor tissues. GAPDH was used as the loading control. (b) Concentrations of ERD-3111 in plasma and tumor tissue in mice in the PD experiment shown in (a). (d) Concentrations of ERD-3111 or ARV-471 in plasma and tumor tissue in mice in the PD experiment shown in (c). Data were provided as mean \pm SD.

V_{ss} of 5.2 L/kg, a low clearance of 11.0 mL/min/kg, a prolonged $T_{1/2}$ of 7.9 h, an excellent oral plasma exposure with C_{max} of 87 ng/mL and AUC of 937 h*ng/mL at 1 mg/kg of oral dosing, and a high oral bioavailability of 66%. In direct comparison, ERD-3111 exhibits a notable superior PK profile to ARV-471 in both rat and mouse species.

Further Evaluation of ERD-3111 in MCF-7 and T47D Cell Lines. The in vitro ER α degradation profile of ERD-3111 was further evaluated in the ER+ MCF-7 and T47D cell lines using traditional western blotting, with ARV-471 and compound 36 included as controls. As shown in Figure 3, ERD-3111 exhibits a similar dose-dependent degradation profile compared

to ARV-471, effectively inducing profound ER α degradation at concentrations as low as 1 nM in both MCF-7 and T47D cell lines. Furthermore, ERD-3111 demonstrates significantly higher degradation potency than compound 36 in the T47D cell line, aligning with the results obtained from the ICW assay in the MCF-7 cell line.

Further Profiling of ERD-3111 for Its Metabolic Stability, hERG, and Cytochrome P450 (CYP) Inhibition. We further profiled ERD-3111 for its microsomal stability and inhibition of human ether-a-go-go related gene (hERG), and cytochromes P450 (CYP), with the data summarized in Table 9. ERD-3111 exhibits excellent microsomal stability, with a $T_{1/2}$

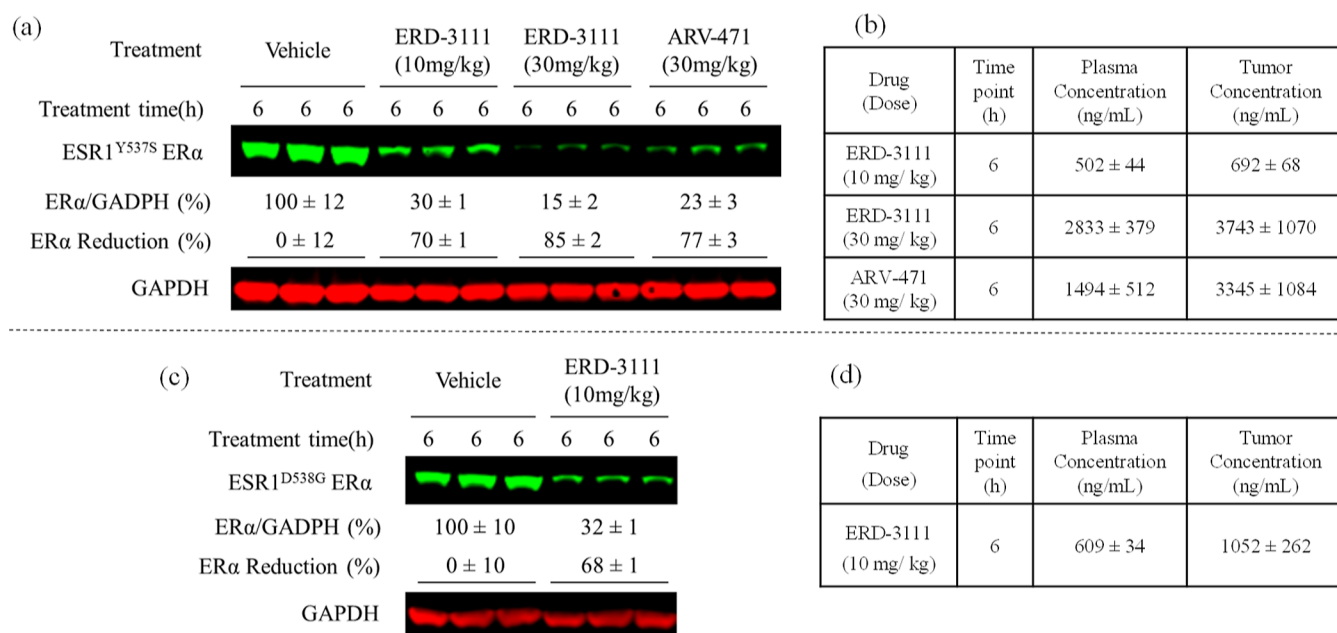


Figure 5. PD analysis and drug concentrations of ERD-3111 and ARV-471 in *ESR1*^{Y537S} or *ESR1*^{D538G} mutant MCF7 tumor bearing mice. Mice were treated with once-daily oral dose for three days and plasma and tumors were collected after the last dose at indicated time points. (a) Western blotting analysis of *ESR1*^{Y537S} mutant protein levels. (b) Drug concentrations of ERD-3111 or ARV-471 in plasma and tumor samples in the PD experiment shown in (a). (c) Western blotting analysis of *ESR1*^{D538G} mutant protein levels. (d) Drug concentrations of ERD-3111 in plasma and tumor samples in the PD experiment shown in (c). Data were provided as mean ± SD.

greater than 60 min in both human and rat microsomes. It also has no significant hERG inhibition at up to 30 μM concentration and no significant CYP inhibition against all the CYP isoforms tested at up to 10 μM concentration.

PK/Pharmacodynamic Studies of ERD-3111 in Wide-Type and *ESR1* Mutant MCF-7 Xenograft Mouse Models. We evaluated ERD-3111 for its PK/pharmacodynamic (PD) in vivo in both wide-type and *ESR1* mutant MCF-7 xenograft mouse models. ERD-3111 was dosed once-daily for 3 days in mice bearing the MCF-7 xenograft tumors, and tumors and plasma were collected at different time-points after the last dose of ERD-3111. Western blotting analysis was performed to determine the levels of ERα protein in the tumor tissues, and drug concentrations were determined in both plasma and tumors. The data are summarized in Figures 4 and 5.

As shown in Figure 4a, ERD-3111 at both 10 and 30 mg/kg effectively reduced the levels of ERα protein in the tumors at 6 and 24 h time-points, ranging from 66 to 78%. Analysis of the drug concentrations showed that while ERD-3111 has similarly high drug exposures in plasma and tumor at 6 h time-point, it has a higher drug exposure in tumor than in plasma at 24 h. ERD-3111 also showed a dose-dependent increase in its exposure in both plasma and tumor. Hence, our PK data in tumor-bearing mice indicated that ERD-3111 has excellent oral bioavailability and importantly good tumor tissue penetration in mice (Figure 4a).

We next directly compared ERD-3111 and ARV-471 for their PK/PD (Figure 4b). ARV-471 and ERD-3111 at 30 mg/kg caused similar levels of reduction in ERα proteins in MCF-7 tumors at both 3 and 24 h time points. Analysis of the drug concentrations showed that while ERD-3111 has 2-times higher drug exposure in plasma compared to ARV-471 at 3 h time-point, both compounds have similar plasma exposures at 24 h time point and have similar drug exposure in tumors at both 3 and 24 h time points.

One of the major objectives for the development of PROTAC ER degraders is to overcome resistance of ER+ human breast cancer to current ET caused by *ESR1* mutations. *ESR1*^{Y537S} and *ESR1*^{D538G} mutations are two of the most common mutations detected in tumors taken from ER+ breast cancer patients who have become resistant to current standard of care endocrine therapies.¹⁰ We have developed and characterized MCF-7 cells harboring the *ESR1*^{Y537S} and *ESR1*^{D538G} mutations via CRISPR technology.⁷⁰ Using these *ESR1* mutant models, we evaluated the ability of ERD-3111 to reduce the *ESR1*^{Y537S} and *ESR1*^{D538G} mutated proteins in vivo, with the data summarized in Figure 5.

ERD-3111 effectively induced dose-dependent *ESR1*^{Y537S} protein depletion in the tumors at 6 h, with 70 and 85% reduction observed for the 10 and 30 mg/kg doses, respectively (Figure 5a). ARV-471 at 30 mg/kg effectively reduced *ESR1*^{Y537S} protein by 77% (Figure 5a). Both ERD-3111 and ARV-471 demonstrated excellent drug exposures in plasma and tumor in mice bearing the MCF-7 *ESR1*^{Y537S} tumors (Figure 5b).

In the MCF-7 *ESR1*^{D538G} xenograft model, ERD-3111 at 10 mg/kg effectively reduced the *ESR1*^{D538G} protein by 68% in the tumor tissue (Figure 5c). Consistent with the drug exposure data in other models, ERD-3111 has a high drug exposure in plasma and tumor in mice bearing the *ESR1*^{D538G} xenograft tumors (Figure 5d).

Collectively, our PK/PD data clearly show that ERD-3111 is very effective in reducing the levels of wild-type ER protein and importantly the *ESR1*^{Y537S} and *ESR1*^{D538G} mutant ER proteins *in vivo* and has high plasma and tumor drug exposures in mice.

Antitumor Efficacy of ERD-3111 in Wide-Type and *ESR1* Mutant MCF7 Xenograft Breast Cancer Models. Based upon the promising PD results, we evaluated ERD-3111 for its antitumor activity in MCF-7 wide-type and *ESR1* mutant tumor models *in vivo*.

In the MCF-7 ER wild-type xenograft tumor model, ERD-3111 demonstrated strong anti-tumor activity (Figure 6). ERD-

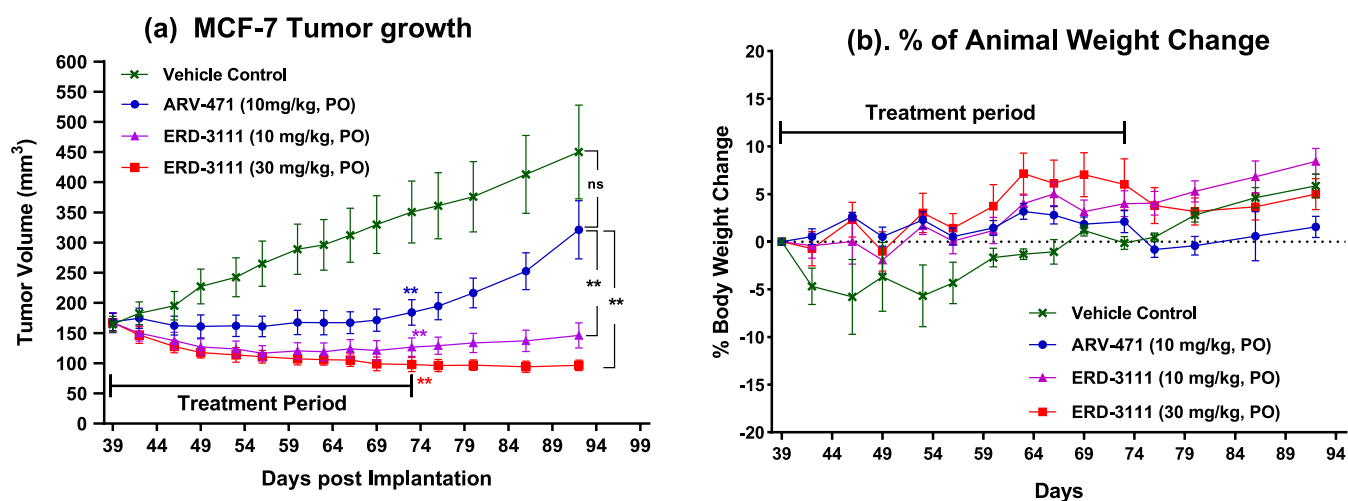


Figure 6. Antitumor efficacy of ERD-3111 in wide-type MCF-7 xenografts. ARV-471 was included as the control. Each compound or vehicle was once-daily and orally administered starting from day 39 post tumor implantation. Drug treatment was discontinued after day 73. (a) Tumor volumes for each group. A method of one-tailed unpaired *t*-test with Welch's correction was used for statistical analysis of the tumor volumes between groups.^{21,27} “**”, $P < 0.01$. (b) Percentage of mouse body weight change over time compared to day 39.

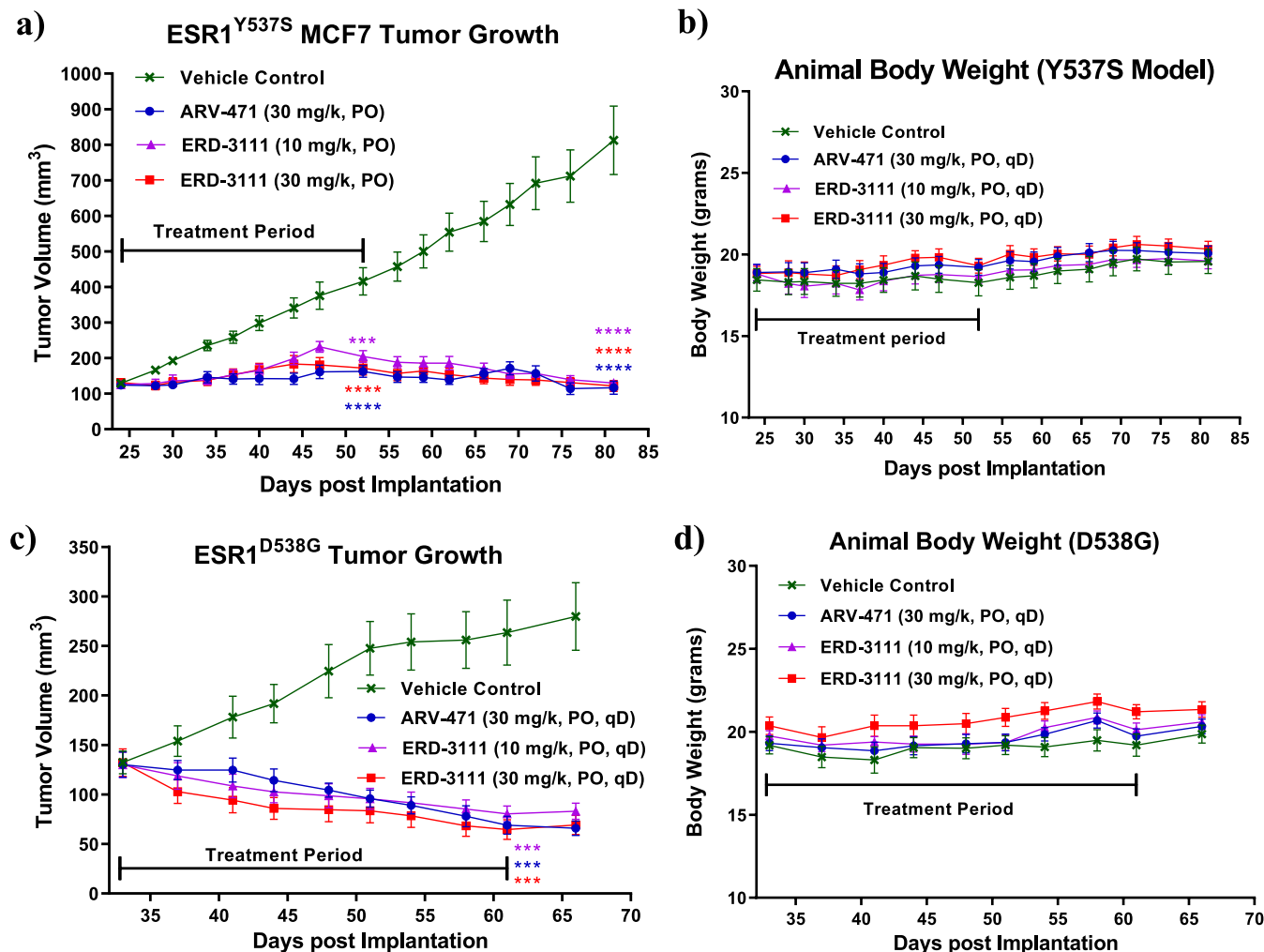
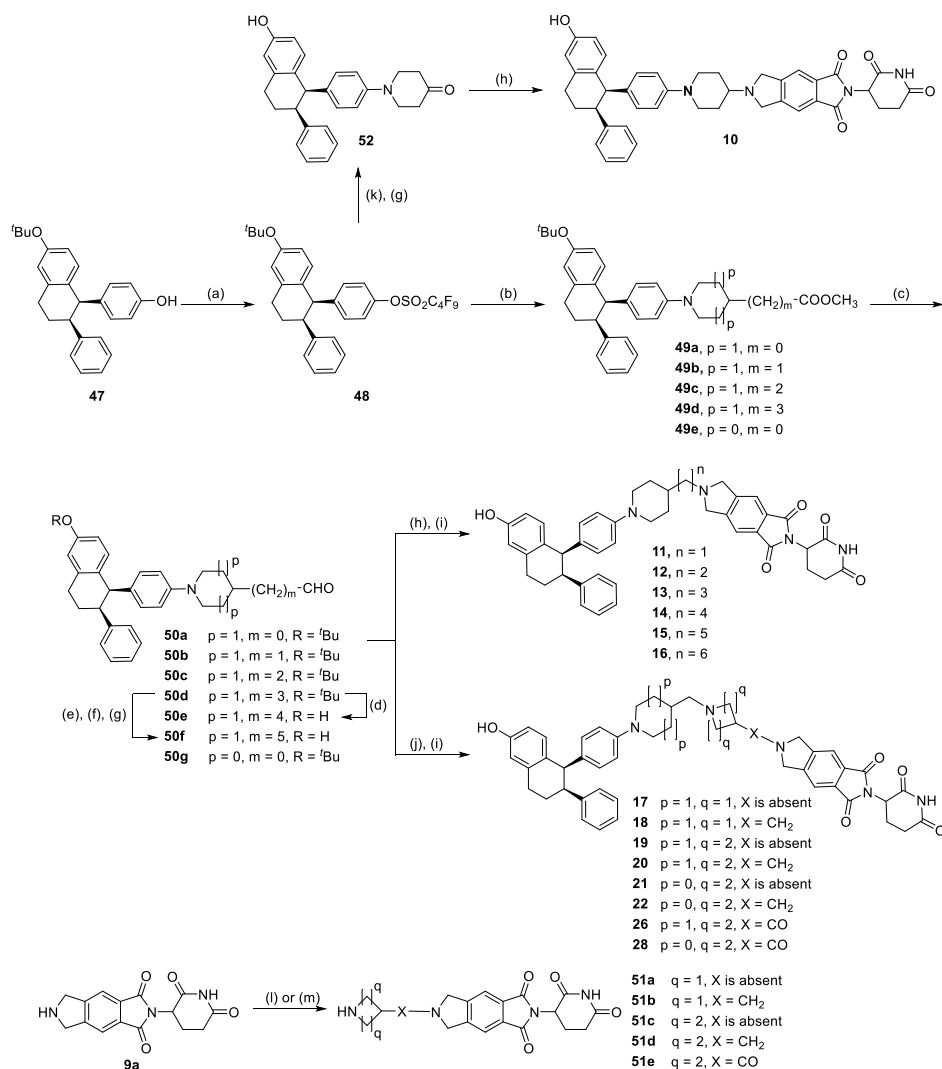


Figure 7. Antitumor efficacy of ERD-3111 in *ESR1* mutant MCF-7 xenograft mouse models: (a) *ESR1*^{Y537S} MCF-7 tumor growth; (b) animal body weight in *ESR1*^{Y537S} MCF-7 xenograft mouse model; (c) *ESR1*^{D538G} MCF-7 tumor growth; (d) animal body weight in *ESR1*^{D538G} MCF-7 xenograft mouse model. A method of one-tailed unpaired *t*-test with Welch's correction was used for statistical analysis of the tumor volumes between groups.^{21,27} “***”, $P < 0.001$; “****”, $P < 0.0001$.

Scheme 1. Synthesis of Compounds 10–22, 26, and 28 in Tables 2 and 3^a

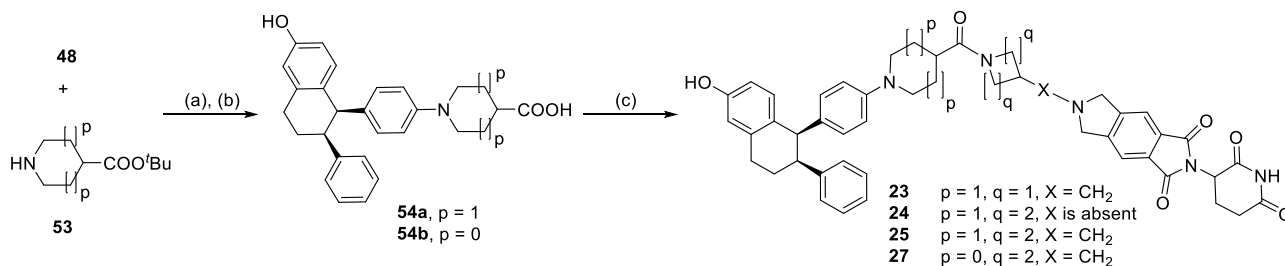
^aReagents and conditions: (a) 1,1,2,2,3,3,4,4,4-nonafluorobutane-1-sulfonyl fluoride, K_2CO_3 , THF/MeCN, rt, 100%; (b) methyl ester functionalized piperidine or azetidine, $\text{Pd}(\text{OAc})_2$, BINAP or XPhos, Cs_2CO_3 , dioxane, 100 °C, 20–96%; (c) diisobutylaluminum hydride (25% in toluene), DCM, -78 °C, 70–89%; (d) $\text{MeOCH}_2\text{PPh}_3\text{Cl}$, NaHDMS, THF, 0 °C, then HCl (12 M), THF, 0 °C, 45%; (e) ((1,3-dioxolan-2-yl)methyl)triphenylphosphonium chloride, *t*-BuOK, THF, 0 °C; (f) H_2 , Pd/C, MeOH/EA, rt; (g) 2% H_2O in TFA, rt; (h) **9a** (TFA salt), $\text{NaBH}(\text{OAc})_3$, DCE/DMF, rt; (i) for **50a–50d** and **50g**, TFA/DCM; (j) **51a–51e**, $\text{NaBH}(\text{OAc})_3$, DCE/DMF, rt; (k) 4,4-dimethoxypiperidine, $\text{Pd}(\text{OAc})_2$, XPhos, *t*-BuONa, toluene, 90 °C; (l) *tert*-butyl 3-oxoazetidine-1-carboxylate, *tert*-butyl 3-formylazetidine-1-carboxylate, *tert*-butyl 4-oxopiperidine-1-carboxylate or *tert*-butyl 4-formylpiperidine-1-carboxylate, $\text{NaBH}(\text{OAc})_3$, DCE/DMF, rt, then TFA/DCM; (m) 1-(*tert*-butoxycarbonyl)piperidine-4-carboxylic acid, HATU, DIPEA, DMF.

3111 dosed daily, PO at 10 mg/kg and 30 mg/kg for 5 weeks were highly effective in inhibiting tumor growth in vivo and resulted in 24 and 42% tumor regression, respectively, at the end of treatment (day 73). In comparison, ARV-471 at 10 mg/kg achieved 87% tumor growth inhibition but no tumor regression at the end of the treatment. Furthermore, the antitumor activity achieved by **ERD-3111** was persistent. Three-weeks after the last dose, **ERD-3111** at 10 and 30 mg/kg exhibited sustained tumor regressions of 13 and 42%, respectively. The antitumor activity achieved by **ERD-3111** at 10 mg/kg at day 93 (three-weeks after the last dose) was also significantly better than that achieved by ARV-471 at 10 mg/kg ($P < 0.01$).

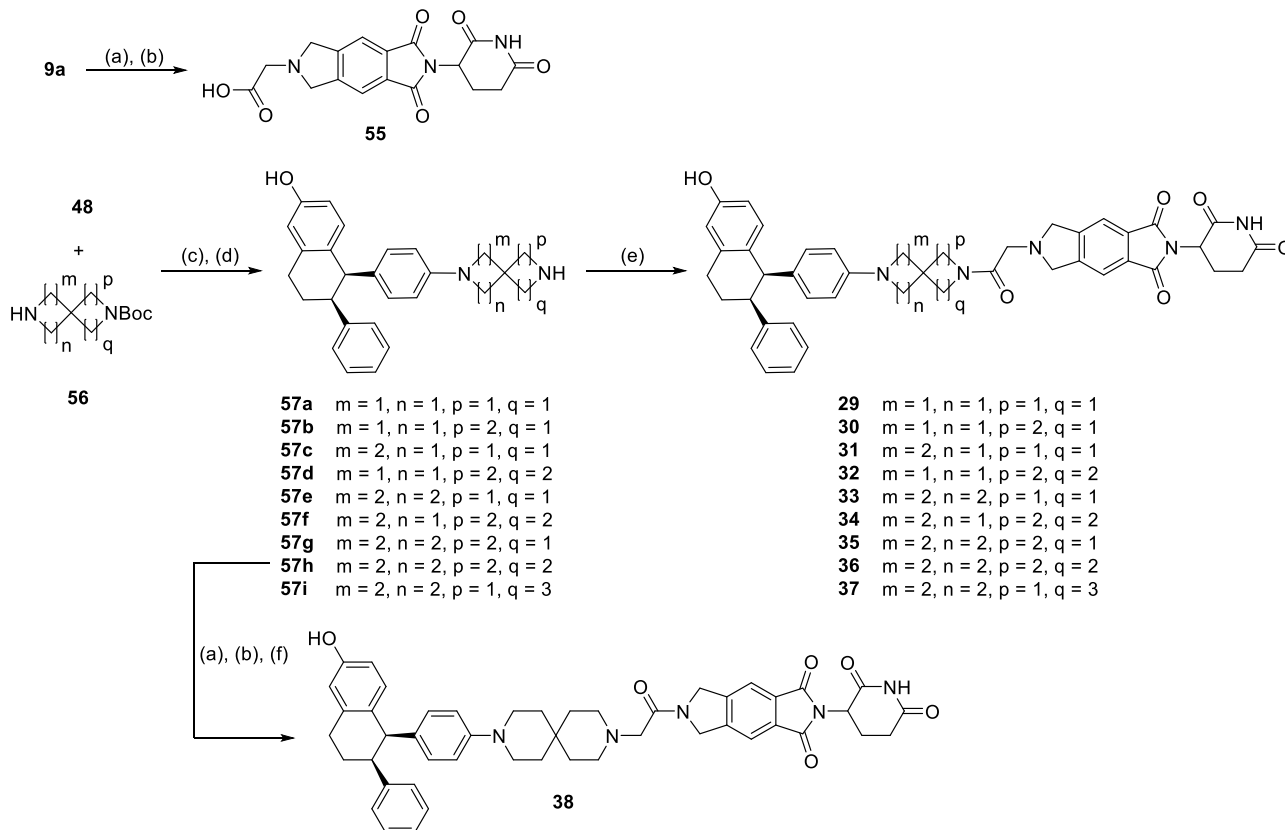
In the $\text{ESR1}^{\text{Y537S}}$ MCF-7 xenograft model, **ERD-3111** achieved strong antitumor activity (Figure 7a). **ERD-3111** dosed at 10 and 30 mg/kg, PO, daily for 4 weeks inhibited tumor growth by 72 and 86%, respectively, at the end of treatment, over

the vehicle control. Importantly, the tumor growth inhibition achieved by **ERD-3111** at both 10 and 30 mg/kg was persistent. At day 82, 30 days after the last treatment, **ERD-3111** at both 10 and 30 mg/kg achieved 99 and 101% tumor growth inhibition, respectively, which are stronger than the antitumor activities displayed at the end of the last treatment. ARV-471 dosed at 30 mg/kg, daily, PO for 4 weeks had virtually the same antitumor activity as **ERD-3111** at 30 mg/kg at all the time-points.

In the $\text{ESR1}^{\text{D538G}}$ mutant MCF-7 xenograft model, **ERD-3111** displayed an even stronger antitumor activity than that achieved in the $\text{ESR1}^{\text{Y537S}}$ mutant MCF-7 xenograft model. **ERD-3111** at both 10 and 30 mg/kg was capable of achieving tumor regression (Figure 7c). **ERD-3111** at 10 and 30 mg/kg dosed daily, PO for 4 weeks achieved tumor regressions of 38 and 51%, respectively, at the end of the treatment. In comparison, ARV-471 dosed at 30 mg/kg for 4 weeks had tumor regression of 47%

Scheme 2. Synthesis of Compounds 23–25 and 27 in Table 4^a

^aReagents and conditions: (a) $\text{Pd}(\text{OAc})_2$, XPhos, *t*-BuONa, toluene, 90 °C; (b) TFA/DCM, rt; (c) **51b**, **51c** or **51d**, HATU, DIPEA, DMF.

Scheme 3. Synthesis of Compounds 29–38 in Table 5^a

^aReagents and conditions: (a) *tert*-butyl 2-bromoacetate, DIPEA, MeCN, rt; (b) TFA/DCM, rt; (c) cyclic amine, $\text{Pd}(\text{OAc})_2$, XPhos, *t*-BuONa, toluene, 90 °C; (d) TFA/DCM, rt; (e) **55**, HATU, DIPEA, DMF; (f) **9a**, HATU, DIPEA, DMF.

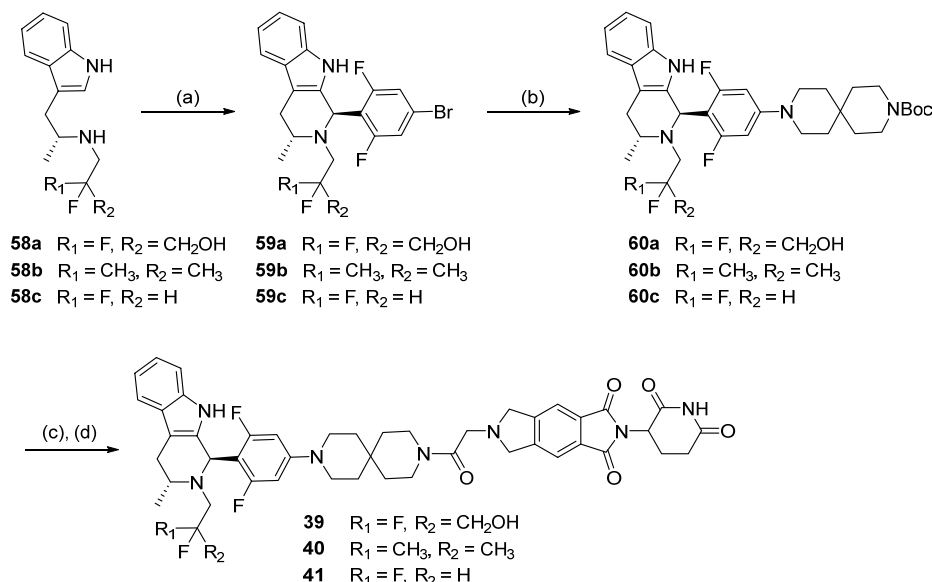
at the end of the treatment, similar to that observed for **ERD-3111** at 30 mg/kg. The antitumor activity achieved by both **ERD-3111** and ARV-471 was persisted and tumors did not grow significantly after the treatment was stopped for 1 week.

Importantly, in all three *in vivo* efficacy experiments, **ERD-3111** was well tolerated and the mice did not show any weight loss or other signs of toxicity (Figure 7b,d).

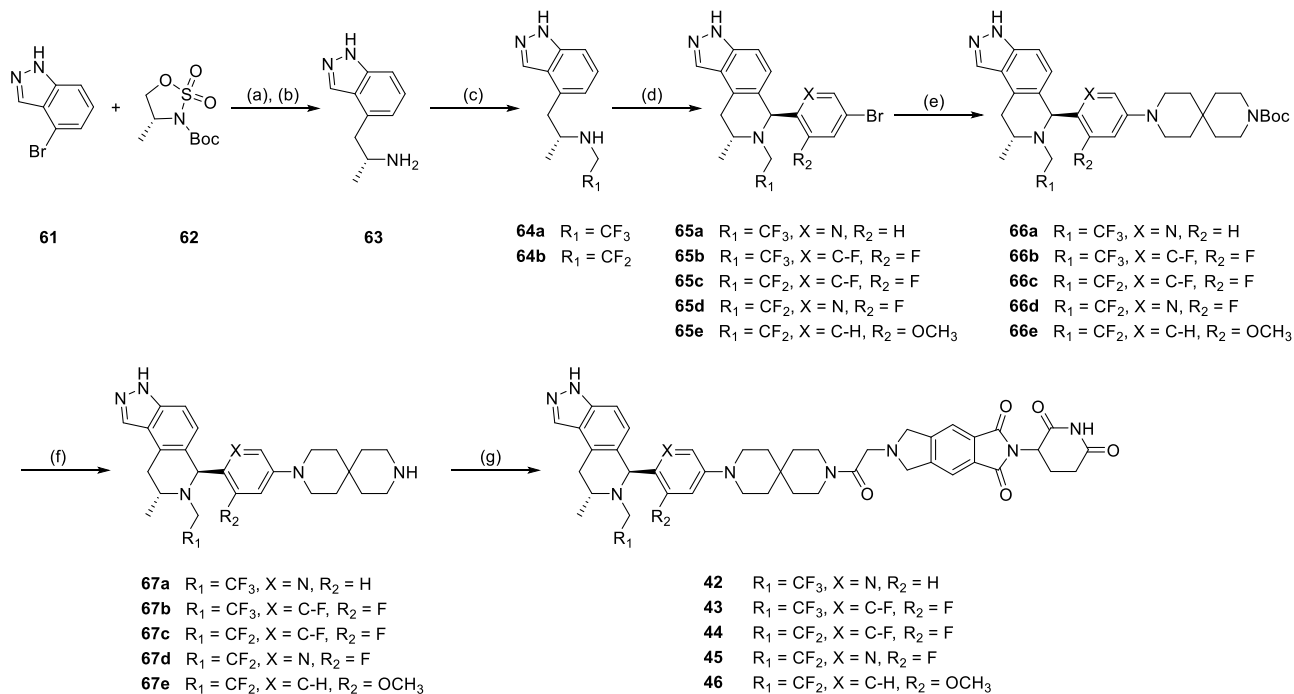
Collectively, our efficacy experiments have demonstrated that **ERD-3111** displays strong antitumor activity in MCF-7 ER wild-type, *ESR1*^{Y537S}, and *ESR1*^{D538G} xenograft tumor models. Specifically, **ERD-3111** achieves persistent tumor regression in the MCF-7 ER wild-type and *ESR1*^{D538G} tumor models and 100% of tumor growth inhibition in the *ESR1*^{Y537S} xenograft tumor model. **ERD-3111** was well tolerated and exhibited no signs of toxicity in mice.

CHEMISTRY

The synthesis of compounds **10–22**, **26**, and **28** are summarized in Scheme 1. Compound **47** was prepared using a reported synthetic procedure.⁷¹ Compound **47** was converted to an activated sulfonate group, resulting in compound **48**. Buchwald amination of compound **48** with various methyl ester functionalized piperidines or azetidines afforded intermediates **49a–49e** in 20–96% yields. Reduction of the methyl esters in intermediates **49a–49e** using 1–2 equiv of DIBAL-H in DCM selectively converted them to the corresponding aldehydes (**50a–50d** and **50g**) in high yields. Aldehyde **50d** was used as a starting point to achieve aldehyde **50e**, which has one more methylene group. This was done through a Wittig reaction with (methoxymethyl)triphenyl-phosphonium, followed by simultaneous deprotection of the methyl group in the linker and *tert*-butyl group in the ER core using concentrated

Scheme 4. Synthesis of Compounds 39–41 in Table 6^a

^aReagents and conditions: (a) aldehyde, AcOH, Toluene, 80 °C; (b) *tert*-butyl 3,9-diazaspiro[5.5]undecane-3-carboxylate, Pd₂(dba)₃, XantPhos, Cs₂CO₃, 1,4-dioxane, 100 °C; (c) TFA, DCM; (d) **55**, HATU, DIPEA, DMF.

Scheme 5. Synthesis of Compounds 42–46 in Table 6^a

^aReagents and conditions: (a) *n*-BuLi, THF, −78 to −50 °C; (b) 4 N HCl/1,4-dioxane; (c) 2,2-difluoroethyl trifluoromethanesulfonate or 2,2,2-trifluoroethyl trifluoromethanesulfonate, DIPEA, 1,4-dioxane, 60 °C; (d) various aldehydes, TFA, toluene, 90 °C; (e) *tert*-butyl 3,9-diazaspiro[5.5]undecane-3-carboxylate, RuPhos Pd G2, RuPhos, *t*-BuONa, 1,4-dioxane, 100 °C; (f) TFA/DCM; (g) **55**, HATU, DIPEA, DMF.

HCl. Similarly, Wittig olefination of aldehyde **50d** with ((1,3-dioxolan-2-yl)methyl)triphenylphosphonium, and subsequent hydrogenation of the resulting alkene, provided aldehyde **50f** after deprotection of the *tert*-butyl group and acetal group using TFA (2% H₂O). To synthesize compounds **17–22**, **26**, and **28**, the appropriate linker portion was introduced to compound **9a**⁶³ first. Reductive amination of compound **9a** with the appropriated aldehydes or ketones, or amide coupling of

compound **9a** with the appropriated acids, followed by Boc deprotection using TFA, yielded intermediates **51a–51e**. Further reductive amination of aldehydes **50a–50g** with amines **9a** and **51a–51e**, and subsequent deprotection of the *tert*-butyl group (if present) using TFA, resulted in the final compounds **11–22**, **26**, and **28**. In addition, Buchwald coupling of intermediate **48** with 4,4-dimethoxypiperidine, followed by deprotection of the ketal and *tert*-butyl groups using TFA,

afforded intermediate **52**. This intermediate was then transformed into the title compound **10** through a reductive amination with compound **9a**.

The synthesis of compounds **23–25** and **27** is described in Scheme 2. Buchwald coupling of intermediate **48** with various amines **53** followed by deprotection of the two *tert*-butyl groups with TFA yielded intermediates **54a** and **54b**, which underwent reductive amination with amines **51 b–51d** to achieve the title compounds **23–25** and **27**.

The synthesis of compounds **29–38** was performed according to Scheme 3. The general intermediate **55** was obtained by substituting **9a** with *tert*-butyl 2-bromoacetate followed by deprotection of the *tert*-butyl group using TFA. On the other hand, key intermediates **57a–57i** were synthesized through Buchwald amination of the common intermediate **48** with various amines (**56**), followed by Boc deprotection. Next, the title compounds **29–37** were obtained by amide coupling of the amines (**57a–57i**) with the acid (**55**). Besides, *N*-substitution of intermediate **57h** with *tert*-butyl 2-bromoacetate followed by deprotection of the *tert*-butyl group, the title compound **38** was obtained by further amide coupling of the modified intermediate with **9a**.

The synthesis of indole-based compounds **39–41** is described in Scheme 4. Compounds **58a–58c** were prepared according to previously reported procedures.²⁶ Pictet–Spengler cyclization of compounds **58a–58c** with various aldehydes were performed in the presence of acetic acid under heating condition. This step yielded key tricyclic indole intermediates **59a–59c** in good yields and with high diastereoselectivity. Subsequent Buchwald amination of bromides (**59a–59c**) with *tert*-butyl 3,9-diazaspiro[5.5]undecane-3-carboxylate provided intermediates **60a–60c**. Treatment of **60a–60c** with TFA to remove the Boc protecting group and then immediately subject to the amide coupling with intermediate **55** afforded the title compounds **39–41**.

The synthesis of indazole compounds **42–46** is shown in Scheme 5. Starting with commercially available compound **61**, the bromo group was subjected to lithium–halogen exchange using *n*-BuLi. Cyclic sulfamidate **62** was added in portions to the reaction mixture, resulting in the formation of intermediate **63** after Boc deprotection by concentrated HCl. *N*-Alkylations of compound **63** with alkyl triflates gave compounds **64a** and **64b**, which underwent Pictet–Spengler cyclization with various aldehydes to generate key intermediates **65a–65e** with high diastereoselectivity.²⁷ Subsequent Buchwald amination with *tert*-butyl 3,9-diazaspiro[5.5]undecane-3-carboxylate using Ru-Phos Pd G2/RuPhos as the catalyst produced intermediates **66a–66e**, which were treated by TFA to deprotect the Boc group to yield intermediates **67a–67e**. Final amide coupling of amines (**67a–67e**) with acid (**55**) afforded the title compounds **42–46**.

SUMMARY

In this study, we have described the design, synthesis, and biological evaluations of novel ER α PROTAC degraders based on our new CRBN ligand TX-16 and three different classes of ER ligands. First, through extensive investigations on the linker portion in PROTAC degraders designed using the ER ligand in Lasofoxifene and ARV-471, the 6,6-spiro-ring-containing linker in compound **36** was identified as an optimal linker for degradation potency and efficiency, as well for pharmacokinetics in mice and rats. To further enhance the degradation potency and improve the oral PK profile, the ER core in compound **36**

was replaced with ER ligands containing either a tricyclic indole or a tricyclic indazole core, which led to the discovery of ERD-3111 as the best ER degrader. ERD-3111 potently and effectively induced degradation of ER α protein in ER+ MCF-7 and T47D cells. Importantly, it achieved an excellent pharmacokinetic profile in rats, mice, and dogs and good oral bioavailability in these species. ERD-3111 showed excellent microsomal stability and exhibits no significant hERG or CYP inhibition. PK/PD studies demonstrated that oral administration of ERD-3111 was highly effective in reducing the levels of wild-type and mutated ER α proteins in xenograft tumor tissues and achieved high plasma and tumor tissue exposures. Consistent with effective depletion of wild-type and ER α mutated proteins in tumor tissues, ERD-3111 demonstrated strong antitumor activity and was capable of achieving persistent tumor regression in the MCF-7 ER wild-type and ESRI^{D538G} xenograft tumor models or 100% of tumor growth inhibition in the MCF-7 ESRI^{Y537S} mutated xenograft tumor model. Significantly, ERD-3111 treatments did not cause animal weight loss or exhibit other signs of toxicity in mice. Taken together, our data show that ERD-3111 is a potent, orally bioavailable and highly efficacious ER α PROTAC degrader and represents a promising lead compound for extensive evaluations for the treatment of ER α + breast cancer.

EXPERIMENTAL SECTION

General Information for Chemistry. Unless otherwise noted, all commercial materials were used as received. NMR spectra were recorded on a Bruker Ascend 400 MHz spectrometer and calibrated using residual solvent peaks as internal reference. In reported spectral data, the format (δ) chemical shift (multiplicity, *J* values in Hz, integration) was used with the following abbreviations: s = singlet, d = doublet, t = triplet, q = quartet, hept = heptet, dd = doublet of doublets, and m = multiplet. Low resolution mass spectrometry (MS) analysis was carried out with a Waters UPLC ACQUITY QDa mass spectrometer. High resolution mass experiments were operated on an Agilent Technologies 6230 TOF LC/MS instrument with APCI ionization. Flash column chromatography was performed by Teledyne CombiFlash RF+ using the RediSep Rf silica gel flash column. The final compounds were all purified by a C18 reverse phase preparative HPLC column (SunFire Prep C18 OBD 5 μ m, 50 \times 100 mm) with solvent A (0.1% TFA or formic acid in H₂O) and solvent B (0.1% TFA or formic acid in MeCN) as eluents at 60 mL/min flow rate. The purity of all the final compounds was measured and confirmed to be >95% by UPLC–MS analysis (10–100% MeCN in H₂O containing 0.1% formic acid in 5 min, 1.0 mL/min flow rate) with a C18 column (ACQUITY UPLC BEH C18 1.7 μ m, 2.1 \times 50 mm).

2-(2,6-Dioxopiperidin-3-yl)-6-(1-(4-((1*R*,2*S*)-6-hydroxy-2-phenyl-1,2,3,4-tetrahydronaphthalen-1-yl)phenyl)piperidin-4-yl)-6,7-dihydropyrrolo[3,4-*f*]isoindole-1,3(2*H*,5*H*)-dione (**10**). Potassium carbonate (2.6 g, 3.5 equiv) was added to a solution of compound 4-((1*R*,2*S*)-6-(*tert*-butoxy)-2-phenyl-1,2,3,4-tetrahydronaphthalen-1-yl)phenol **47**⁷¹ (2.0 g, 1 equiv) and 1,1,2,2,3,3,4,4,4-nonafluorobutane-1-sulfonyl fluoride (3.24 g, 2.0 equiv) in tetrahydrofuran (10 mL) and MeCN (10 mL). The reaction mixture was stirred at rt for 16 h. TLC indicated the starting material was consumed completely, and one new spot formed. The reaction mixture was concentrated under reduced pressure. The residue was purified by flash column chromatography. The desired compound 4-((1*R*,2*S*)-6-(*tert*-butoxy)-2-phenyl-1,2,3,4-tetrahydronaphthalen-1-yl)phenyl 4,4,4,4,4,4,4-nonafluoro-4H12-butyl-1,3-diyne-1-sulfonate (**48**)⁷¹ (3.5 g, 100% yield) was obtained as a colorless oil. ¹H NMR (400 MHz, CDCl₃): δ 7.21–7.11 (m, 3H), 6.94–6.86 (m, 3H), 6.84–6.73 (m, 4H), 6.46 (d, *J* = 8.8 Hz, 2H), 4.33 (d, *J* = 5.2 Hz, 1H), 3.50–3.40 (m, 1H), 3.16–2.95 (m, 2H), 2.20–2.02 (m, 1H), 1.91–1.79 (m, 1H), 1.38 (s, 9H).

A mixture of intermediate **48** (300 mg, 1.0 equiv), 4,4-dimethylpiperidine (133 mg, 2.0 equiv), Pd(OAc)₂ (20.6 mg, 0.2

equiv), XPhos (65.5 mg, 0.3 equiv) and *t*-BuONa (176 mg, 4.0 equiv) in toluene (10 mL) was degassed and purged with 3 times with N₂ and then stirred at 90 °C under a N₂ atmosphere for 10 h. UPLC–MS showed one main peak with the desired MS was detected. TLC indicated that the starting material was completely consumed, and a new spot formed. The mixture was cooled, diluted with DCM, and filtered through Celite to remove insoluble catalyst and salts, and the filter cake was washed with DCM. The filtrate was concentrated under reduced pressure. The residue was purified by flash column chromatography (*n*-hexane/EtOAc = 100:0 to 90:10). The resulting pure product was dissolved in TFA (containing 2% H₂O) and stirred for 4 h. The solvent was removed, and the residue was lyophilized to give compound 1-(4-((1*R*,2*S*)-6-hydroxy-2-phenyl-1,2,3,4-tetrahydronaphthalen-1-yl)phenyl)piperidin-4-one (**52**) as a white solid (180 mg, yield = 99%); UPLC–MS (ESI) *m/z*: calcd, 398.21 for C₂₇H₂₇N₂O₂ [M + H]⁺; found, 398.38; ¹H NMR (400 MHz, DMSO-*d*₆): δ 9.00 (s, 1H), 7.18–7.08 (m, 3H), 6.86–6.80 (m, 2H), 6.68–6.59 (m, 4H), 6.48 (dd, *J* = 8.3, 2.6 Hz, 1H), 6.26 (d, *J* = 8.7 Hz, 2H), 4.15 (d, *J* = 5.0 Hz, 1H), 3.45 (t, *J* = 6.0 Hz, 4H), 3.34–3.22 (m, 1H), 3.04–2.85 (m, 2H), 2.35 (t, *J* = 6.0 Hz, 4H), 2.18–2.02 (m, 1H), 1.79–1.64 (m, 1H).

Compound 2-(2,6-dioxopiperidin-3-yl)-6,7-dihydropyrrolo[3,4-*f*]-isoindole-1,3(2*H*,5*H*)-dione (**9a**)⁶³ was prepared according to our previous reported procedures as a dark powder; UPLC–MS (ESI) *m/z*: calcd, 300.10 for C₁₅H₁₃N₃O₄ [M + H]⁺; found, 300.25; ¹H NMR (400 MHz, MeOD): δ 7.95 (s, 2H), 5.17 (dd, *J* = 12.6, 5.4 Hz, 1H), 4.78 (s, 4H), 2.94–2.82 (m, 1H), 2.81–2.67 (m, 2H), 2.20–2.10 (m, 1H); ¹³C NMR (101 MHz, MeOD): δ 174.51, 171.33, 167.93, 143.06, 134.09, 119.56, 51.79, 50.80, 32.13, 23.55.

Intermediate **52** (30 mg, 1.0 equiv) was added to a suspension of TFA salt of compound **9a** (31 mg, 1.0 equiv) in DCE/DMF (4 mL/2 mL), and the mixture was stirred at rt for 3 h. NaBH(OAc)₃ (48 mg, 3 equiv) was then added into two portions, after which the reaction was kept stirring overnight. The reaction mixture was concentrated under reduced pressure to remove most of the solvent DCE and subsequently purified by pre-HPLC (MeCN/H₂O = 25–100% in 75 min) to afford title compound 2-(2,6-dioxopiperidin-3-yl)-6-(1-(4-((1*R*,2*S*)-6-hydroxy-2-phenyl-1,2,3,4-tetrahydronaphthalen-1-yl)phenyl)piperidin-4-yl)-6,7-dihydropyrrolo[3,4-*f*]isoindole-1,3(2*H*,5*H*)-dione (**10**) as a white solid (34 mg, yield = 66%); UPLC–MS: 1.73 min, purity >95%; MS (ESI) *m/z*: calcd, 681.31 for C₄₂H₄₀N₄O₅ [M + H]⁺; found, 681.44; ¹H NMR (400 MHz, MeOD): δ 7.93 (s, 2H), 7.17–7.06 (m, 3H), 6.86–6.78 (m, 4H), 6.70–6.64 (m, 2H), 6.52 (dd, *J* = 8.3, 2.7 Hz, 1H), 6.43 (d, *J* = 8.7 Hz, 2H), 5.17 (dd, *J* = 12.6, 5.4 Hz, 1H), 4.92 (s, 4H), 4.25 (d, *J* = 5.1 Hz, 1H), 3.82–3.63 (m, 3H), 3.40–3.33 (m, 1H), 3.09–2.94 (m, 4H), 2.93–2.81 (m, 1H), 2.80–2.66 (m, 2H), 2.35 (d, *J* = 11.7 Hz, 2H), 2.27–2.11 (m, 2H), 2.05–1.91 (m, 2H), 1.84–1.75 (m, 1H).

2-(2,6-Dioxopiperidin-3-yl)-6-((1-(4-((1*R*,2*S*)-6-hydroxy-2-phenyl-1,2,3,4-tetrahydronaphthalen-1-yl)phenyl)piperidin-4-yl)methyl)-6,7-dihydropyrrolo[3,4-*f*]isoindole-1,3(2*H*,5*H*)-dione (**11**). Compound **11** was prepared using a similar procedure for the synthesis of compound **14**. It was obtained as a white solid; UPLC–MS: 1.74 min, purity >95%; MS (ESI) *m/z*: calcd, 695.32 for C₄₃H₄₂N₄O₅ [M + H]⁺; found, 695.40; ¹H NMR (400 MHz, MeOD): δ 7.93 (s, 2H), 7.29–7.08 (m, 5H), 6.89–6.79 (m, 2H), 6.71–6.58 (m, 4H), 6.53 (dd, *J* = 8.3, 2.5 Hz, 1H), 5.17 (dd, *J* = 12.6, 5.4 Hz, 1H), 4.93 (s, 4H), 4.41–4.33 (m, 1H), 3.73–3.61 (m, 2H), 3.56–3.38 (m, 5H), 3.12–2.97 (m, 2H), 2.95–2.82 (m, 1H), 2.81–2.66 (m, 2H), 2.39–2.25 (m, 1H), 2.25–2.09 (m, 4H), 1.91–1.73 (m, 3H).

2-(2,6-Dioxopiperidin-3-yl)-6-(2-(1-(4-((1*R*,2*S*)-6-hydroxy-2-phenyl-1,2,3,4-tetrahydronaphthalen-1-yl)phenyl)piperidin-4-yl)ethyl)-6,7-dihydropyrrolo[3,4-*f*]isoindole-1,3(2*H*,5*H*)-dione (**12**). Compound **12** was prepared using a similar procedure for the synthesis of compound **14**. It was obtained as a white solid; UPLC–MS: 1.56 min, purity >95%; MS (ESI) *m/z*: calcd, 709.34 for C₄₄H₄₄N₄O₅ [M + H]⁺; found, 709.39; ¹H NMR (400 MHz, MeOD): δ 7.93 (s, 2H), 7.23 (d, *J* = 8.7 Hz, 2H), 7.18–7.08 (m, 3H), 6.83 (dd, *J* = 7.6, 1.9 Hz, 2H), 6.72–6.60 (m, 4H), 6.53 (dd, *J* = 8.3, 2.6 Hz, 1H), 5.17 (dd, *J* = 12.6, 5.5 Hz, 1H), 4.90 (s, 4H), 4.38 (d, *J* = 5.4 Hz, 1H), 3.66–3.41 (m, 7H), 3.13–

2.97 (m, 2H), 2.94–2.81 (m, 1H), 2.80–2.66 (m, 2H), 2.23–2.06 (m, 4H), 1.93–1.67 (m, 6H).

2-(2,6-Dioxopiperidin-3-yl)-6-(3-(1-(4-((1*R*,2*S*)-6-hydroxy-2-phenyl-1,2,3,4-tetrahydronaphthalen-1-yl)phenyl)piperidin-4-yl)-propyl)-6,7-dihydropyrrolo[3,4-*f*]isoindole-1,3(2*H*,5*H*)-dione (**13**). Compound **13** was prepared using a similar procedure for the synthesis of compound **14**. It was obtained as a white solid; UPLC–MS: 1.56 min, purity >95%; MS (ESI) *m/z*: calcd, 723.35 for C₄₅H₄₆N₄O₅ [M + H]⁺; found, 723.44; ¹H NMR (400 MHz, MeOD): δ 7.93 (s, 2H), 7.23 (d, *J* = 8.7 Hz, 2H), 7.18–7.08 (m, 3H), 6.88–6.79 (m, 2H), 6.72–6.61 (m, 4H), 6.53 (dd, *J* = 8.4, 2.5 Hz, 1H), 5.17 (dd, *J* = 12.5, 5.5 Hz, 1H), 4.89 (s, 4H), 4.38 (d, *J* = 5.4 Hz, 1H), 3.64–3.41 (m, 7H), 3.12–2.98 (m, 2H), 2.95–2.82 (m, 1H), 2.81–2.66 (m, 2H), 2.23–2.05 (m, 4H), 1.95–1.86 (m, 2H), 1.86–1.60 (m, 4H), 1.54–1.44 (m, 2H).

2-(2,6-Dioxopiperidin-3-yl)-6-(4-(1-(4-((1*R*,2*S*)-6-hydroxy-2-phenyl-1,2,3,4-tetrahydronaphthalen-1-yl)phenyl)piperidin-4-yl)-butyl)-6,7-dihydropyrrolo[3,4-*f*]isoindole-1,3(2*H*,5*H*)-dione (**14**). A mixture of intermediate **48** (600 mg, 1.0 equiv), methyl 4-(piperidin-4-yl)butanoate hydrochloride (406 mg, 2.0 equiv), Pd(OAc)₂ (41 mg, 0.2 equiv), XPhos (131 mg, 0.3 equiv), and Cs₂CO₃ (1.5 g, 5.0 equiv) in toluene (15 mL) was degassed and purged 3 times with N₂, and the reaction was stirred at 100 °C under a N₂ atmosphere for 16 h. After cooling to rt, the reaction mixture was diluted with DCM and filtered through Celite to remove insoluble catalysts and salts, and the filter cake was washed with DCM. The resulting filtration was concentrated to dryness, which was purified by flash column chromatography (*n*-hexane/EtOAc = 100:0 to 85:15) to provide compound methyl 4-(1-(4-((1*R*,2*S*)-6-(*tert*-butoxy)-2-phenyl-1,2,3,4-tetrahydronaphthalen-1-yl)phenyl)piperidin-4-yl)butanoate (**49d**) as a light yellow oil (480 mg, yield = 97%); UPLC–MS: 2.66 min; MS (ESI) *m/z*: calcd, 540.35 for C₃₆H₄₅NO₃ [M + H]⁺; found, 540.43; ¹H NMR (400 MHz, CDCl₃): δ 7.22–7.10 (m, 3H), 6.90–6.71 (m, 6H), 6.58 (m, 1H), 6.29 (m, 2H), 4.23 (d, *J* = 4.3 Hz, 1H), 3.67 (s, 3H), 3.59–3.48 (m, 2H), 3.42–3.32 (m, 1H), 3.12–2.95 (m, 2H), 2.58 (s, 2H), 2.30 (t, *J* = 7.5 Hz, 2H), 2.24–2.09 (m, 1H), 1.84–1.71 (m, 3H), 1.70–1.60 (m, 3H), 1.36 (s, 9H), 1.34–1.26 (m, 3H).

A solution of compound **49d** (668 mg, 1.0 equiv) in DCM (20 mL) was degassed and purged 3 times with N₂ and then cooled down to –78 °C. DIBAL-H (25% in toluene, 1.42 mL, 1.7 equiv) was added dropwise under a N₂ atmosphere over 30 min, and the reaction was stirred for 1 h. After that, the reaction was quenched with 12 mL aqueous potassium sodium tartrate solution. The resulting mixture was warmed to rt and kept stirring until became clear, which was subsequently extracted with DCM, washed with brine, dried over Na₂SO₄, and purified by flash column chromatography (*n*-hexane/EtOAc = 100:0 to 85:15) to afford compound 4-(1-(4-((1*R*,2*S*)-6-(*tert*-butoxy)-2-phenyl-1,2,3,4-tetrahydronaphthalen-1-yl)phenyl)piperidin-4-yl)butanal (**50d**) as a gray solid (440 mg, yield = 70%); UPLC–MS: 2.48 min; MS (ESI) *m/z*: calcd, 510.34 for C₃₅H₄₃NO₂ [M + H]⁺; found, 510.43; ¹H NMR (400 MHz, CDCl₃): δ 9.77 (t, *J* = 1.7 Hz, 1H), 7.20–7.10 (m, 3H), 6.88–6.70 (m, 6H), 6.68–6.53 (m, 1H), 6.35–6.23 (m, 2H), 4.24 (d, *J* = 4.5 Hz, 1H), 3.59–3.48 (m, 2H), 3.41–3.33 (m, 1H), 3.11–2.96 (m, 2H), 2.61 (s, 1H), 2.43 (td, *J* = 7.3, 1.6 Hz, 2H), 2.23–2.08 (m, 1H), 1.86–1.71 (m, 3H), 1.71–1.61 (m, 3H), 1.40–1.34 (m, 11H), 1.34–1.24 (m, 3H).

To a suspension of TFA salt of compound **9a** (24 mg, 1.0 equiv) in DCE/DMF (4 mL/2 mL) was added intermediate **50d** (30 mg, 1.0 equiv), and the mixture was stirred at rt for 3 h. NaBH(OAc)₃ (75 mg, 6 equiv) was then added into portion wise over 12 h, after which the reaction was kept stirring for another 24 h. The reaction mixture was concentrated under reduced pressure to remove most of the solvent DCE and purified by pre-HPLC (MeCN/H₂O = 40–100% in 60 min) to afford a pure product. The resulting product was dissolved in TFA/DCM (2 mL/4 mL) and stirred at rt for 3–4 h. Then the solution was concentrated to a dryness, which was further lyophilized to give the title compound 2-(2,6-dioxopiperidin-3-yl)-6-(4-(1-(4-((1*R*,2*S*)-6-hydroxy-2-phenyl-1,2,3,4-tetrahydronaphthalen-1-yl)phenyl)piperidin-4-yl)butyl)-6,7-dihydropyrrolo[3,4-*f*]isoindole-1,3(2*H*,5*H*)-dione (**14**) as a white solid (9 mg, yield = 21%); UPLC–MS: 1.54 min, purity >95%; MS (ESI) *m/z*: calcd, 737.37 for C₄₆H₄₈N₄O₅ [M + H]⁺; found,

737.43; $^1\text{H NMR}$ (400 MHz, MeOD): δ 7.93 (s, 2H), 7.24 (d, J = 8.8 Hz, 2H), 7.17–7.08 (m, 3H), 6.77–6.81 (m, 2H), 6.72–6.61 (m, 4H), 6.53 (dd, J = 8.3, 2.6 Hz, 1H), 5.17 (dd, J = 12.6, 5.5 Hz, 1H), 4.90 (s, 4H), 4.38 (d, J = 5.4 Hz, 1H), 3.62–3.42 (m, 7H), 3.12–2.97 (m, 2H), 2.93–2.82 (m, 1H), 2.81–2.67 (m, 2H), 2.23–2.04 (m, 4H), 1.88–1.80 (m, 3H), 1.76–1.58 (m, 3H), 1.57–1.41 (m, 4H).

2-(2,6-Dioxopiperidin-3-yl)-6-(5-(1-(4-((1R,2S)-6-hydroxy-2-phenyl-1,2,3,4-tetrahydronaphthalen-1-yl)phenyl)piperidin-4-yl)-pentyl)-6,7-dihydropyrrolo[3,4-*f*]isoindole-1,3(2H,5H)-dione (15). To a suspension of $\text{MeOCH}_2\text{PPh}_3\text{Cl}$ (353 mg, 3.5 equiv) in THF (10 mL) was added NaHDMS (1.0 M in THF, 881 μL , 3.0 equiv) at 0 $^\circ\text{C}$, and the mixture was stirred at 0 $^\circ\text{C}$ for 30 min. A solution of intermediate **50d** (120 mg, 0.8 equiv) in THF (2 mL) was added, and the reaction was kept stirred at 0 $^\circ\text{C}$ for 5 h, after which the reaction was quenched with aqueous NH_4Cl . The mixture was extracted with EA, washed with brine, dried over Na_2SO_4 , and concentrated to a dryness, which was purified by flash column chromatography (EtOAc/*n*-hexane = 0–15%) to give a pure colorless oil. The resulting product was dissolved in THF (4 mL), and then 12 N HCl (3 mL) was added at 0 and the reaction was stirred at $^\circ\text{C}$ for 5 min until UPLC–MS showed that the starting material was completely conversion to the desired product. The reaction was quenched with 20 mL aqueous saturated NaHCO_3 . The mixture was extracted with EA, washed with brine, dried over Na_2SO_4 , and concentrated to a dryness, which was purified by flash column chromatography (EtOAc/*n*-hexane = 0–20%) to afford compound **5-(1-(4-((1R,2S)-6-hydroxy-2-phenyl-1,2,3,4-tetrahydronaphthalen-1-yl)phenyl)piperidin-4-yl)pentanal (50e)** as a colorless oil (50 mg, yield = 57); UPLC–MS: 1.92 min; MS (ESI) m/z : calcd, 468.29 for $\text{C}_{32}\text{H}_{37}\text{NO}_2$ [$\text{M} + \text{H}$] $^+$; found, 468.41; $^1\text{H NMR}$ (400 MHz, CDCl_3): δ 9.77 (t, J = 1.8 Hz, 1H), 7.19–7.10 (m, 3H), 6.84–6.60 (m, 6H), 6.51 (dd, J = 8.3, 2.6 Hz, 1H), 6.31 (d, J = 8.1 Hz, 2H), 5.19 (s, 1H), 4.20 (d, J = 4.9 Hz, 1H), 3.52 (d, J = 12.0 Hz, 2H), 3.38–3.30 (m, 1H), 3.09–2.93 (m, 2H), 2.61 (s, 2H), 2.44 (td, J = 7.3, 1.8 Hz, 2H), 2.22–2.09 (m, 1H), 1.83–1.71 (m, 3H), 1.63 (p, J = 7.3 Hz, 3H), 1.40–1.29 (m, 6H).

To a suspension of TFA salt of compound **9a** (21.8 mg, 1.0 equiv) in DCE/DMF (4 mL/2 mL) was added intermediate **50e** (25 mg, 1.0 equiv), and the mixture was stirred at rt for 3.5 h. $\text{NaBH}(\text{OAc})_3$ (68 mg, 6 equiv) was then added into portion wise over 12 h, after which the reaction was kept stirring for another 24 h. The reaction mixture was concentrated under reduced pressure to remove most of the solvent DCE and purified by pre-HPLC (MeCN/ H_2O = 30–100% in 70 min) to provide the title compound **2-(2,6-dioxopiperidin-3-yl)-6-(5-(1-(4-((1R,2S)-6-hydroxy-2-phenyl-1,2,3,4-tetrahydronaphthalen-1-yl)phenyl)piperidin-4-yl)pentyl)-6,7-dihydropyrrolo[3,4-*f*]isoindole-1,3(2H,5H)-dione (15)** as a white solid (8.1 mg, yield = 20%); UPLC–MS: 1.62 min, purity >95%; MS (ESI) m/z : calcd, 751.39 for $\text{C}_{47}\text{H}_{50}\text{N}_4\text{O}_5$ [$\text{M} + \text{H}$] $^+$; found, 751.44; $^1\text{H NMR}$ (400 MHz, MeOD): δ 7.92 (s, 2H), 7.24 (d, J = 8.7 Hz, 2H), 7.18–7.07 (m, 3H), 6.84 (d, J = 9.1 Hz, 2H), 6.73–6.61 (m, 4H), 6.53 (dd, J = 8.3, 2.6 Hz, 1H), 5.17 (dd, J = 12.6, 5.4 Hz, 1H), 4.90 (s, 4H), 4.38 (d, J = 5.3 Hz, 1H), 3.61–3.40 (m, 7H), 3.12–2.97 (m, 2H), 2.95–2.82 (m, 1H), 2.81–2.66 (m, 2H), 2.23–2.01 (m, 4H), 1.92–1.79 (m, 3H), 1.76–1.57 (m, 3H), 1.54–1.36 (m, 6H).

2-(2,6-Dioxopiperidin-3-yl)-6-(6-(1-(4-((1R,2S)-6-hydroxy-2-phenyl-1,2,3,4-tetrahydronaphthalen-1-yl)phenyl)piperidin-4-yl)-hexyl)-6,7-dihydropyrrolo[3,4-*f*]isoindole-1,3(2H,5H)-dione (16). To a suspension of ((1,3-dioxolan-2-yl)methyl)triphenylphosphonium chloride (403 mg, 4.0 equiv) in THF (10 mL) was added *t*-BuOK (92 mg, 3.0 equiv) at 0 $^\circ\text{C}$, and the mixture was stirred at 0 $^\circ\text{C}$ for 30 min. A solution of intermediate **50d** (120 mg, 1.0 equiv) in THF (2 mL) was added dropwise, after which the reaction was kept stirred at 0 $^\circ\text{C}$ for 30 min. Then the reaction was quenched with aqueous NH_4Cl , and the mixture was extracted with EA, washed with brine, dried over Na_2SO_4 , and concentrated to a dryness, which was purified by flash column chromatography (*n*-hexane/EtOAc = 100:0 to 80:20) to give a pure colorless oil (130 mg). The resulting product was dissolved in MeOH/EtOAc (3 mL/3 mL), and the solution was degassed and purged with N_2 , after which Pd/C (20% Pd, 65 mg) was added, and the result reaction mixture was stirred under a H_2 atmosphere until UPLC–

MS indicated that the starting material was completely consumed. Next, the reaction mixture was filtered, and the filtration was concentrated to give a crude product, which was treated with TFA (containing 2% H_2O) for 30 min until completely conversion as monitored by UPLC–MS. The reaction mixture was concentrated under reduced pressure to give a crude mixture, which was dissolved in EA, washed with aqueous NaHCO_3 and brine, dried over Na_2SO_4 , and purified by flash column chromatography to afford compound **6-(1-(4-((1R,2S)-6-hydroxy-2-phenyl-1,2,3,4-tetrahydronaphthalen-1-yl)phenyl)piperidin-4-yl)-hexanal (50f)** as a white solid (60 mg, yield = 53); UPLC–MS: 2.05 min; MS (ESI) m/z : calcd, 482.31 for $\text{C}_{33}\text{H}_{39}\text{NO}_2$ [$\text{M} + \text{H}$] $^+$; found, 482.40; $^1\text{H NMR}$ (400 MHz, CDCl_3): δ 9.76 (t, J = 1.7 Hz, 1H), 7.22–7.08 (m, 5H), 6.80–6.67 (m, 4H), 6.59 (dd, J = 8.3, 2.6 Hz, 1H), 6.52 (d, J = 8.5 Hz, 2H), 4.29 (d, J = 5.4 Hz, 1H), 3.64 (d, J = 12.7 Hz, 2H), 3.47–3.37 (m, 1H), 3.21–3.08 (m, 2H), 3.07–2.97 (m, 2H), 2.44 (td, J = 7.2, 1.7 Hz, 2H), 2.11–1.98 (m, 1H), 1.98–1.79 (m, 5H), 1.70–1.58 (m, 2H), 1.58–1.47 (m, 1H), 1.39–1.26 (m, 6H).

To a suspension of TFA salt of compound **9a** (21.2 mg, 1.0 equiv) in DCE/DMF (4 mL/2 mL) was added intermediate **50f** (25 mg, 1.0 equiv), and the mixture was stirred at rt for 3.5 h. $\text{NaBH}(\text{OAc})_3$ (66 mg, 6 equiv) was then added into portion wise over 12 h, after which the reaction was kept stirring for another 24 h. The reaction mixture was concentrated under reduced pressure to remove most of the solvent DCE and purified by pre-HPLC (MeCN/ H_2O = 30–100% in 70 min) to afford the title compound **2-(2,6-dioxopiperidin-3-yl)-6-(6-(1-(4-((1R,2S)-6-hydroxy-2-phenyl-1,2,3,4-tetrahydronaphthalen-1-yl)phenyl)piperidin-4-yl)hexyl)-6,7-dihydropyrrolo[3,4-*f*]isoindole-1,3(2H,5H)-dione (16)** as a white solid (20.6 mg, yield = 52%); UPLC–MS: 1.69 min, purity >95%; MS (ESI) m/z : calcd, 765.40 for $\text{C}_{48}\text{H}_{52}\text{N}_4\text{O}_5$ [$\text{M} + \text{H}$] $^+$; found, 765.42; $^1\text{H NMR}$ (400 MHz, MeOD): δ 7.93 (s, 2H), 7.24 (d, J = 8.8 Hz, 2H), 7.13 (d, J = 7.2 Hz, 3H), 6.88–6.79 (m, 2H), 6.72–6.62 (m, 4H), 6.53 (dd, J = 8.3, 2.6 Hz, 1H), 5.17 (dd, J = 12.6, 5.4 Hz, 1H), 4.90 (s, 4H), 4.39 (d, J = 5.3 Hz, 1H), 3.61–3.41 (m, 7H), 3.12–2.97 (m, 2H), 2.94–2.82 (m, 1H), 2.81–2.67 (m, 2H), 2.23–2.11 (m, 2H), 2.11–2.01 (m, 2H), 1.90–1.78 (m, 3H), 1.77–1.55 (m, 3H), 1.54–1.33 (m, 8H).

2-(2,6-Dioxopiperidin-3-yl)-6-(1-(4-((1R,2S)-6-hydroxy-2-phenyl-1,2,3,4-tetrahydronaphthalen-1-yl)phenyl)piperidin-4-yl)-methyl)azetidin-3-yl)-6,7-dihydropyrrolo[3,4-*f*]isoindole-1,3(2H,5H)-dione (17). Intermediate **6-(azetidin-3-yl)-2-(2,6-dioxopiperidin-3-yl)-6,7-dihydropyrrolo[3,4-*f*]isoindole-1,3(2H,5H)-dione (51a)** was synthesized using a similar procedure for the preparation of intermediate **51c**, and it was obtained as a white solid (31% yield from **9a**); UPLC–MS: 0.91 min; MS (ESI) m/z : calcd, 355.14 for $\text{C}_{18}\text{H}_{18}\text{N}_4\text{O}_4$ [$\text{M} + \text{H}$] $^+$; found, 355.29; $^1\text{H NMR}$ (400 MHz, MeOD): δ 7.78 (s, 2H), 5.14 (dd, J = 12.6, 5.5 Hz, 1H), 4.26 (dd, J = 11.6, 7.3 Hz, 2H), 4.20–4.10 (m, 6H), 4.03–3.95 (m, 1H), 2.93–2.82 (m, 1H), 2.80–2.66 (m, 2H), 2.19–2.10 (m, 1H).

The title compound **17** was prepared from intermediates **50a** and **51a** using a similar procedure for producing **21** from intermediates **50g** and **51c**, and it was afforded as a white solid (59% yield); UPLC–MS: 1.68 min, purity >95%; MS (ESI) m/z : calcd, 750.37 for $\text{C}_{46}\text{H}_{47}\text{N}_5\text{O}_5$ [$\text{M} + \text{H}$] $^+$; found, 750.37; $^1\text{H NMR}$ (400 MHz, MeCN- d_3): δ 9.08 (s, 1H), 7.87 (s, 2H), 7.28–7.20 (m, 5H), 6.96–6.89 (m, 2H), 6.83–6.77 (m, 2H), 6.71–6.63 (m, 3H), 5.12 (dd, J = 12.4, 5.3 Hz, 1H), 4.68–4.29 (m, 8H), 4.22 (p, J = 6.4 Hz, 1H), 3.62 (d, J = 11.7 Hz, 2H), 3.56–3.49 (m, 1H), 3.47–3.25 (m, 4H), 3.22–3.05 (m, 2H), 2.93–2.74 (m, 3H), 2.31–2.19 (m, 2H), 2.18–2.06 (m, 3H), 2.02–1.80 (m, 4H).

2-(2,6-Dioxopiperidin-3-yl)-6-(1-(4-((1R,2S)-6-hydroxy-2-phenyl-1,2,3,4-tetrahydronaphthalen-1-yl)phenyl)piperidin-4-yl)-methyl)azetidin-3-yl)methyl)-6,7-dihydropyrrolo[3,4-*f*]isoindole-1,3(2H,5H)-dione (18). Intermediate **6-(azetidin-3-ylmethyl)-2-(2,6-dioxopiperidin-3-yl)-6,7-dihydropyrrolo[3,4-*f*]isoindole-1,3(2H,5H)-dione (51b)** was synthesized using a similar procedure for the preparation of intermediate **51c**, and it was obtained as a white solid (42% yield from **9a**). UPLC–MS: 0.75 min; MS (ESI) m/z : calcd, 369.16 for $\text{C}_{19}\text{H}_{20}\text{N}_4\text{O}_4$ [$\text{M} + \text{H}$] $^+$; found, 369.31; $^1\text{H NMR}$ (400 MHz, MeOD): δ 7.91 (s, 2H), 5.16 (dd, J = 12.7, 5.4 Hz, 1H), 4.81 (s, 4H), 4.30–4.21 (m, 2H), 4.14–4.05 (m, 2H), 3.76 (d, J = 7.2 Hz, 2H),

3.58–3.45 (m, 1H), 2.94–2.82 (m, 1H), 2.81–2.66 (m, 2H), 2.21–2.10 (m, 1H).

The title compound **18** was prepared from intermediates **50a** and **51b** using a similar procedure for producing **21** from intermediates **50g** and **51c**, and it was afforded as a white solid. UPLC–MS: 1.50 min, purity >95%; MS (ESI) m/z : calcd, 764.38 for $C_{47}H_{49}N_5O_5$ $[M + H]^+$; found, 764.4; 1H NMR (400 MHz, MeOD): δ 7.90 (s, 2H), 7.16–7.09 (m, 5H), 6.86–6.81 (m, 2H), 6.70–6.65 (m, 2H), 6.59 (d, J = 8.7 Hz, 2H), 6.53 (dd, J = 8.3, 2.6 Hz, 1H), 5.16 (dd, J = 12.6, 5.4 Hz, 1H), 4.75 (s, 4H), 4.50–4.32 (m, 3H), 4.30–4.13 (m, 2H), 3.73 (d, J = 7.0 Hz, 2H), 3.62 (d, J = 12.0 Hz, 2H), 3.53–3.32 (m, 6H), 3.12–2.99 (m, 2H), 2.94–2.82 (m, 1H), 2.81–2.67 (m, 2H), 2.23–2.01 (m, 5H), 1.87–1.64 (m, 3H).

2-(2,6-Dioxopiperidin-3-yl)-6-(1-((1-(4-((1R,2S)-6-hydroxy-2-phenyl-1,2,3,4-tetrahydronaphthalen-1-yl)phenyl)piperidin-4-yl)methyl)piperidin-4-yl)-6,7-dihydropyrrolo[3,4-f]isoindole-1,3-(2H,5H)-dione (19). The title compound **19** was prepared from intermediates **50a** and **51c** using a similar procedure for producing **21** from intermediates **50g** and **51c**, and it was afforded as a white solid. UPLC–MS: 2.69 min, purity >95%; MS (ESI) m/z : calcd, 778.40 for $C_{48}H_{51}N_5O_5$ $[M + H]^+$; found, 778.28; 1H NMR (400 MHz, MeOD): δ 7.90 (s, 2H), 7.18–7.09 (m, 5H), 6.83 (dd, J = 7.4, 1.7 Hz, 2H), 6.71–6.64 (m, 2H), 6.61 (d, J = 8.7 Hz, 2H), 6.53 (dd, J = 8.3, 2.6 Hz, 1H), 5.16 (dd, J = 12.6, 5.4 Hz, 1H), 4.79 (s, 4H), 4.36 (d, J = 5.3 Hz, 1H), 3.87–3.57 (m, 5H), 3.50–3.36 (m, 3H), 3.26–2.97 (m, 6H), 2.93–2.81 (m, 1H), 2.81–2.66 (m, 2H), 2.55–2.39 (m, 2H), 2.36–2.04 (m, 7H), 1.87–1.67 (m, 3H).

2-(2,6-Dioxopiperidin-3-yl)-6-(1-((1-(4-((1R,2S)-6-hydroxy-2-phenyl-1,2,3,4-tetrahydronaphthalen-1-yl)phenyl)piperidin-4-yl)methyl)piperidin-4-yl)methyl)-6,7-dihydropyrrolo[3,4-f]isoindole-1,3-(2H,5H)-dione (20). Intermediate **2-(2,6-dioxopiperidin-3-yl)-6-(piperidin-4-ylmethyl)-6,7-dihydropyrrolo[3,4-f]isoindole-1,3-(2H,5H)-dione (51d)** was synthesized using a similar procedure for the preparation of intermediate **51c**, and it was obtained as a dark solid (83% yield from **9a**). UPLC–MS: 0.78 min; MS (ESI) m/z : calcd, 397.19 for $C_{21}H_{24}N_4O_4$ $[M + H]^+$; found, 397.37; 1H NMR (400 MHz, MeOD): δ 7.12 (s, 2H), 4.36 (dd, J = 12.6, 5.5 Hz, 1H), 4.13 (s, 4H), 2.68 (d, J = 7.0 Hz, 4H), 2.28 (td, J = 12.9, 2.6 Hz, 2H), 2.14–2.01 (m, 1H), 2.00–1.86 (m, 2H), 1.55–1.43 (m, 1H), 1.40–1.27 (m, 3H), 0.86–0.72 (m, 2H).

The title compound **20** was prepared from intermediates **50a** and **51d** using a similar procedure for producing **21** from intermediates **50g** and **51c**, and it was afforded as a white solid. UPLC–MS: 1.49 min, purity >95%; MS (ESI) m/z : calcd, 792.41 for $C_{49}H_{53}N_5O_5$ $[M + H]^+$; found, 792.5; 1H NMR (400 MHz, MeOD): δ 7.93 (s, 2H), 7.20 (d, J = 8.8 Hz, 2H), 7.17–7.09 (m, 3H), 6.84 (dd, J = 7.5, 1.7 Hz, 2H), 6.72–6.60 (m, 4H), 6.53 (dd, J = 8.3, 2.6 Hz, 1H), 5.17 (dd, J = 12.6, 5.4 Hz, 1H), 4.94 (s, 4H), 4.37 (d, J = 5.3 Hz, 1H), 3.82–3.58 (m, 4H), 3.56–3.41 (m, 5H), 3.24–2.97 (m, 6H), 2.94–2.66 (m, 3H), 2.41–2.10 (m, 8H), 1.88–1.70 (m, 5H).

2-(2,6-Dioxopiperidin-3-yl)-6-(1-((1-(4-((1R,2S)-6-hydroxy-2-phenyl-1,2,3,4-tetrahydronaphthalen-1-yl)phenyl)azetidide-3-yl)methyl)piperidin-4-yl)-6,7-dihydropyrrolo[3,4-f]isoindole-1,3-(2H,5H)-dione (21). A mixture of intermediate **48** (500 mg, 1.0 equiv), methyl azetidide-3-carboxylate hydrochloride (232 mg, 2.0 equiv), Pd(OAc)₂ (34 mg, 0.2 equiv), BINAP (143 mg, 0.3 equiv), and Cs₂CO₃ (996 mg, 4.0 equiv) in toluene (15 mL) was degassed and purged with 3 times N₂, and the reaction was stirred at 100 °C under a N₂ atmosphere for 16 h. After cooling to rt, the reaction mixture was diluted with DCM and filtered through Celite to remove insoluble catalyst and salts, and the filter cake was washed with DCM. The resulting filtration was concentrated to dryness, which was purified by flash column chromatography (*n*-hexane/EtOAc = 100:0 to 85:15) to provide compound methyl 1-(4-((1R,2S)-6-(*tert*-butoxy)-2-phenyl-1,2,3,4-tetrahydronaphthalen-1-yl)phenyl)azetidide-3-carboxylate (**49e**) as a light yellow oil (286 mg, yield = 80%); UPLC–MS (ESI) m/z : calcd, 470.27 for $C_{31}H_{35}NO_3$ $[M + H]^+$; found, 470.65; 1H NMR (400 MHz, CDCl₃): δ 7.23–7.07 (m, 3H), 6.94–6.67 (m, 6H), 6.50–6.24 (m, 3H), 4.36–3.90 (m, 5H), 3.78–3.52 (m, 4H), 3.48–3.32 (m, 1H), 3.15–2.95 (m, 2H), 2.22–2.06 (m, 1H), 1.89–1.76 (m, 1H), 1.37 (d, 9H).

A solution of compound **49e** (250 mg, 1.0 equiv) in DCM (10 mL) was degassed and purged with 3 times N₂ and then cooled down to –78 °C. DIBAL-H (25% in toluene, 608 μ L, 1.7 equiv) was added dropwise under a N₂ atmosphere over 30 min, and the reaction was stirred for 1 h. After that, the reaction was quenched with 8 mL of aqueous potassium sodium tartrate solution. The resulting mixture was warmed to rt and kept stirring until it became clear, which was subsequently extracted with DCM, washed with brine, dried over Na₂SO₄, and purified by flash column chromatography (*n*-hexane/EtOAc = 100:0 to 70:30) to afford compound 1-(4-((1R,2S)-6-(*tert*-butoxy)-2-phenyl-1,2,3,4-tetrahydronaphthalen-1-yl)phenyl)azetidide-3-carbaldehyde (**50g**) as a white solid (200 mg, yield = 85%); UPLC–MS (ESI) m/z : calcd, 440.26 for $C_{30}H_{33}NO_2$ $[M + H]^+$; found, 440.41; 1H NMR (400 MHz, DMSO-*d*₆): δ 9.79 (d, J = 2.0 Hz, 1H), 7.21–7.06 (m, 3H), 6.87–6.79 (m, 3H), 6.74 (d, J = 8.4 Hz, 1H), 6.67 (dd, J = 8.3, 2.4 Hz, 1H), 6.19 (d, J = 8.5 Hz, 2H), 6.09 (d, J = 8.6 Hz, 2H), 4.19 (d, J = 4.9 Hz, 1H), 3.85–3.74 (m, 4H), 3.52–3.43 (m, 1H), 3.42–3.27 (m, 2H), 3.10–2.89 (m, 2H), 2.11 (tq, J = 12.8, 6.2 Hz, 1H), 1.72 (dd, J = 12.2, 6.0 Hz, 1H), 1.29 (s, 9H).

To a suspension of TFA salt of compound **9a** (300 mg, 1.0 equiv) in DMF (5 mL) was added *tert*-butyl 4-oxopiperidine-1-carboxylate (174 mg, 1.0 equiv), and the mixture was stirred at rt for 12 h. NaBH(OAc)₃ (462 mg, 3.0 equiv) was then added into portion wise over 6 h, after which the reaction was kept stirring for another 12 h. The reaction mixture directly purified by pre-HPLC (MeCN/H₂O = 15–100% in 85 min) to afford a pure product. The resulting product was treated with TFA/DCM (2 mL/4 mL) at rt for 20 min, and then the solution was concentrated to a dryness, which was further lyophilized to give compound 2-(2,6-dioxopiperidin-3-yl)-6-(piperidin-4-yl)-6,7-dihydropyrrolo[3,4-f]isoindole-1,3-(2H,5H)-dione (**51c**) as a white solid (346 mg, yield = 96%); UPLC–MS (ESI) m/z : calcd, 383.17 for $C_{20}H_{22}N_4O_4$ $[M + H]^+$; found, 383.10; 1H NMR (400 MHz, MeOD): δ 7.91 (s, 2H), 5.17 (dd, J = 12.6, 5.4 Hz, 1H), 4.83 (s, 4H), 3.75–3.56 (m, 3H), 3.15 (td, J = 12.9, 2.6 Hz, 2H), 2.95–2.82 (m, 1H), 2.81–2.66 (m, 2H), 2.47 (d, J = 13.7 Hz, 2H), 2.19–2.11 (m, 1H), 2.10–1.96 (m, 2H).

To a suspension of TFA salt of compound **51c** (30 mg, 1.0 equiv) in DCE/DMF (4 mL/2 mL) was added intermediate **50g** (32 mg, 1.2 equiv), and the mixture was stirred at rt for 6 h. NaBH(OAc)₃ (38 mg, 3.0 equiv) was then added into portions over 12 h, after which the reaction was kept stirring for another 12 h. The reaction mixture was concentrated under reduced pressure to remove most of the solvent DCE and purified by pre-HPLC (MeCN/H₂O = 35–100% in 65 min) to afford a pure product. The resulting product was treated with TFA/DCM (2 mL/4 mL) at rt for 3–4 h. Then the solution was concentrated to a dryness, which was further lyophilized to give the title compound 2-(2,6-dioxopiperidin-3-yl)-6-(1-((1-(4-((1R,2S)-6-hydroxy-2-phenyl-1,2,3,4-tetrahydronaphthalen-1-yl)phenyl)azetidide-3-yl)methyl)piperidin-4-yl)-6,7-dihydropyrrolo[3,4-f]isoindole-1,3-(2H,5H)-dione (**21**) as a white solid (35 mg, yield = 77%); UPLC–MS: 1.72 min, purity >95%; MS (ESI) m/z : calcd, 750.37 for $C_{46}H_{47}N_5O_5$ $[M + H]^+$; found, 750.44; 1H NMR (400 MHz, Acetone-*d*₆): δ 9.91 (s, 1H), 7.91 (s, 2H), 7.17–7.09 (m, 3H), 6.85 (dd, J = 7.6, 1.6 Hz, 2H), 6.72–6.67 (m, 2H), 6.57 (dd, J = 8.3, 2.5 Hz, 1H), 6.26 (d, J = 8.5 Hz, 2H), 6.07 (d, J = 8.6 Hz, 2H), 5.16 (dd, J = 12.6, 5.4 Hz, 1H), 4.98 (s, 4H), 4.17 (d, J = 5.0 Hz, 1H), 4.03–3.68 (m, 5H), 3.62–3.48 (m, 4H), 3.42–3.22 (m, 4H), 3.08–2.89 (m, 3H), 2.86–2.71 (m, 2H), 2.57–2.36 (m, 4H), 2.30–2.12 (m, 2H), 1.78–1.71 (m, 1H).

2-(2,6-Dioxopiperidin-3-yl)-6-(1-((1-(4-((1R,2S)-6-hydroxy-2-phenyl-1,2,3,4-tetrahydronaphthalen-1-yl)phenyl)azetidide-3-yl)methyl)piperidin-4-yl)methyl)-6,7-dihydropyrrolo[3,4-f]isoindole-1,3-(2H,5H)-dione (22). The title compound **22** was prepared from intermediates **50g** and **51d** using a similar procedure for producing **21** from intermediates **50g** and **51c**, and it was afforded as a light-yellow solid (67% yield). UPLC–MS: 1.55 min, purity >95%; MS (ESI) m/z : calcd, 764.38 for $C_{47}H_{49}N_5O_5$ $[M + H]^+$; found, 764.44; 1H NMR (400 MHz, MeOD): δ 7.93 (s, 2H), 7.14–7.07 (m, 3H), 6.83–6.78 (m, 2H), 6.70–6.63 (m, 2H), 6.51 (dd, J = 8.3, 2.6 Hz, 1H), 6.29 (d, J = 8.6 Hz, 2H), 6.19 (d, J = 8.6 Hz, 2H), 5.17 (dd, J = 12.6, 5.4 Hz, 1H), 4.93 (s, 4H), 4.18 (d, J = 4.9 Hz, 1H), 4.07–3.96 (m, 2H), 3.68–3.40 (m, 8H),

3.25–2.81 (m, 7H), 2.80–2.67 (m, 2H), 2.33–2.09 (m, 5H), 1.81–1.61 (m, 3H).

2-(2,6-Dioxopiperidin-3-yl)-6-((1-(1-(4-((1R,2S)-6-hydroxy-2-phenyl-1,2,3,4-tetrahydronaphthalen-1-yl)phenyl)piperidine-4-carbonyl)azetid-3-yl)methyl)-6,7-dihydropyrrolo[3,4-f]isoindole-1,3(2H,5H)-dione (23). A mixture of intermediate **48** (300 mg, 1.0 equiv), *tert*-butyl piperidine-4-carboxylate (170 mg, 2.0 equiv), Pd(OAc)₂ (20.6 mg, 0.2 equiv), XPhos (65.5 mg, 0.3 equiv), and *t*-BuONa (176 mg, 4.0 equiv) in toluene (10 mL) was degassed and purged with 3 times N₂ and then stirred at 90 °C under a N₂ atmosphere for 10 h. The mixture was cooled, diluted with DCM, and filtered through Celite to remove insoluble catalyst and salts, and the filter cake was washed with DCM. The filtrate was concentrated under reduced pressure. The residue was purified by flash column chromatography (*n*-hexane/EtOAc = 100:0 to 90:10). The resulting pure product was treated with TFA at rt for 6 h, after which the solvent was removed and the residue was lyophilized to give compound **1-(4-((1R,2S)-6-hydroxy-2-phenyl-1,2,3,4-tetrahydronaphthalen-1-yl)phenyl)piperidine-4-carboxylic acid (54a)** as a white solid (192 mg, yield = 98%); UPLC–MS (ESI) *m/z*: calcd, 428.22 for C₂₈H₂₉NO₃ [M + H]⁺; found, 428.36; ¹H NMR (400 MHz, DMSO-*d*₆): δ 7.29–7.10 (m, 4H), 7.02–6.78 (m, 4H), 6.71–6.60 (m, 2H), 6.49 (dd, *J* = 8.3, 2.5 Hz, 1H), 6.37 (d, *J* = 7.4 Hz, 2H), 4.23 (d, *J* = 4.8 Hz, 1H), 3.53–3.41 (m, 2H), 3.38–3.28 (m, 1H), 3.09–2.85 (m, 3H), 2.49–2.39 (m, 1H), 2.06 (td, *J* = 12.6, 11.5, 6.2 Hz, 1H), 2.01–1.89 (m, 2H), 1.81–1.63 (m, 3H).

To a solution of intermediate **54a** (36 mg, 1.2 equiv) and HATU (26 mg, 1.1 equiv) in DMF (2 mL) was added DIPEA (65 μL, 6.0 equiv). 10 min later, **51b** (30 mg, 1.0 equiv) was added, and the reaction was stirred at rt for 10 min. Then the crude mixture was directly purified by pre-HPLC (25–100% MeCN/H₂O in 75 min) to give title compound **2-(2,6-dioxopiperidin-3-yl)-6-((1-(1-(4-((1R,2S)-6-hydroxy-2-phenyl-1,2,3,4-tetrahydronaphthalen-1-yl)phenyl)piperidine-4-carbonyl)azetid-3-yl)methyl)-6,7-dihydropyrrolo[3,4-f]isoindole-1,3(2H,5H)-dione (23)** as a white solid (40 mg, 83% yield); UPLC–MS: 1.44 min, purity >95%; MS (ESI) *m/z*: calcd, 778.36 for C₄₇H₄₇N₅O₆ [M + H]⁺; found, 778.41; ¹H NMR (400 MHz, MeOD): δ 7.93 (s, 2H), 7.21 (d, *J* = 8.8 Hz, 2H), 7.18–7.09 (m, 3H), 6.87–6.81 (m, 2H), 6.71–6.62 (m, 4H), 6.53 (dd, *J* = 8.3, 2.6 Hz, 1H), 5.17 (dd, *J* = 12.6, 5.4 Hz, 1H), 4.90 (s, 4H), 4.54 (t, *J* = 8.7 Hz, 1H), 4.38 (d, *J* = 5.3 Hz, 1H), 4.28–4.16 (m, 2H), 3.89 (dd, *J* = 10.2, 5.8 Hz, 1H), 3.83 (d, *J* = 7.3 Hz, 2H), 3.73–3.62 (m, 2H), 3.60–3.42 (m, 3H), 3.30–3.21 (m, 1H), 3.12–2.98 (m, 2H), 2.94–2.82 (m, 1H), 2.81–2.66 (m, 3H), 2.23–2.04 (m, 6H), 1.89–1.78 (m, 1H).

2-(2,6-Dioxopiperidin-3-yl)-6-((1-(1-(4-((1R,2S)-6-hydroxy-2-phenyl-1,2,3,4-tetrahydronaphthalen-1-yl)phenyl)piperidine-4-carbonyl)piperidin-4-yl)-6,7-dihydropyrrolo[3,4-f]isoindole-1,3(2H,5H)-dione (24). Compound **24** was produced using a similar procedure for the preparation of compound **23**. White solid; UPLC–MS: 1.50 min, purity >95%; MS (ESI) *m/z*: calcd, 792.38 for C₄₈H₄₉N₅O₆ [M + H]⁺; found, 792.4; ¹H NMR (400 MHz, MeOD): δ 7.93 (s, 2H), 7.24 (d, *J* = 8.8 Hz, 2H), 7.18–7.08 (m, 3H), 6.84 (dd, *J* = 7.5, 1.7 Hz, 2H), 6.72–6.63 (m, 4H), 6.53 (dd, *J* = 8.3, 2.6 Hz, 1H), 5.17 (dd, *J* = 12.6, 5.4 Hz, 1H), 4.95 (s, 4H), 4.74 (d, *J* = 13.4 Hz, 1H), 4.39 (d, *J* = 5.4 Hz, 1H), 4.29 (d, *J* = 15.2 Hz, 1H), 3.87–3.76 (m, 1H), 3.72–3.53 (m, 4H), 3.50–3.41 (m, 1H), 3.30–3.15 (m, 2H), 3.13–2.96 (m, 2H), 2.94–2.82 (m, 1H), 2.81–2.66 (m, 3H), 2.34 (t, *J* = 15.0 Hz, 2H), 2.23–2.05 (m, 6H), 1.88–1.61 (m, 3H).

2-(2,6-Dioxopiperidin-3-yl)-6-((1-(1-(4-((1R,2S)-6-hydroxy-2-phenyl-1,2,3,4-tetrahydronaphthalen-1-yl)phenyl)piperidine-4-carbonyl)piperidin-4-yl)methyl)-6,7-dihydropyrrolo[3,4-f]isoindole-1,3(2H,5H)-dione (25). Compound **25** was synthesized using a similar procedure with the preparation of compound **23**. White solid; UPLC–MS: 1.51 min, purity >95%; MS (ESI) *m/z*: calcd, 806.39 for C₄₉H₅₁N₅O₆ [M + H]⁺; found, 806.4; ¹H NMR (400 MHz, MeOD): δ 7.94 (s, 2H), 7.21 (d, *J* = 8.8 Hz, 2H), 7.18–7.08 (m, 3H), 6.84 (dd, *J* = 7.5, 1.7 Hz, 2H), 6.72–6.62 (m, 4H), 6.53 (dd, *J* = 8.3, 2.6 Hz, 1H), 5.17 (dd, *J* = 12.6, 5.4 Hz, 1H), 4.94 (s, 4H), 4.62 (d, *J* = 13.3 Hz, 1H), 4.39 (d, *J* = 5.4 Hz, 1H), 4.17 (d, *J* = 14.1 Hz, 1H), 3.71–3.51 (m, 4H), 3.49–3.42 (m, 3H), 3.29–2.98 (m, 4H), 2.94–2.82 (m, 1H), 2.81–2.66 (m, 3H), 2.31–2.05 (m, 7H), 1.97 (dd, *J* = 26.5, 12.3 Hz, 2H), 1.84 (dd, *J* = 14.2, 3.7 Hz, 1H), 1.39–1.24 (m, 2H).

2-(2,6-Dioxopiperidin-3-yl)-6-((1-(1-(4-((1R,2S)-6-hydroxy-2-phenyl-1,2,3,4-tetrahydronaphthalen-1-yl)phenyl)piperidin-4-yl)-methyl)piperidine-4-carbonyl)-6,7-dihydropyrrolo[3,4-f]isoindole-1,3(2H,5H)-dione (26). To a solution of 1-(*tert*-butoxycarbonyl)-piperidine-4-carboxylic acid (117 mg, 1.4 equiv) and HATU (179 mg, 1.3 equiv) in DMF (2 mL) was added DIPEA (253 μL, 4.0 equiv), followed by **9a** (150 mg, 1.0 equiv), and the reaction was stirred at rt for 10 min. Then the crude mixture was directly purified by pre-HPLC (30–100% MeCN/H₂O in 70 min) to provide a pure product, which was further treated with TFA at rt for 15 min to remove the Boc group. After concentration to remove TFA and lyophilization, compound **2-(2,6-dioxopiperidin-3-yl)-6-((1-(1-(4-((1R,2S)-6-hydroxy-2-phenyl-1,2,3,4-tetrahydronaphthalen-1-yl)phenyl)piperidin-4-yl)-methyl)piperidine-4-carbonyl)-6,7-dihydropyrrolo[3,4-f]isoindole-1,3(2H,5H)-dione (51e)** was obtained as a white solid (102 mg, yield = 37%); UPLC–MS: 0.55 min; MS (ESI) *m/z*: calcd, 411.17 for C₂₁H₂₂N₄O₅ [M + H]⁺; found, 411.06; ¹H NMR (400 MHz, DMSO-*d*₆): δ 11.12 (s, 1H), 8.61–8.48 (m, 1H), 8.42–8.23 (m, 1H), 7.94 (s, 1H), 7.89 (s, 1H), 5.16 (dd, *J* = 12.9, 5.4 Hz, 1H), 5.07 (s, 2H), 4.78 (s, 2H), 3.35 (d, *J* = 12.6 Hz, 2H), 3.06–2.82 (m, 4H), 2.65–2.52 (m, 2H), 2.12–2.03 (m, 1H), 1.98–1.88 (m, 2H), 1.85–1.71 (m, 2H).

The title compound **26** was prepared from intermediates **50a** and **51e** using a similar procedure for producing **21** from intermediates **50g** and **51c**, and it was afforded as a white solid (52% yield). UPLC–MS: 1.59 min, purity >95%; MS (ESI) *m/z*: calcd, 806.39 for C₄₉H₅₁N₅O₆ [M + H]⁺; found, 806.46; ¹H NMR (400 MHz, MeOD): δ 7.86 (d, *J* = 15.5 Hz, 2H), 7.18–7.07 (m, 5H), 6.83 (dd, *J* = 7.5, 1.8 Hz, 2H), 6.71–6.64 (m, 2H), 6.59 (d, *J* = 8.7 Hz, 2H), 6.53 (dd, *J* = 8.3, 2.6 Hz, 1H), 5.21–5.09 (m, 3H), 4.90 (s, 2H), 4.35 (d, *J* = 5.3 Hz, 1H), 3.83–3.60 (m, 4H), 3.47–3.33 (m, 3H), 3.27–2.94 (m, 7H), 2.94–2.67 (m, 3H), 2.37–2.04 (m, 9H), 1.88–1.66 (m, 3H).

2-(2,6-Dioxopiperidin-3-yl)-6-((1-(1-(4-((1R,2S)-6-hydroxy-2-phenyl-1,2,3,4-tetrahydronaphthalen-1-yl)phenyl)azetid-3-carbonyl)piperidin-4-yl)methyl)-6,7-dihydropyrrolo[3,4-f]isoindole-1,3(2H,5H)-dione (27). Compound **27** was synthesized using a similar procedure for the preparation of compound **23**. White solid; UPLC–MS: 1.82 min, purity >95%; MS (ESI) *m/z*: calcd, 778.36 for C₄₇H₄₇N₅O₆ [M + H]⁺; found, 778.5; ¹H NMR (400 MHz, MeOD): δ 7.93 (s, 2H), 7.17–7.07 (m, 3H), 6.85–6.78 (m, 2H), 6.70–6.64 (m, 2H), 6.56–6.48 (m, 3H), 6.40 (d, *J* = 8.5 Hz, 2H), 5.17 (dd, *J* = 12.6, 5.4 Hz, 1H), 4.93 (s, 4H), 4.59 (d, *J* = 13.0 Hz, 1H), 4.30–4.08 (m, 5H), 3.92 (p, *J* = 7.4 Hz, 1H), 3.79 (d, *J* = 14.3 Hz, 1H), 3.45 (d, *J* = 7.1 Hz, 2H), 3.38–3.33 (m, 1H), 3.23–3.14 (m, 1H), 3.09–2.96 (m, 2H), 2.94–2.67 (m, 4H), 2.28–2.11 (m, 3H), 1.95–1.86 (m, 2H), 1.82–1.73 (m, 1H), 1.38–1.22 (m, 2H).

2-(2,6-Dioxopiperidin-3-yl)-6-((1-(1-(4-((1R,2S)-6-hydroxy-2-phenyl-1,2,3,4-tetrahydronaphthalen-1-yl)phenyl)azetid-3-yl)-methyl)piperidine-4-carbonyl)-6,7-dihydropyrrolo[3,4-f]isoindole-1,3(2H,5H)-dione (28). The title compound **28** was prepared from intermediates **50g** and **51e** by a similar procedure for producing **21** from intermediates **50g** and **51c**, and it was afforded as a white solid (88% yield). UPLC–MS: 1.77 min, purity >95%; MS (ESI) *m/z*: calcd, 778.36 for C₄₇H₄₇N₅O₆ [M + H]⁺; found, 778.41; ¹H NMR (400 MHz, MeOD): δ 7.85 (d, *J* = 16.6 Hz, 2H), 7.16–7.06 (m, 3H), 6.80 (dd, *J* = 7.4, 1.9 Hz, 2H), 6.71–6.62 (m, 2H), 6.51 (dd, *J* = 8.3, 2.6 Hz, 1H), 6.29 (d, *J* = 8.5 Hz, 2H), 6.20 (d, *J* = 8.6 Hz, 2H), 5.20–5.09 (m, 3H), 4.89 (s, 2H), 4.18 (d, *J* = 4.9 Hz, 1H), 4.07–3.98 (m, 2H), 3.67–3.52 (m, 4H), 3.47 (d, *J* = 7.4 Hz, 2H), 3.30–3.27 (m, 1H), 3.24–3.04 (m, 3H), 3.04–2.81 (m, 4H), 2.81–2.66 (m, 2H), 2.27–1.89 (m, 6H), 1.84–1.72 (m, 1H).

2-(2,6-Dioxopiperidin-3-yl)-6-((2-(6-(4-((1R,2S)-6-hydroxy-2-phenyl-1,2,3,4-tetrahydronaphthalen-1-yl)phenyl)-2,6-diazaspiro[3.3]heptan-2-yl)-2-oxoethyl)-6,7-dihydropyrrolo[3,4-f]isoindole-1,3(2H,5H)-dione (29). Compound **29** was synthesized using a similar procedure for the preparation of compound **36**. White solid; UPLC–MS: 1.80 min, purity >95%; MS (ESI) *m/z*: calcd, 736.31 for C₄₄H₄₁N₅O₆ [M + H]⁺; found, 736.40; ¹H NMR (400 MHz, MeOD): δ 7.92 (d, *J* = 3.9 Hz, 2H), 7.15–7.07 (m, 3H), 6.85–6.77 (m, 2H), 6.70–6.62 (m, 2H), 6.53–6.45 (m, 1H), 6.39–6.24 (m, 4H), 5.16 (dd, *J* = 12.6, 5.4 Hz, 1H), 4.93 (s, 4H), 4.46–3.96 (m, 10H), 3.34 (s, 1H), 3.08–2.96 (m, 2H), 2.93–2.66 (m, 4H), 2.27–2.10 (m, 2H), 1.76 (dd, *J* = 11.7, 3.7 Hz, 1H).

2-(2,6-Dioxopiperidin-3-yl)-6-(2-(2-(4-((1R,2S)-6-hydroxy-2-phenyl-1,2,3,4-tetrahydronaphthalen-1-yl)phenyl)-2,6-diazaspiro[3.4]octan-6-yl)-2-oxoethyl)-6,7-dihydropyrrolo[3,4-f]isoindole-1,3-(2H,5H)-dione (**30**). Compound **30** was synthesized using a similar procedure for the preparation of compound **36**. White solid; UPLC–MS: 1.82 min, purity >95%; MS (ESI) m/z : calcd, 750.33 for $C_{45}H_{43}N_5O_6$ [M + H]⁺; found, 750.38; ¹H NMR (400 MHz, MeOD): δ 7.94 (s, 2H), 7.16–7.05 (m, 3H), 6.86–6.76 (m, 2H), 6.71–6.62 (m, 2H), 6.51 (dt, J = 8.3, 2.5 Hz, 1H), 6.38–6.24 (m, 4H), 5.17 (dd, J = 12.6, 5.4 Hz, 1H), 4.97 (s, 4H), 4.50 (d, J = 2.6 Hz, 2H), 4.20 (t, J = 5.4 Hz, 1H), 3.90–3.77 (m, 4H), 3.68 (d, J = 24.5 Hz, 2H), 3.63–3.50 (m, 2H), 3.39–3.32 (m, 1H), 3.09–2.95 (m, 2H), 2.93–2.82 (m, 1H), 2.81–2.66 (m, 2H), 2.29 (t, J = 6.9 Hz, 1H), 2.26–2.10 (m, 3H), 1.83–1.71 (m, 1H).

2-(2,6-Dioxopiperidin-3-yl)-6-(2-(6-(4-((1R,2S)-6-hydroxy-2-phenyl-1,2,3,4-tetrahydronaphthalen-1-yl)phenyl)-2,6-diazaspiro[3.4]octan-2-yl)-2-oxoethyl)-6,7-dihydropyrrolo[3,4-f]isoindole-1,3-(2H,5H)-dione (**31**). Compound **31** was synthesized using a similar procedure for the preparation of compound **36**. White solid; UPLC–MS: 1.88 min, purity >95%; MS (ESI) m/z : calcd, 750.33 for $C_{45}H_{43}N_5O_6$ [M + H]⁺; found, 750.38; ¹H NMR (400 MHz, MeOD): δ 7.93 (s, 2H), 7.16–7.05 (m, 3H), 6.86–6.78 (m, 2H), 6.71–6.62 (m, 2H), 6.51 (dd, J = 8.3, 2.6 Hz, 1H), 6.31 (q, J = 8.7 Hz, 4H), 5.16 (dd, J = 12.6, 5.4 Hz, 1H), 4.94 (s, 4H), 4.35 (s, 2H), 4.23–4.13 (m, 3H), 4.08 (q, J = 10.1 Hz, 2H), 3.52–3.41 (m, 2H), 3.36–3.32 (m, 2H), 3.30–3.26 (m, 1H), 3.09–2.94 (m, 2H), 2.93–2.81 (m, 1H), 2.80–2.67 (m, 2H), 2.32–2.10 (m, 4H), 1.82–1.70 (m, 1H).

2-(2,6-Dioxopiperidin-3-yl)-6-(2-(2-(4-((1R,2S)-6-hydroxy-2-phenyl-1,2,3,4-tetrahydronaphthalen-1-yl)phenyl)-2,7-diazaspiro[3.5]nonan-7-yl)-2-oxoethyl)-6,7-dihydropyrrolo[3,4-f]isoindole-1,3-(2H,5H)-dione (**32**). Compound **32** was synthesized using a similar procedure for the preparation of compound **36**. White solid; UPLC–MS: 1.85 min, purity >95%; MS (ESI) m/z : calcd, 764.34 for $C_{46}H_{45}N_5O_6$ [M + H]⁺; found, 764.39; ¹H NMR (400 MHz, MeOD): δ 7.93 (s, 2H), 7.16–7.04 (m, 3H), 6.82 (dd, J = 7.5, 1.8 Hz, 2H), 6.71–6.61 (m, 2H), 6.51 (dd, J = 8.3, 2.6 Hz, 1H), 6.42–6.31 (m, 4H), 5.17 (dd, J = 12.6, 5.4 Hz, 1H), 4.96 (s, 4H), 4.63 (s, 2H), 4.21 (d, J = 5.0 Hz, 1H), 3.80–3.70 (m, 4H), 3.68–3.59 (m, 2H), 3.44–3.32 (m, 3H), 3.09–2.96 (m, 2H), 2.96–2.82 (m, 1H), 2.81–2.66 (m, 2H), 2.27–2.10 (m, 2H), 1.94–1.73 (m, 5H).

2-(2,6-Dioxopiperidin-3-yl)-6-(2-(7-(4-((1R,2S)-6-hydroxy-2-phenyl-1,2,3,4-tetrahydronaphthalen-1-yl)phenyl)-2,7-diazaspiro[3.5]nonan-2-yl)-2-oxoethyl)-6,7-dihydropyrrolo[3,4-f]isoindole-1,3-(2H,5H)-dione (**33**). Compound **33** was synthesized using a similar procedure for the preparation of compound **36**. White solid; UPLC–MS: 2.56 min, purity >95%; MS (ESI) m/z : calcd, 764.34 for $C_{46}H_{45}N_5O_6$ [M + H]⁺; found, 764.40; ¹H NMR (400 MHz, MeOD): δ 7.93 (s, 2H), 7.21–7.07 (m, 5H), 6.83 (dd, J = 7.5, 1.7 Hz, 2H), 6.71–6.64 (m, 2H), 6.61 (d, J = 8.7 Hz, 2H), 6.53 (dd, J = 8.3, 2.6 Hz, 1H), 5.17 (dd, J = 12.6, 5.4 Hz, 1H), 4.94 (s, 4H), 4.42–4.30 (m, 3H), 4.07 (s, 2H), 3.96 (s, 2H), 3.57–3.38 (m, 5H), 3.13–2.96 (m, 2H), 2.94–2.82 (m, 1H), 2.82–2.66 (m, 2H), 2.29–2.08 (m, 6H), 1.89–1.77 (m, 1H).

2-(2,6-Dioxopiperidin-3-yl)-6-(2-(2-(4-((1R,2S)-6-hydroxy-2-phenyl-1,2,3,4-tetrahydronaphthalen-1-yl)phenyl)-2,8-diazaspiro[4.5]decan-8-yl)-2-oxoethyl)-6,7-dihydropyrrolo[3,4-f]isoindole-1,3-(2H,5H)-dione (**34**). The key intermediate (1R,6S)-5-(4-(2,8-diazaspiro[4.5]decan-2-yl)phenyl)-6-phenyl-5,6,7,8-tetrahydronaphthalen-2-ol (**57f**) was prepared using a similar procedure for the synthesis of **57h**, and it was obtained as a white solid (172 mg, 68% yield); UPLC–MS (ESI) m/z : calcd, 439.27 for $C_{30}H_{34}N_2O$ [M + H]⁺; found, 439.40; ¹H NMR (400 MHz, MeOD): δ 7.15–7.06 (m, 3H), 6.81 (dd, J = 7.5, 1.7 Hz, 2H), 6.68 (d, J = 8.4 Hz, 1H), 6.64 (d, J = 2.5 Hz, 1H), 6.50 (dd, J = 8.3, 2.6 Hz, 1H), 6.26 (s, 4H), 4.15 (d, J = 5.0 Hz, 1H), 3.30–3.26 (m, 3H), 3.26–3.16 (m, 4H), 3.15–3.11 (m, 2H), 3.07–2.92 (m, 2H), 2.29–2.15 (m, 1H), 1.95 (t, J = 7.0 Hz, 2H), 1.88–1.72 (m, 5H).

The title compound **34** was synthesized from **57f** and **55** using a similar procedure for the preparation of compound **36**, and it was afforded as a white solid (71 yield). UPLC–MS: 1.95 min, purity >95%; MS (ESI) m/z : calcd, 778.36 for $C_{47}H_{47}N_5O_6$ [M + H]⁺; found, 764.39;

¹H NMR (400 MHz, MeOD): δ 7.93 (s, 2H), 7.17–7.05 (m, 3H), 6.82 (dd, J = 7.6, 1.6 Hz, 2H), 6.71–6.62 (m, 2H), 6.51 (dd, J = 8.3, 2.6 Hz, 1H), 6.43–6.25 (m, 4H), 5.17 (dd, J = 12.6, 5.4 Hz, 1H), 4.96 (s, 4H), 4.62 (s, 2H), 4.18 (d, J = 4.6 Hz, 1H), 3.76–3.58 (m, 2H), 3.50–3.39 (m, 2H), 3.39–3.32 (m, 3H), 3.18 (s, 2H), 3.08–2.94 (m, 2H), 2.93–2.82 (m, 1H), 2.81–2.66 (m, 2H), 2.29–2.10 (m, 2H), 1.96 (t, J = 7.5 Hz, 2H), 1.81–1.59 (m, 5H).

2-(2,6-Dioxopiperidin-3-yl)-6-(2-(8-(4-((1R,2S)-6-hydroxy-2-phenyl-1,2,3,4-tetrahydronaphthalen-1-yl)phenyl)-2,8-diazaspiro[4.5]decan-2-yl)-2-oxoethyl)-6,7-dihydropyrrolo[3,4-f]isoindole-1,3-(2H,5H)-dione (**35**). Compound **35** was synthesized using a similar procedure for the preparation of compound **36**. White solid; UPLC–MS: 1.58 min, purity >95%; MS (ESI) m/z : calcd, 778.36 for $C_{47}H_{47}N_5O_6$ [M + H]⁺; found, 764.39; ¹H NMR (400 MHz, MeOD): δ 7.94 (d, J = 2.0 Hz, 2H), 7.23 (dd, J = 8.7, 7.4 Hz, 2H), 7.17–7.07 (m, 3H), 6.89–6.78 (m, 2H), 6.72–6.59 (m, 4H), 6.53 (dt, J = 8.3, 2.3 Hz, 1H), 5.17 (dd, J = 12.5, 5.3 Hz, 1H), 4.98 (s, 4H), 4.53 (d, J = 5.6 Hz, 2H), 4.41–4.34 (m, 1H), 3.69–3.40 (m, 9H), 3.11–2.95 (m, 2H), 2.94–2.82 (m, 1H), 2.81–2.67 (m, 2H), 2.25–1.94 (m, 8H), 1.88–1.78 (m, 1H).

2-(2,6-Dioxopiperidin-3-yl)-6-(2-(9-(4-((1R,2S)-6-hydroxy-2-phenyl-1,2,3,4-tetrahydronaphthalen-1-yl)phenyl)-3,9-diazaspiro[5.5]undecan-3-yl)-2-oxoethyl)-6,7-dihydropyrrolo[3,4-f]isoindole-1,3-(2H,5H)-dione (**36**). To a solution of **9a** (500 mg, 1.0 equiv) in MeCN (25 mL) was added DIPEA (2.59 mL, 10.0 equiv) and BrCH₂CO^tBu (264 μ L, 1.2 equiv), and then the mixture was stirred at rt for 6 h. LC–MS showed that one main peak with the desired MS was detected. TLC (DCM/MeOH = 20:1) indicated that a new spot formed. Then the reaction mixture was concentrated under reduced pressure, and the residue was purified by flash column chromatography (DCM/MeOH = 100:0 to 95:5) to provide a pure product, which was further treated with TFA at rt to remove the *tert*-butyl group. Compound 2-(6-(2,6-dioxopiperidin-3-yl)-5,7-dioxo-3,5,6,7-tetrahydropyrrolo[3,4-f]isoindol-2(1H)-yl)acetic acid (**55**) was obtained as a white solid (392 mg, 74% yield); UPLC–MS: 0.22 min; MS (ESI) m/z : calcd, 358.10 for $C_{17}H_{13}N_3O_6$ [M + H]⁺; found, 358.19; ¹H NMR (400 MHz, MeOD): δ 7.94 (s, 2H), 5.17 (dd, J = 12.7, 5.5 Hz, 1H), 4.97 (s, 4H), 4.44 (s, 2H), 2.95–2.82 (m, 1H), 2.82–2.67 (m, 2H), 2.22–2.10 (m, 1H).

A mixture of intermediate **48** (300 mg, 1.0 equiv), *tert*-butyl 3,9-diazaspiro[5.5]undecane-3-carboxylate (220 mg, 2.0 equiv), Pd(OAc)₂ (20.6 mg, 0.2 equiv), XPhos (65.5 mg, 0.3 equiv), and *t*-BuONa (176 mg, 4.0 equiv) in toluene (10 mL) was degassed and purged with N₂ 3 times and then stirred at 90 °C under a N₂ atmosphere for 10 h. The mixture was cooled, diluted with DCM, and filtered through Celite to remove insoluble catalyst and salts, and the filter cake was washed with DCM. The filtrate was concentrated under reduced pressure. The residue was purified by flash column chromatography (*n*-hexane/EtOAc = 100:0 to 90:10). The resulting pure product was treated with TFA at rt for 6 h, after which the solvent was removed, and the residue was lyophilized to give compound (1R,6S)-5-(4-(3,9-diazaspiro[5.5]undecan-3-yl)phenyl)-6-phenyl-5,6,7,8-tetrahydronaphthalen-2-ol (**57h**) as a white solid (250 mg, yield = 96%); UPLC–MS (ESI) m/z : calcd, 453.29 for $C_{31}H_{36}N_2O$ [M + H]⁺; found, 453.40; ¹H NMR (400 MHz, MeOD): δ 7.25 (d, J = 8.8 Hz, 2H), 7.17–7.07 (m, 3H), 6.87–6.80 (m, 2H), 6.71–6.61 (m, 4H), 6.53 (dd, J = 8.3, 2.6 Hz, 1H), 4.38 (d, J = 5.4 Hz, 1H), 3.60–3.49 (m, 4H), 3.49–3.41 (m, 1H), 3.26–3.18 (m, 4H), 3.13–2.97 (m, 2H), 2.23–2.10 (m, 1H), 2.02–1.94 (m, 4H), 1.91–1.79 (m, 5H).

To a solution of intermediate **55** (166 mg, 1.0 equiv) and HATU (134 mg, 1.0 equiv) in DMF (6 mL) was added DIPEA (369 μ L, 6.0 equiv). 10 min later, **57h** (200 mg, 1.0 equiv) was added, and the reaction was stirred at rt for 10 min. Then the crude mixture was directly purified by pre-HPLC (25–100% MeCN/H₂O in 75 min) to give title compound 2-(2,6-dioxopiperidin-3-yl)-6-(2-(9-(4-((1R,2S)-6-hydroxy-2-phenyl-1,2,3,4-tetrahydronaphthalen-1-yl)phenyl)-3,9-diazaspiro[5.5]undecan-3-yl)-2-oxoethyl)-6,7-dihydropyrrolo[3,4-f]isoindole-1,3-(2H,5H)-dione (**36**) as a white solid (186 mg, 67% yield); UPLC–MS: 2.49 min, purity >95%; MS (ESI) m/z : calcd for $C_{48}H_{49}N_5O_6$ [M + H]⁺ 792.38; found, 792.22; HRMS (APCI) m/z :

calcd for $C_{48}H_{49}N_5O_6$ $[M + H]^+$ 792.3756; found, 792.3775; 1H NMR (400 MHz, DMSO- d_6): δ 11.14 (s, 1H), 8.01 (s, 2H), 7.27–7.09 (m, 4H), 7.06–6.79 (m, 4H), 6.68–6.60 (m, 2H), 6.50 (dd, J = 8.2, 2.4 Hz, 1H), 6.40 (d, J = 8.0 Hz, 2H), 5.17 (dd, J = 12.9, 5.3 Hz, 1H), 4.87 (s, 3H), 4.65 (s, 2H), 4.25 (d, J = 4.7 Hz, 1H), 3.54 (s, 2H), 3.41–3.15 (m, 7H), 3.04–2.85 (m, 3H), 2.66–2.51 (m, 2H), 2.15–2.01 (m, 2H), 1.85–1.31 (m, 10H); ^{13}C NMR (101 MHz, DMSO): δ 172.72, 169.75, 166.59, 162.96, 155.49, 143.91, 141.46, 137.14, 131.72, 131.07, 130.88, 129.60, 127.78, 127.59, 125.90, 118.54, 114.45, 113.62, 58.85, 55.81, 49.46, 49.19, 44.32, 37.28, 33.35, 30.94, 29.25, 28.93, 21.98, 21.50.

2-(2,6-Dioxopiperidin-3-yl)-6-(2-(9-(4-((1R,2S)-6-hydroxy-2-phenyl-1,2,3,4-tetrahydronaphthalen-1-yl)phenyl)-2,9-diazaspiro[5.5]undecan-2-yl)-2-oxoethyl)-6,7-dihydropyrrolo[3,4-f]isoindole-1,3-(2H,5H)-dione (37). Compound 37 was synthesized using a similar procedure for the preparation of compound 36. White solid; UPLC–MS: 1.61 min, purity >95%; MS (ESI) m/z : calcd, 792.38 for $C_{48}H_{49}N_5O_6$ $[M + H]^+$; found, 792.45; 1H NMR (400 MHz, MeOD): δ 7.93 (s, 2H), 7.33–7.23 (m, 2H), 7.18–7.08 (m, 3H), 6.88–6.80 (m, 2H), 6.72–6.60 (m, 4H), 6.53 (dd, J = 8.3, 2.6 Hz, 1H), 5.17 (dd, J = 12.6, 5.4 Hz, 1H), 4.97 (s, 4H), 4.73–4.58 (m, 2H), 4.39 (d, J = 5.3 Hz, 1H), 3.75–3.38 (m, 9H), 3.30–3.27 (m, 1H), 3.12–2.97 (m, 2H), 2.94–2.82 (m, 1H), 2.81–2.67 (m, 2H), 2.23–2.09 (m, 2H), 2.00–1.64 (m, 9H).

2-(2,6-Dioxopiperidin-3-yl)-6-(2-(9-(4-((1R,2S)-6-hydroxy-2-phenyl-1,2,3,4-tetrahydronaphthalen-1-yl)phenyl)-3,9-diazaspiro[5.5]undecan-3-yl)acetyl)-6,7-dihydropyrrolo[3,4-f]isoindole-1,3-(2H,5H)-dione (38). To a solution of 57h (60 mg, 1.0 equiv) in MeCN (25 mL) was added DIPEA (184 μ L, 10.0 equiv) and BrCH₂COO^tBu (17 μ L, 1.1 equiv), and then the mixture was stirred at rt for 6 h until LC–MS showed complete conversion of 57h and a main peak with desired MS was detected. Then the reaction mixture was concentrated under reduced pressure, and the residue was purified by pre-HPLC (30–100% MeCN/H₂O in 70 min) to provide a pure product, which was further treated with TFA at rt to remove the *tert*-butyl group. The key intermediate 2-(6-(2,6-dioxopiperidin-3-yl)-5,7-dioxo-3,5,6,7-tetrahydropyrrolo[3,4-f]isoindol-2(1H)-yl)acetic acid (57j) was obtained as a white solid (48 mg, yield = 89%); UPLC–MS (ESI) m/z : calcd, 511.30 for $C_{33}H_{38}N_2O_3$ $[M + H]^+$; found, 511.28; 1H NMR (400 MHz, MeOD): δ 7.20 (d, J = 8.8 Hz, 2H), 7.16–7.08 (m, 3H), 6.86–6.81 (m, 2H), 6.71–6.59 (m, 4H), 6.53 (dd, J = 8.3, 2.6 Hz, 1H), 4.37 (d, J = 5.3 Hz, 1H), 4.06 (s, 2H), 3.59–3.32 (m, 9H), 3.12–2.97 (m, 2H), 2.22–2.11 (m, 1H), 2.09–1.78 (m, 9H).

To a solution of intermediate 57j (4 mg, 1.0 equiv) and HATU (2.7 mg, 1.1 equiv) in DMF (2 mL) was added DIPEA (6.7 μ L, 6.0 equiv). 10 min later, TFA salt of 9a (3.4 mg, 1.3 equiv) was added, and the reaction was stirred at rt for 10 min. Then the crude mixture was directly purified by pre-HPLC (30–100% MeCN/H₂O in 70 min) to give the title compound 2-(2,6-dioxopiperidin-3-yl)-6-(2-(9-(4-((1R,2S)-6-hydroxy-2-phenyl-1,2,3,4-tetrahydronaphthalen-1-yl)phenyl)-3,9-diazaspiro[5.5]undecan-3-yl)acetyl)-6,7-dihydropyrrolo[3,4-f]isoindole-1,3(2H,5H)-dione (38) as a white solid (5.0 mg, yield = 99%); UPLC–MS: 1.61 min, purity >95%; MS (ESI) m/z : calcd, 792.38 for $C_{48}H_{49}N_5O_6$ $[M + H]^+$; found, 792.46; 1H NMR (400 MHz, MeOD): δ 7.89 (d, J = 15.1 Hz, 2H), 7.22 (d, J = 8.8 Hz, 2H), 7.17–7.07 (m, 3H), 6.84 (dd, J = 7.6, 1.7 Hz, 2H), 6.72–6.59 (m, 4H), 6.53 (dd, J = 8.3, 2.6 Hz, 1H), 5.16 (dd, J = 12.6, 5.4 Hz, 1H), 4.99 (d, J = 12.6 Hz, 4H), 4.37 (d, J = 5.3 Hz, 1H), 4.32 (s, 2H), 3.75–3.32 (m, 9H), 3.12–2.97 (m, 2H), 2.94–2.82 (m, 1H), 2.81–2.66 (m, 2H), 2.23–1.78 (m, 11H).

6-(2-(9-(4-((1R,3R)-2-(2,2-difluoro-3-hydroxypropyl)-3-methyl-2,3,4,9-tetrahydro-1H-pyrido[3,4-b]indol-1-yl)-3,5-difluorophenyl)-3,9-diazaspiro[5.5]undecan-3-yl)-2-oxoethyl)-2-(2,6-dioxopiperidin-3-yl)-6,7-dihydropyrrolo[3,4-f]isoindole-1,3(2H,5H)-dione (39). To a mixture of (R)-3-((1-(1H-indol-3-yl)propan-2-yl)amino)-2,2-difluoropropan-1-ol²⁶ (58a, 500 mg, 1.0 equiv) and 4-bromo-2,6-difluorobenzaldehyde (449 mg, 1.1 equiv) in toluene (6 mL) was added AcOH (316 μ L, 3.0 equiv) and then kept the reaction stirring at 90 °C for 12 h. After cooling to rt, the reaction mixture was concentrated under reduced pressure and purified by flash column chromatography (*n*-hexane/EtOAc = 100:0 to 80:20) to give compound 3-((1R,3R)-1-(4-bromo-2,6-difluorophenyl)-3-methyl-1,3,4,9-tetrahydro-2H-

pyrido[3,4-*b*]indol-2-yl)-2,2-difluoropropan-1-ol (59a) as a white foam (630 mg, yield = 73%); UPLC–MS (ESI) m/z : calcd, 471.07 for $C_{21}H_{19}BrF_4N_2O$ $[M + H]^+$; found, 471.11; 1H NMR (400 MHz, CDCl₃): δ 7.55–7.50 (m, 1H), 7.43 (s, 1H), 7.26–7.22 (m, 1H), 7.18–7.09 (m, 4H), 5.27 (s, 1H), 3.78–3.66 (m, 3H), 3.32–3.20 (m, 1H), 3.09 (ddd, J = 15.6, 5.0, 1.8 Hz, 1H), 2.91–2.78 (m, 1H), 2.68 (ddd, J = 15.6, 4.3, 1.3 Hz, 1H), 1.19 (d, J = 6.6 Hz, 3H).

A mixture of intermediate 59a (50 mg, 1.0 equiv), *tert*-butyl 3,9-diazaspiro[5.5]undecane-3-carboxylate (54 mg, 2.0 equiv), Pd₃(dba)₃ (29 mg, 0.3 equiv), XantPhos (30 mg, 0.6 equiv), and Cs₂CO₃ (138 mg, 4.0 equiv) in 1,4-dioxane (6 mL) was degassed and purged with N₂ 3 times and then was stirred under a N₂ atmosphere at 100 °C for 10 h. After cooling to rt, the reaction mixture was diluted with DCM and filtered through Celite, and the filter cake was washed with DCM. The filtration was concentrated under reduced pressure to give a dryness, which was purified by pre-HPLC (70–100% MeCN/H₂O in 30 min) to afford compound *tert*-butyl 9-(4-((1R,3R)-2-(2,2-difluoro-3-hydroxypropyl)-3-methyl-2,3,4,9-tetrahydro-1H-pyrido[3,4-*b*]indol-1-yl)-3,5-difluorophenyl)-3,9-diazaspiro[5.5]undecane-3-carboxylate (60a) as a white solid (32.7 mg, yield = 48%); UPLC–MS: 2.62 min; MS (ESI) m/z : calcd, 645.34 for $C_{35}H_{44}F_4N_4O_3$ $[M + H]^+$; found, 645.31; 1H NMR (400 MHz, MeOD): δ 7.43–7.37 (m, 1H), 7.22–7.17 (m, 1H), 7.04–6.92 (m, 2H), 6.51–6.41 (m, 2H), 5.20 (s, 1H), 3.87–3.73 (m, 1H), 3.62 (h, J = 6.3 Hz, 1H), 3.55–3.35 (m, 5H), 3.28–3.09 (m, 5H), 2.97 (dd, J = 14.6, 4.3 Hz, 1H), 2.86–2.70 (m, 1H), 2.61 (dd, J = 15.4, 4.9 Hz, 1H), 1.69–1.56 (m, 4H), 1.54–1.40 (m, 13H), 1.15 (d, J = 6.6 Hz, 3H); ^{13}C NMR (101 MHz, CDCl₃): δ 162.03, 155.11, 152.80, 136.34, 131.54, 127.74, 121.80, 119.59, 118.38, 110.88, 107.73, 103.46, 98.06, 97.80, 79.66, 67.25, 64.74, 64.42, 51.49, 50.03, 43.40, 34.80, 29.76, 28.62, 27.16, 21.20, 14.35.

Intermediate 60a was treated with TFA/DCM (1 mL/3 mL) at rt for 5 min to remove the Boc group. After concentration to remove the solvent and lyophilization, the resulting product was immediately used in the next step.

To a solution of 55 (21 mg, 1.0 equiv) and HATU (16.8 mg, 1.0 equiv) in DMF was added DIPEA (46 μ L, 6.0 equiv). 10 min later, the de-Boc product of 60a (35 mg, 1.2 equiv) was added, and the reaction was stirred for 5 min, after which the crude mixture was directly purified by pre-HPLC (30–100% MeCN/H₂O (containing 0.1% formic acid) in 70 min) to afford the title compound 6-(2-(9-(4-((1R,3R)-2-(2,2-difluoro-3-hydroxypropyl)-3-methyl-2,3,4,9-tetrahydro-1H-pyrido[3,4-*b*]indol-1-yl)-3,5-difluorophenyl)-3,9-diazaspiro[5.5]undecan-3-yl)-2-oxoethyl)-2-(2,6-dioxopiperidin-3-yl)-6,7-dihydropyrrolo[3,4-f]isoindole-1,3(2H,5H)-dione (39) as a light yellow solid (21 mg, yield = 54%); UPLC–MS: 1.79 min, purity >95%; MS (ESI) m/z : calcd, 884.38 for $C_{47}H_{49}F_4N_7O_6$ $[M + H]^+$; found, 884.45; 1H NMR (400 MHz, MeOD): δ 7.86 (s, 2H), 7.40 (d, J = 7.2 Hz, 1H), 7.19 (d, J = 7.6 Hz, 1H), 7.05–6.93 (m, 2H), 6.48 (d, J = 12.8 Hz, 2H), 5.23 (s, 1H), 5.15 (dd, J = 12.6, 5.4 Hz, 1H), 4.66 (s, 4H), 4.27 (s, 2H), 3.86–3.73 (m, 1H), 3.69–3.59 (m, 3H), 3.53–3.42 (m, 3H), 3.28–3.13 (m, 5H), 3.01–2.59 (m, 6H), 2.22–2.07 (m, 1H), 1.71–1.63 (m, 4H), 1.62–1.53 (m, 4H), 1.17 (d, J = 6.5 Hz, 3H).

6-(2-(9-(3,5-Difluoro-4-((1R,3R)-2-(2-fluoro-2-methylpropyl)-3-methyl-2,3,4,9-tetrahydro-1H-pyrido[3,4-*b*]indol-1-yl)phenyl)-3,9-diazaspiro[5.5]undecan-3-yl)-2-oxoethyl)-2-(2,6-dioxopiperidin-3-yl)-6,7-dihydropyrrolo[3,4-f]isoindole-1,3(2H,5H)-dione (40). Intermediate (1R,3R)-1-(4-bromo-2,6-difluorophenyl)-2-(2-fluoro-2-methylpropyl)-3-methyl-2,3,4,9-tetrahydro-1H-pyrido[3,4-*b*]indole (59b) was prepared using a similar procedure for the procedure for synthesizing compound 59a, and it was obtained as a light-yellow solid; UPLC–MS (ESI) m/z : calcd, 451.10 for $C_{22}H_{22}BrF_3N_2$ $[M + H]^+$; found, 451.11; 1H NMR (400 MHz, CDCl₃): δ 7.54 (d, J = 7.0 Hz, 1H), 7.47 (s, 1H), 7.25–7.21 (m, 1H), 7.17–7.09 (m, 2H), 7.06 (d, J = 8.3 Hz, 2H), 5.28 (s, 1H), 3.65 (h, J = 6.1 Hz, 1H), 3.08 (dd, J = 15.2, 4.8 Hz, 1H), 2.88 (dd, J = 21.7, 15.0 Hz, 1H), 2.64 (dd, J = 15.2, 4.5 Hz, 1H), 2.42 (dd, J = 23.7, 15.0 Hz, 1H), 1.28 (d, J = 20.5 Hz, 3H), 1.21 (d, J = 21.4 Hz, 3H), 1.12 (d, J = 6.6 Hz, 3H); ^{13}C NMR (101 MHz, CDCl₃): δ 183.64, 183.60, 183.55, 163.48, 163.40, 160.94, 160.85, 136.40, 131.28, 127.65, 122.01, 121.89, 121.76, 121.68, 119.48, 118.35, 117.24, 117.10, 116.95, 116.92, 116.89, 116.68, 116.64, 116.07, 116.03,

115.81, 115.77, 110.89, 109.16, 98.00, 96.34, 77.48, 77.16, 76.84, 57.20, 56.98, 51.29, 27.02, 25.28, 25.03, 24.93, 24.68.

Intermediate *tert*-butyl 9-(3,5-difluoro-4-((1*R*,3*R*)-2-(2-fluoro-2-methylpropyl)-3-methyl-2,3,4,9-tetrahydro-1*H*-pyrido[3,4-*b*]indol-1-yl)phenyl)-3,9-diazaspiro[5.5]undecane-3-carboxylate (**60b**) was prepared using a similar procedure for the synthesis of compound **60a**, and it was obtained as a light yellow solid; UPLC–MS (ESI) *m/z*: calcd, 625.37 for C₃₆H₄₇F₃N₄O₂ [M + H]⁺; found, 625.3; ¹H NMR (400 MHz, CDCl₃): δ 7.53–7.48 (m, 1H), 7.41 (s, 1H), 7.23–7.19 (m, 1H), 7.12–7.06 (m, 2H), 6.32 (d, *J* = 12.4 Hz, 2H), 5.15 (s, 1H), 3.70–3.65 (m, 1H), 3.45–3.36 (m, 4H), 3.23–3.15 (m, 4H), 3.13–3.06 (m, 1H), 2.86 (dd, *J* = 17.6, 15.1 Hz, 1H), 2.59 (dd, *J* = 15.0, 2.5 Hz, 1H), 2.40 (dd, *J* = 26.4, 14.8 Hz, 1H), 1.66–1.59 (m, 4H), 1.59–1.54 (m, 2H), 1.50–1.48 (m, 2H), 1.46 (s, 9H), 1.23 (d, *J* = 3.9 Hz, 3H), 1.18 (d, *J* = 4.2 Hz, 3H), 1.10 (d, *J* = 6.5 Hz, 3H).

The title compound 6-(2-(9-(3,5-difluoro-4-((1*R*,3*R*)-2-(2-fluoro-2-methylpropyl)-3-methyl-2,3,4,9-tetrahydro-1*H*-pyrido[3,4-*b*]indol-1-yl)phenyl)-3,9-diazaspiro[5.5]undecan-3-yl)-2-oxoethyl)-2-(2,6-dioxopiperidin-3-yl)-6,7-dihydropyrrolo[3,4-*f*]isoindole-1,3(2*H*,5*H*)-dione (**40**) was produced from intermediate **60b** and **55** using a similar procedure for the preparation of compound **39**, and it was afforded as a light yellow solid; UPLC–MS: 1.64 min, purity >95%; MS (ESI) *m/z*: calcd, 864.41 for C₄₈H₅₂F₃N₇O₅ [M + H]⁺; found, 864.33; ¹H NMR (400 MHz, DMSO-*d*₆): δ 11.10 (s, 1H), 10.48 (s, 1H), 7.81 (s, 2H), 7.37 (d, *J* = 7.4 Hz, 1H), 7.17 (d, *J* = 7.7 Hz, 1H), 7.02–6.87 (m, 2H), 6.52 (d, *J* = 13.2 Hz, 2H), 5.13 (dd, *J* = 12.8, 5.4 Hz, 1H), 5.07 (s, 1H), 4.10 (s, 4H), 3.62 (s, 2H), 3.50–3.44 (m, 4H), 3.24–3.15 (m, 4H), 2.95–2.74 (m, 3H), 2.65–2.52 (m, 3H), 2.46–2.28 (m, 2H), 2.10–2.02 (m, 1H), 1.58–1.49 (m, 4H), 1.48–1.39 (m, 4H), 1.21–1.11 (m, 6H), 1.03 (d, *J* = 6.5 Hz, 3H).

6-(2-(9-(4-((1*R*,3*R*)-2-(2,2-difluoroethyl)-3-methyl-2,3,4,9-tetrahydro-1*H*-pyrido[3,4-*b*]indol-1-yl)-3,5-difluorophenyl)-3,9-diazaspiro[5.5]undecan-3-yl)-2-oxoethyl)-2-(2,6-dioxopiperidin-3-yl)-6,7-dihydropyrrolo[3,4-*f*]isoindole-1,3(2*H*,5*H*)-dione (**41**). Intermediate (1*R*,3*R*)-1-(4-bromo-2,6-difluorophenyl)-2-(2,2-difluoroethyl)-3-methyl-2,3,4,9-tetrahydro-1*H*-pyrido[3,4-*b*]indole (**59c**) was prepared using a similar procedure for the synthesis of compound **59a**, and it was obtained as a light yellow solid; ¹H NMR (400 MHz, CDCl₃): δ 7.57–7.51 (m, 1H), 7.48 (s, 1H), 7.28–7.25 (m, 1H), 7.19–7.07 (m, 4H), 5.70 (tt, *J* = 56.3, 4.4 Hz, 1H), 5.26 (s, 1H), 3.49 (h, *J* = 6.3 Hz, 1H), 3.15–3.00 (m, 2H), 2.82–2.71 (m, 1H), 2.65 (ddd, *J* = 15.5, 5.7, 1.4 Hz, 1H), 1.18 (d, *J* = 6.6 Hz, 3H).

Intermediate *tert*-butyl 9-(4-((1*R*,3*R*)-2-(2,2-difluoroethyl)-3-methyl-2,3,4,9-tetrahydro-1*H*-pyrido[3,4-*b*]indol-1-yl)-3,5-difluorophenyl)-3,9-diazaspiro[5.5]undecane-3-carboxylate **60c** was prepared using a similar procedure for the synthesis of compound **60a**, and it was obtained as a yellow oil; UPLC–MS: 2.86 min; MS (ESI) *m/z*: calcd, 615.33 for [M + H]⁺; found, 615.29; ¹H NMR (400 MHz, MeOD): δ 7.43–7.38 (m, 1H), 7.23–7.18 (m, 1H), 7.03–6.94 (m, 2H), 6.47 (d, *J* = 12.7 Hz, 2H), 5.83–5.47 (m, 1H), 5.20 (s, 1H), 3.49 (q, *J* = 5.7 Hz, 1H), 3.45–3.36 (m, 4H), 3.27–3.18 (m, 4H), 3.07–2.92 (m, 2H), 2.83–2.71 (m, 1H), 2.60 (ddd, *J* = 15.3, 5.7, 1.2 Hz, 1H), 1.66–1.57 (m, 4H), 1.51–1.42 (m, 13H), 1.16 (d, *J* = 6.6 Hz, 3H).

The title compound 6-(2-(9-(4-((1*R*,3*R*)-2-(2,2-difluoroethyl)-3-methyl-2,3,4,9-tetrahydro-1*H*-pyrido[3,4-*b*]indol-1-yl)-3,5-difluorophenyl)-3,9-diazaspiro[5.5]undecan-3-yl)-2-oxoethyl)-2-(2,6-dioxopiperidin-3-yl)-6,7-dihydropyrrolo[3,4-*f*]isoindole-1,3(2*H*,5*H*)-dione (**41**) was produced from intermediate **60c** and **55** using a similar procedure for the preparation of compound **39** and it was afforded as a light yellow solid; UPLC–MS: 1.95 min, purity >95%; MS (ESI) *m/z*: calcd, 854.36 for C₄₆H₄₇F₄N₇O₅ [M + H]⁺; found, 854.41; ¹H NMR (400 MHz, MeOD): δ 7.93 (s, 2H), 7.43 (d, *J* = 7.7 Hz, 1H), 7.23 (d, *J* = 7.9 Hz, 1H), 7.07–6.96 (m, 2H), 6.53 (d, *J* = 12.9 Hz, 2H), 6.01–5.67 (m, 1H), 5.45 (s, 1H), 5.16 (dd, *J* = 12.6, 5.4 Hz, 1H), 4.94 (s, 4H), 4.59 (s, 2H), 3.71–3.62 (m, 3H), 3.45–3.38 (m, 2H), 3.30–3.21 (m, 4H), 3.09–2.82 (m, 3H), 2.79–2.67 (m, 3H), 2.20–2.10 (m, 1H), 1.70–1.56 (m, 9H), 1.27 (d, *J* = 6.6 Hz, 3H).

2-(2,6-Dioxopiperidin-3-yl)-6-(2-(9-(6-((6*S*,8*R*)-8-methyl-7-(2,2,2-trifluoroethyl)-6,7,8,9-tetrahydro-3*H*-pyrazolo[4,3-*f*]isoquinolin-6-yl)pyridin-3-yl)-3,9-diazaspiro[5.5]undecan-3-yl)-2-oxoethyl)-6,7-

*dihydropyrrolo[3,4-*f*]isoindole-1,3(2*H*,5*H*)-dione* (**42**). Intermediate (6*S*,8*R*)-6-(5-bromopyridin-2-yl)-8-methyl-7-(2,2,2-trifluoroethyl)-6,7,8,9-tetrahydro-3*H*-pyrazolo[4,3-*f*]isoquinoline (**65a**) was prepared using a similar procedure for the synthesis of **65c**, and it was obtained as a light-yellow foam; UPLC–MS (ESI) *m/z*: calcd, 425.06 for C₁₈H₁₆BrF₃N₄ [M + H]⁺; found, 424.94; ¹H NMR (400 MHz, CDCl₃): δ 8.58 (d, *J* = 2.5 Hz, 1H), 8.13 (d, *J* = 1.0 Hz, 1H), 7.80 (dd, *J* = 8.5, 2.3 Hz, 1H), 7.43 (d, *J* = 8.5 Hz, 1H), 7.33 (d, *J* = 8.7 Hz, 1H), 7.03 (d, *J* = 8.7 Hz, 1H), 5.18 (s, 1H), 3.64–3.49 (m, 1H), 3.38–3.24 (m, 2H), 3.10–2.95 (m, 1H), 2.90 (dd, *J* = 16.8, 6.5 Hz, 1H), 1.16 (d, *J* = 6.6 Hz, 3H).

Intermediate *tert*-butyl 9-(6-((6*S*,8*R*)-8-methyl-7-(2,2,2-trifluoroethyl)-6,7,8,9-tetrahydro-3*H*-pyrazolo[4,3-*f*]isoquinolin-6-yl)-pyridin-3-yl)-3,9-diazaspiro[5.5]undecane-3-carboxylate (**66a**) was prepared using a similar procedure for the synthesis of **66c**, and it was obtained as a yellow solid; UPLC–MS (ESI) *m/z*: calcd, 599.33 for C₃₂H₄₁F₃N₆O₂ [M + H]⁺; found, 599.33; ¹H NMR (400 MHz, CDCl₃): δ 8.17 (d, *J* = 2.7 Hz, 1H), 7.98 (s, 1H), 7.29 (d, *J* = 8.8 Hz, 1H), 7.18 (dd, *J* = 8.8, 2.9 Hz, 1H), 7.11 (d, *J* = 8.7 Hz, 1H), 6.88 (d, *J* = 8.7 Hz, 1H), 5.07 (s, 1H), 3.65–3.55 (m, 1H), 3.43–3.37 (m, 4H), 3.31–3.17 (m, 6H), 3.05–2.95 (m, 1H), 2.83 (dd, *J* = 16.8, 6.7 Hz, 1H), 1.68–1.61 (m, 4H), 1.51–1.44 (m, 13H), 1.14 (d, *J* = 6.6 Hz, 3H).

The title compound 2-(2,6-dioxopiperidin-3-yl)-6-(2-(9-(6-((6*S*,8*R*)-8-methyl-7-(2,2,2-trifluoroethyl)-6,7,8,9-tetrahydro-3*H*-pyrazolo[4,3-*f*]isoquinolin-6-yl)pyridin-3-yl)-3,9-diazaspiro[5.5]undecan-3-yl)-2-oxoethyl)-6,7-dihydropyrrolo[3,4-*f*]isoindole-1,3(2*H*,5*H*)-dione (**42**) was prepared from intermediate **66a** and **55** in a similar manner with the procedure for production of compound **44**. It was afforded as a white solid; UPLC–MS: 1.22 min, purity >95%; MS (ESI) *m/z*: calcd, 838.36 for C₄₄H₄₆F₃N₉O₅ [M + H]⁺; found, 838.42; ¹H NMR (400 MHz, MeOD): δ 8.16 (d, *J* = 0.8 Hz, 1H), 8.08 (d, *J* = 3.0 Hz, 1H), 8.02 (dd, *J* = 9.2, 3.0 Hz, 1H), 7.94 (s, 2H), 7.77 (d, *J* = 9.2 Hz, 1H), 7.40 (d, *J* = 8.7 Hz, 1H), 6.96 (d, *J* = 8.7 Hz, 1H), 5.38 (s, 1H), 5.17 (dd, *J* = 12.6, 5.4 Hz, 1H), 4.97 (s, 4H), 4.64 (s, 2H), 3.73–3.65 (m, 2H), 3.64–3.52 (m, 1H), 3.50–3.37 (m, 8H), 3.14–3.00 (m, 2H), 2.94–2.82 (m, 1H), 2.81–2.67 (m, 2H), 2.20–2.11 (m, 1H), 1.75 (t, *J* = 5.5 Hz, 4H), 1.69–1.56 (m, 4H), 1.21 (d, *J* = 6.4 Hz, 3H).

6-(2-(9-(3,5-Difluoro-4-((6*S*,8*R*)-8-methyl-7-(2,2,2-trifluoroethyl)-6,7,8,9-tetrahydro-3*H*-pyrazolo[4,3-*f*]isoquinolin-6-yl)phenyl)-3,9-diazaspiro[5.5]undecan-3-yl)-2-oxoethyl)-2-(2,6-dioxopiperidin-3-yl)-6,7-dihydropyrrolo[3,4-*f*]isoindole-1,3(2*H*,5*H*)-dione (**43**). The title compound **43** was prepared using a similar procedure for the synthesis of compound **44**, and it was afforded as a light-yellow solid; UPLC–MS: 1.92 min, purity >95%; MS (ESI) *m/z*: calcd, 873.35 for C₄₅H₄₅F₃N₈O₅ [M + H]⁺; found, 873.39; ¹H NMR (400 MHz, MeOD): δ 8.07 (s, 1H), 7.94 (s, 2H), 7.23 (d, *J* = 8.7 Hz, 1H), 6.80 (d, *J* = 8.7 Hz, 1H), 6.47 (d, *J* = 12.6 Hz, 2H), 5.32 (s, 1H), 5.17 (dd, *J* = 12.6, 5.4 Hz, 1H), 4.96 (s, 4H), 4.62 (s, 2H), 3.72–3.60 (m, 3H), 3.46–3.34 (m, 5H), 3.27–3.22 (m, 4H), 2.99–2.91 (m, 1H), 2.90–2.83 (m, 1H), 2.80–2.68 (m, 2H), 2.19–2.12 (m, 1H), 1.74–1.66 (m, 4H), 1.66–1.57 (m, 4H), 1.14 (d, *J* = 6.5 Hz, 3H).

6-(2-(9-(4-((6*S*,8*R*)-2-(2,2-difluoroethyl)-8-methyl-6,7,8,9-tetrahydro-3*H*-pyrazolo[4,3-*f*]isoquinolin-6-yl)-3,5-difluorophenyl)-3,9-diazaspiro[5.5]undecan-3-yl)-2-oxoethyl)-2-(2,6-dioxopiperidin-3-yl)-6,7-dihydropyrrolo[3,4-*f*]isoindole-1,3(2*H*,5*H*)-dione (**44**, **ERD-3111**). To a solution of 4-bromo-1*H*-indazole (**61**, 5.9 g, 1.0 equiv) in THF (70 mL) was added *n*-BuLi (47 mL, 2.5 equiv) dropwise at –78 °C, and the mixture was stirred for 10 min, after which the reaction was warmed to –50 °C for 30 min. Then the reaction was cooled back to –78 °C, and *tert*-butyl (*R*)-4-methyl-1,2,3-oxathiazolidine-3-carboxylate **62**, 10 g, 1.4 equiv) was added in portionwise. After stirring for 1.5 h, the reaction was quenched with water, warmed to rt, and neutralized with 2 N HCl. The resulting mixture was extracted with EA, washed with brine, dried over Na₂SO₄, and concentrated under reduced pressure to give a crude mixture, which was purified by flash column chromatography (EA/*n*-hexane = 0/100 to 35/65) to afford a pure product. The resulting product was further treated with 4 N HCl in dioxane at rt for 10 min to remove the Boc group. After removal of the solvent, compound (*R*)-1-(1*H*-indazol-4-yl)propan-2-amine di-hydro-

chlorides (**63**)²⁷ was obtained as a white powder (3.5 g, yield = 47% yield); UPLC–MS: 0.19 min; MS (ESI) *m/z*: calcd, 176.12 for C₁₀H₁₃N₃ [M + H]⁺; found, 176.01; ¹H NMR (400 MHz, DMSO-*d*₆): δ 8.34–8.14 (m, 4H), 7.44 (d, *J* = 8.4 Hz, 1H), 7.29 (dd, *J* = 8.3, 6.9 Hz, 1H), 6.95 (d, *J* = 6.9 Hz, 1H), 3.55–3.48 (m, 1H), 3.39 (dd, *J* = 13.7, 4.4 Hz, 1H), 2.97 (dd, *J* = 13.2, 9.3 Hz, 1H), 1.13 (d, *J* = 6.5 Hz, 3H).

To a suspension of **63** (500 mg, 1.0 equiv) was added DIPEA (1.4 mL, 4.0 equiv). After the solution became clear, 2,2-difluoroethyl trifluoromethanesulfonate (362 μL, 1.25 equiv) was added, and the mixture was stirred at 60 °C for 12 h. The reaction was cooled down to rt and concentrated under reduced pressure to give an oil, which was purified by flash column chromatography (EA/*n*-hexane = 0–50%) to give compound (R)-*N*-(2,2-difluoroethyl)-1-(1H-indazol-4-yl)propan-2-amine (**64b**) as a colorless oil (370 mg, yield = 77%); UPLC–MS: 0.49 min; MS (ESI) *m/z*: calcd, 240.13 for C₁₂H₁₅F₂N₃ [M + H]⁺; found, 240.08; ¹H NMR (400 MHz, CDCl₃): δ 10.54 (s, 1H), 8.13 (s, 1H), 7.41–7.29 (m, 2H), 7.01–6.94 (m, 1H), 5.78 (tt, *J* = 56.5, 4.3 Hz, 1H), 3.23–3.06 (m, 2H), 3.05–2.87 (m, 3H), 1.12 (d, *J* = 6.2 Hz, 3H); ¹³C NMR (101 MHz, CDCl₃): δ 140.43, 133.10, 132.00, 127.02, 123.51, 121.40, 115.72 (t, *J* = 240.6 Hz), 108.50, 54.22, 48.75 (t, *J* = 24.7 Hz), 40.86, 20.09.

To a mixture of **64b** (570 mg, 1.0 equiv) and 4-bromo-2,6-difluorobenzaldehyde (2.62 g, 5.0 equiv) in toluene (10 mL) was added TFA (1 mL), and the mixture was stirred at 90 °C for 16 h. Then the reaction mixture was cooled down to rt and concentrated under reduced pressure to give a sticky oil, which was purified by pre-HPLC (MeCN/H₂O = 50–100% in 50 min) to afford product (6*S*,8*R*)-6-(4-bromo-2,6-difluorophenyl)-7-(2,2-difluoroethyl)-8-methyl-6,7,8,9-tetrahydro-3*H*-pyrazolo[4,3-*f*]isoquinoline (**65c**) as a white solid (860 mg, yield = 82%); UPLC–MS: 2.22 min; MS (ESI) *m/z*: calcd, 442.05 for C₁₉H₁₆BrF₄N₃ [M + H]⁺; found, 442.09; ¹H NMR (400 MHz, MeOD): δ 8.12 (d, *J* = 1.0 Hz, 1H), 7.32 (d, *J* = 8.7 Hz, 1H), 7.24 (d, *J* = 8.5 Hz, 2H), 6.86 (d, *J* = 8.7 Hz, 1H), 5.85 (tt, *J* = 55.7, 4.1 Hz, 1H), 5.59 (s, 1H), 3.71 (h, *J* = 6.3 Hz, 1H), 3.44 (dd, *J* = 16.9, 4.9 Hz, 1H), 3.39–3.25 (m, 1H), 3.07 (dd, *J* = 16.9, 6.1 Hz, 1H), 2.92 (qd, *J* = 14.9, 3.6 Hz, 1H), 1.23 (d, *J* = 6.5 Hz, 3H).

To a mixture of intermediate **65c** (770 mg, 1.0 equiv), *tert*-butyl 3,9-diazaspiro[5.5]undecane-3-carboxylate (926 mg, 2.0 equiv), RuPhos Pd G2 (283 mg, 0.2 equiv), RuPhos (170 mg, 0.2 equiv), and *t*-BuONa (699 mg, 4.0 equiv) in dioxane (20 mL) was degassed and purged with 3 times N₂, and then the mixture was stirred at 100 °C for 12 h. LC–MS showed **65c** was completely consumed, and a main peak with desired MS was formed. The mixture was cooled, diluted with DCM, and filtered through Celite, the filter cake was washed with DCM, and the filtrate was concentrated under reduced pressure. The residue was purified by pre-HPLC (MeCN/H₂O = 55–100% in 45 min) to give compound *tert*-butyl 9-(4-((6*S*,8*R*)-7-(2,2-difluoroethyl)-8-methyl-6,7,8,9-tetrahydro-3*H*-pyrazolo[4,3-*f*]isoquinolin-6-yl)-3,5-difluorophenyl)-3,9-diazaspiro[5.5]undecane-3-carboxylate (**66c**) as a light yellow foam (520 mg, yield = 48%); UPLC–MS: 2.58 min; MS (ESI) *m/z*: calcd, 616.33 for C₃₃H₄₁F₄N₃O₂ [M + H]⁺; found, 616.50; ¹H NMR (400 MHz, MeOD): δ 8.18 (d, *J* = 1.0 Hz, 1H), 7.44 (d, *J* = 9.2 Hz, 1H), 7.00 (d, *J* = 8.8 Hz, 1H), 6.57 (d, *J* = 14.0 Hz, 2H), 6.35 (tt, *J* = 53.9, 3.4 Hz, 1H), 6.08 (s, 1H), 4.21–4.09 (m, 1H), 3.91–3.75 (m, 1H), 3.61 (dd, *J* = 18.4, 5.1 Hz, 1H), 3.56–3.32 (m, 9H), 3.29–3.22 (m, 1H), 1.62 (t, *J* = 8.1 Hz, 5H), 1.54 (d, *J* = 6.5 Hz, 3H), 1.51–1.47 (m, 4H), 1.45 (s, 9H).

To a solution of **66c** (520 mg) in DCM (10 mL) was added TFA (2 mL). 10 min later, the mixture was concentrated to give a dryness, which was lyophilized to give compound (6*S*,8*R*)-6-(2,6-difluoro-4-(3,9-diazaspiro[5.5]undecan-3-yl)phenyl)-7-(2,2-difluoroethyl)-8-methyl-6,7,8,9-tetrahydro-3*H*-pyrazolo[4,3-*f*]isoquinoline (**67c**) as a yellow solid (720 mg); UPLC–MS: 1.57 min; MS (ESI) *m/z*: calcd, 516.27 for [M + H]⁺; found, 516.34; ¹H NMR (400 MHz, MeOD): δ 8.16 (d, *J* = 0.9 Hz, 1H), 7.41 (d, *J* = 8.6 Hz, 1H), 6.97 (d, *J* = 8.8 Hz, 1H), 6.57 (d, *J* = 13.6 Hz, 2H), 6.26 (tt, *J* = 54.0, 3.2 Hz, 1H), 5.98 (s, 1H), 4.13–4.02 (m, 1H), 3.74 (qd, *J* = 14.9, 3.9 Hz, 1H), 3.58 (dd, *J* = 18.2, 5.0 Hz, 1H), 3.47–3.37 (m, 1H), 3.37–3.32 (m, 4H), 3.28–3.17 (m, 5H), 1.81–1.73 (m, 4H), 1.71–1.64 (m, 4H), 1.49 (d, *J* = 6.5 Hz, 3H).

To a solution of **55** (646 mg, 1.2 equiv) and HATU (478 mg, 1.1 equiv) in DMF (10 mL) was added DIPEA (1.19 mL, 6.0 equiv). 5 min later, **67c** (720 mg, 1.0 equiv) was added, and the reaction mixture was stirred for 10 min. Then the reaction was quenched with water 5 mL and immediately purified by pre-HPLC (MeCN/H₂O = 25–100% in 75 min), and the desired product came out when MeCN/H₂O = 33%. The title compound 6-(2-(9-(4-((6*S*,8*R*)-7-(2,2-difluoroethyl)-8-methyl-6,7,8,9-tetrahydro-3*H*-pyrazolo[4,3-*f*]isoquinolin-6-yl)-3,5-difluorophenyl)-3,9-diazaspiro[5.5]undecan-3-yl)-2-oxoethyl)-2-(2,6-dioxopiperidin-3-yl)-6,7-dihydropyrrolo[3,4-*f*]isoindole-1,3(2*H*,5*H*)-dione (**44**, ERD-3111) was obtained as a light yellow solid (500 mg, yield = 45%) after concentrated and lyophilized. UPLC–MS: 1.79 min, purity >95%; MS (ESI) *m/z*: calcd for C₄₅H₄₆F₄N₈O₅ [M + H]⁺ 855.36; found, 855.14; HRMS (APCI) *m/z*: calcd for C₄₅H₄₆F₄N₈O₅ [M + H]⁺ 855.36; found, 855.3631; ¹H NMR (400 MHz, MeOD): δ 8.17 (d, *J* = 0.8 Hz, 1H), 7.93 (s, 2H), 7.43 (d, *J* = 8.7 Hz, 1H), 6.99 (d, *J* = 8.8 Hz, 1H), 6.57 (d, *J* = 13.9 Hz, 2H), 6.32 (tt, *J* = 54.1, 3.2 Hz, 1H), 6.03 (s, 1H), 5.17 (dd, *J* = 12.6, 5.4 Hz, 1H), 4.97 (s, 4H), 4.63 (s, 2H), 4.18–4.07 (m, 1H), 3.87–3.72 (m, 1H), 3.70–3.56 (m, 3H), 3.52–3.32 (m, 7H), 3.30–3.22 (m, 1H), 3.00–2.82 (m, 1H), 2.80–2.67 (m, 2H), 2.20–2.11 (m, 1H), 1.70–1.56 (m, 8H), 1.52 (d, *J* = 6.5 Hz, 3H); ¹³C NMR (101 MHz, MeOD): δ 174.47, 171.31, 167.88, 165.51, 165.41, 163.98, 163.07, 162.97, 155.17, 155.03, 154.90, 142.13, 140.89, 134.18, 133.10, 127.43, 126.34, 123.51, 123.17, 119.53, 115.27, 110.57, 98.64, 98.37, 60.60, 59.28, 57.56, 53.53, 50.82, 44.23, 41.82, 39.06, 36.23, 35.53, 35.50, 32.12, 31.04, 30.38, 23.56, 15.20.

6-(2-(9-(6-((6*S*,8*R*)-7-(2,2-difluoroethyl)-8-methyl-6,7,8,9-tetrahydro-3*H*-pyrazolo[4,3-*f*]isoquinolin-6-yl)pyridin-3-yl)-3,9-diazaspiro[5.5]undecan-3-yl)-2-oxoethyl)-2-(2,6-dioxopiperidin-3-yl)-6,7-dihydropyrrolo[3,4-*f*]isoindole-1,3(2*H*,5*H*)-dione (**45**). The title compound **45** was prepared using a similar procedure for the preparation of compound **44**. It was obtained as a white solid: UPLC–MS: 1.15 min, purity >95%; MS (ESI) *m/z*: calcd, 820.37 for C₄₄H₄₇F₂N₉O₅ [M + H]⁺; found, 820.29; ¹H NMR (400 MHz, MeOD): δ 8.19–8.09 (m, 2H), 7.99–7.90 (m, 3H), 7.64 (d, *J* = 9.2 Hz, 1H), 7.42 (d, *J* = 8.7 Hz, 1H), 7.01 (d, *J* = 8.7 Hz, 1H), 6.20–5.83 (m, 1H), 5.34 (s, 1H), 5.17 (dd, *J* = 12.6, 5.4 Hz, 1H), 4.97 (s, 4H), 4.63 (s, 2H), 3.74–3.64 (m, 2H), 3.52–3.32 (m, 7H), 3.29–3.19 (m, 1H), 3.07–2.99 (m, 1H), 2.94–2.82 (m, 1H), 2.81–2.70 (m, 2H), 2.21–2.11 (m, 1H), 1.82–1.70 (m, 4H), 1.69–1.57 (m, 4H), 1.22 (d, *J* = 6.4 Hz, 3H).

6-(2-(9-(4-((6*S*,8*R*)-7-(2,2-difluoroethyl)-8-methyl-6,7,8,9-tetrahydro-3*H*-pyrazolo[4,3-*f*]isoquinolin-6-yl)-3-methoxyphenyl)-3,9-diazaspiro[5.5]undecan-3-yl)-2-oxoethyl)-2-(2,6-dioxopiperidin-3-yl)-6,7-dihydropyrrolo[3,4-*f*]isoindole-1,3(2*H*,5*H*)-dione (**46**). Intermediate (6*S*,8*R*)-6-(4-bromo-2-methoxyphenyl)-7-(2,2-difluoroethyl)-8-methyl-6,7,8,9-tetrahydro-3*H*-pyrazolo[4,3-*f*]isoquinoline (**65e**) was prepared following the procedure for synthesis of **65c**, and it was obtained as a white solid: UPLC–MS (ESI) *m/z*: calcd, 436.08 for C₂₀H₂₀BrF₂N₃O [M + H]⁺; found, 436.21; ¹H NMR (400 MHz, MeOD): δ 8.22 (d, *J* = 1.0 Hz, 1H), 7.50 (d, *J* = 8.7 Hz, 1H), 7.39 (d, *J* = 1.8 Hz, 1H), 7.09 (dd, *J* = 8.2, 1.8 Hz, 1H), 6.93 (d, *J* = 8.8 Hz, 1H), 6.79–6.47 (m, 2H), 6.42 (s, 1H), 4.19–4.08 (m, 1H), 4.04 (s, 3H), 4.00–3.84 (m, 1H), 3.64 (dd, *J* = 18.7, 4.8 Hz, 1H), 3.61–3.50 (m, 1H), 3.30–3.22 (m, 1H), 1.57 (d, *J* = 6.5 Hz, 3H).

Intermediate (6*S*,8*R*)-7-(2,2-difluoroethyl)-6-(2-methoxy-4-(3,9-diazaspiro[5.5]undecan-3-yl)phenyl)-8-methyl-6,7,8,9-tetrahydro-3*H*-pyrazolo[4,3-*f*]isoquinoline (**66e**) was synthesized following the procedure for preparation of **66c** and was obtained as a light yellow solid: UPLC–MS (ESI) *m/z*: calcd, 510.30 for C₂₉H₃₇F₂N₅O [M + H]⁺; found, 510.20; ¹H NMR (400 MHz, MeOD): δ 8.21 (d, *J* = 0.9 Hz, 1H), 7.48 (d, *J* = 8.7 Hz, 1H), 6.91 (d, *J* = 8.8 Hz, 1H), 6.86 (s, 1H), 6.75–6.44 (m, 3H), 6.35 (s, 1H), 4.22–4.10 (m, 1H), 4.02 (s, 3H), 3.94–3.80 (m, 1H), 3.63 (dd, *J* = 18.7, 4.8 Hz, 1H), 3.59–3.49 (m, 1H), 3.43–3.35 (m, 4H), 3.29–3.18 (m, 5H), 1.83–1.74 (m, 8H), 1.56 (d, *J* = 6.5 Hz, 3H).

The title compound 6-(2-(9-(4-((6*S*,8*R*)-7-(2,2-difluoroethyl)-8-methyl-6,7,8,9-tetrahydro-3*H*-pyrazolo[4,3-*f*]isoquinolin-6-yl)-3-methoxyphenyl)-3,9-diazaspiro[5.5]undecan-3-yl)-2-oxoethyl)-2-(2,6-dioxopiperidin-3-yl)-6,7-dihydropyrrolo[3,4-*f*]isoindole-1,3(2*H*,5*H*)-

dione (**46**) was synthesized from **67e** using a similar procedure for the preparation of **44** from **67c**. It was obtained as a white solid; UPLC–MS: 1.63 min, purity >95%; MS (ESI) m/z : calcd, 849.39 for $C_{46}H_{50}F_2N_8O_6$ $[M + H]^+$; found, 849.41; 1H NMR (400 MHz, MeOD): δ 8.21 (d, $J = 0.8$ Hz, 1H), 7.94 (s, 2H), 7.48 (d, $J = 8.7$ Hz, 1H), 6.91 (d, $J = 9.0$ Hz, 2H), 6.74–6.42 (m, 3H), 6.33 (s, 1H), 5.17 (dd, $J = 12.6, 5.4$ Hz, 1H), 4.97 (s, 4H), 4.64 (s, 2H), 4.19–4.08 (m, 1H), 4.02 (s, 3H), 3.92–3.78 (m, 1H), 3.71–3.57 (m, 3H), 3.57–3.38 (m, 7H), 3.24 (dd, $J = 18.7, 11.3$ Hz, 1H), 2.93–2.83 (m, 1H), 2.80–2.67 (m, 2H), 2.20–2.11 (m, 1H), 1.84–1.75 (m, 4H), 1.70–1.60 (m, 4H), 1.55 (d, $J = 6.5$ Hz, 3H).

Cereblon Binding Assay. The binding to cereblon (CRBN) was determined using the Cereblon Binding Kit (Cisbio, #64BDCRBNPEG) following the manufacturer's instructions. Briefly, serially diluted compounds were incubated with GST-tagged wild-type human CRBN protein, XL665-labelled Thalidomide and Europium Cryptate labeled GST antibody at room temperature for ~3 h. Time resolved fluorescence resonance energy transfer (TR-FRET) measurements were acquired on a CALRIOstar plate reader with MARS data analysis software (BMG Labtech), with the following settings: 665/10 nm and 620/10 nm emission, 60 μ s delay, and 400 μ s integration. The TR-FRET ratio was taken as the 665/620 nm intensity ratio. The readings were normalized to the control (0.5%), and the IC_{50} was calculated by nonlinear regression (four parameters sigmoid fitted with variable slope) analysis using the GraphPad Prism 8 software.

ICW Blot Analysis. The protocol is as follows: (a) seeded cells in black-sided/clear bottom 384-well plates at 40,000 or 10,000 cells/well, overnight; (b) added diluted compounds (final 0.5% DMSO), incubated for 12 h, removed medium, added 50 μ L of 3.7% formaldehyde (PBS/FA = 9:1) and kept at room temp (RT) for 20 min without shaking; (c) washed with PBS, and permeabilized with 70 μ L/well of 1 \times PBS + 0.1% Triton X-100 for 5 min; (d) blocked with 50 μ L Intercept blocking buffer (LI-COR), kept at RT for 1 h with moderate shaking; (e) added 50 μ L of anti-ER (cs-8644, 1: 1-000) + GAPDH (Millipore MAB374, 1:1000) in intercept block buffer, and kept at RT for 2 h with gentle shaking. Negative control: cells plus secondary antibodies (no primary antibodies); (f) washed with PBS containing 0.1% Tween 20 with gentle shaking 10 min for 4 times; (g) washed 5 min with PBS + 0.1% Tween 20 for four times; and (h) added 70 μ L of PBS to each well and scan with ODYSSEY CLX machine from LI-COR. The data were collected based on triplicate experiments, unless otherwise stated. The maximum level of ER α degradation achieved by fulvestrant was set as 100% to minimize the effect of non-specific signal. The relative ER α degradation achieved by other compounds was calculated as follows: % degradation = $100 \times (1 - (\text{tested compound} - \text{fulvestrant}) / (\text{DMSO} - \text{fulvestrant}))$. The definitions for the degradation profiling are as follows: DC_{50} = the concentration needed to reduce ER α protein by 50%; D_{max} = maximal ER α degradation. The data were provided as mean \pm SEM.

Western Blot Analysis. Western blot analysis was performed as described previously.⁷² The cells treated with indicated compounds were lysed in radioimmunoprecipitation assay protein lysis and extraction buffer (25 mmol/L Tris, HCl, pH 7.6, 150 mmol/L NaCl, 1% Nonidet P-40, 1% sodium deoxycholate, and 0.1% sodium dodecyl sulfate) containing proteinase inhibitor cocktail (Roche Diagnostics, Mannheim, Germany). 20 μ g amounts of total protein was separated in 10% SDS-polyacrylamide gels after quantified by BCA assay (Fisher Scientific, Pittsburgh, PA). The separated protein bands were transferred onto PVDF membranes (GE Healthcare Life Sciences, Marlborough, MA) and blotted against different antibodies, as indicated. The blots were scanned, and the band intensities were quantified with the Image Studio software (Version 5.2). The relative mean intensity of target proteins was expressed after normalization to the intensity of glyceraldehyde-3-phosphate dehydrogenase or β -actin bands.

PK Studies in Rat, Mouse, and Beagle Dog. Pharmacokinetic (PK) studies were performed in Shanghai Medicilon Inc. Shanghai, 201200, China. For the PK studies in rats and mice, male Sprague

Dawley (SD) rats and male ICR mice were purchased from Sino-British SIPPR/BK Lab Animal Ltd., Shanghai, China. One group of three mice or rats was dosed intravenously (IV) with a dose level of 1 mg/kg, and a second group of three mice or rats was dosed orally with a dose level of 3 mg/kg. The animals were fasted prior to oral administration and food supply to the animals dosed orally were resumed 4 h post-administration. The drug solution was freshly prepared before administration. For the IV route, each compound was formulated in 5% DMSO + 10% solutol + 85% saline or 100% PEG200 (compound **9**) as a clear solution, a dosage volume of 5 mL/kg, and a theoretical concentration of 0.2 mg/mL. For the oral route, each was formulated in 5% DMSO + 10% solutol + 85% saline or 100% PEG200 (compound **9**) as a clear solution, a dosage volume of 10 mL/kg, and a theoretical concentration of 0.3 mg/mL. Blood samples were collected at the following time points: 5 min, 15 min, 30 min, 1 h, 2 h, 4 h, 6 h, 8 h, and 24 h post dose administration. 200 μ L (for rat) or 30 μ L (for mouse) of blood was collected, and the samples were placed in tubes containing heparin sodium and stored on ice. The samples were centrifuged at ~6800 G for 6 min at 2–8 $^{\circ}C$, and the resulting plasma was transferred to appropriately labeled tubes within 1 h of blood collection/centrifugation and then stored frozen at –80 $^{\circ}C$.

For the PK studies in dogs, male non-naive beagle dogs were used in Medicilon Inc. One group of three dogs was dosed IV with a dose level of 0.5 or 1 mg/kg, and a second group of three dogs was dosed orally with a dose level of 1 mg/kg. The animals were fasted for 10–18 h prior to oral administration and food supply to the animals dosed orally were resumed 4 h post-administration. The drug solution was freshly prepared before administration. For the IV route, each compound was formulated in 10% PEG400 + 90% PBS (adjust pH = 3 with 0.1 N HCl) as a clear solution, a dosage volume of 2 mL/kg, and a theoretical concentration of 0.25 or 0.5 mg/mL. For the oral route, each was formulated in 10% PEG400 + 90% PBS (adjust pH = 3 with 0.1 N HCl) as a clear solution, a dosage volume of 5 mL/kg, and a theoretical concentration of 0.2 mg/mL. Blood samples were collected at the following time points: 5 min, 15 min, 30 min, 1 h, 2 h, 4 h, 6 h, 8 h, and 24 h post dose administration. At each timepoint, 1 mL of blood was collected and the samples were placed in tubes containing heparin sodium and stored on ice. Then the samples were centrifuged at ~2200 G for 10 min at 2–8 $^{\circ}C$, and the resulting plasma was transferred to appropriately labeled tubes within 1 h of blood collection/centrifugation and then stored frozen at –80 $^{\circ}C$.

Method development and biological samples analysis for the test articles (sodium heparin anticoagulant) were performed by Testing Facility by means of LC–MS/MS. The analytical results were confirmed using quality control samples for intra-assay variation. The accuracy of >66.7% of the quality control samples was between 80 and 120% of the known value(s). The standard set of parameters including $T_{1/2}$ (elimination half-life), $AUC_{(0-t)}$ (area-under-the-curve), V_{ss} (volume of distribution at steady state), Cl (clearance), C_{max} (maximum drug concentration), and F (oral bioavailability) were calculated using Phoenix WinNonlin 7.0 (Pharsight, USA) by the Study Director.

Determination of Oral Plasma Exposure in Rats. The oral plasma exposure of selected compounds was evaluated in female SD rats (Charles River Laboratories). These studies in rats were performed under animal protocols (PRO00011174 and PRO00009463) approved by the Institutional Animal Care & Use Committee (IACUC) of the University of Michigan, in accordance with the recommendations in the Guide for the Care and Use of Laboratory Animals of the National Institutes of Health.

A group of three rats was dosed orally for each compound with a dose level of 3 or 5 mg/kg. The drug solution was freshly prepared using 100% PEG200 as the dosing vehicle before administration. Blood samples were collected at the time points of 1, 3, 6, and 24 h (for some cases) post dose, and 250–300 μ L of blood was collected at each time point from the rats' saphenous vein. The blood was collected into 1.5 mL microfuge tubes pretreated with Heparin and put on ice immediately. Samples will be centrifuged at 15,000 rpm for 10 min. A minimum of 100 μ L of blood plasma will be collected from the upper layer, leaving the blood cells behind in the microfuge tube. The plasma was transferred into a fresh 1.5 mL microfuge tube and frozen at –80 $^{\circ}C$

for future LC–MS analysis. For the LC–MS experiments, the chromatographic conditions are as follows: column, 50 × 2.1 mm I.D., packed with 3.5 μm C18 (Waters XBridge); mobile phase A, 0.1% formic acid in purified deionized water; mobile phase B, 0.1% formic acid in MeCN; flow rate: 0.5 mL/min; Injection Volume: 15 μL; run time: 5.7 min. MS/MS Conditions in 4500Q: electrospray, Turbo-Ionspray Interface used in the positive ion-mode.

Permeability and Efflux Ratio Determination in Caco-2 Cells.

The Caco-2 permeability evaluation of compound 9 was carried out in Shanghai Medicilon Inc. Shanghai, 201200, China. Caco-2 cells were seeded onto polyethylene membranes (PET) in 96-well Falcon insert systems at 2 × 10⁵ cells/cm² and cultured for 21–28 days for confluent cell monolayer formation. The cell culture media was changed every 3–4 days. Test compounds were diluted with the transport buffer (HBSS or HBSS with BSA) from a 10 mM stock solution to a concentration of 10 μM and applied to the apical or basolateral side of the cell monolayer. Permeation of the test compounds from A to B direction or B to A direction was determined in duplicate over a 120 min incubation at 37 °C and 5% CO₂ with a relative humidity of 95%. In addition, the efflux ratio of each compound was also determined. Test and reference compounds were quantified by LC–MS/MS analysis based on the peak area ratio of analyte/IS. The apparent permeability coefficient P_{app} (cm/s) was calculated using the equation: $P_{app} = (dC_r/dt) \times V_r / (A \times C_0)$, where dC_r/dt is the cumulative concentration of compound in the receiver chamber as a function of time (S); V_r is the solution volume in the receiver chamber (0.1 mL on the apical side, 0.25 mL on the basolateral side); A is the surface area for the transport, that is 0.0804 cm² for the area of the monolayer; and C_0 is the initial concentration in the donor chamber. The efflux ratio was calculated using the equation: efflux ratio = P_{app} (BA)/ P_{app} (AB). The LC/MS/MS condition is as follows: detection method, LC–MS/MS-20 (TQ-6500+); matrix, HBSS; internal standard, Tolbutamide; MS conditions, positive ion ESI for Atenolol and Propranolol and ERD-3111 and negative ion ESI for Digoxin and Tolbutamide; mobile phase, A = 0.1% FA in H₂O, B = 0.1% FA in MeCN; column, ACQUITY UPLC HSS T3 1.8 μm (50 mm × 2.10 mm).

Microsomal Metabolic Stability Studies. Pooled human and rat microsomes (10 μL aliquot) were prepared and stored at –80 °C prior to use. Master-mix containing microsome, phosphate buffer, and test compound solution was made as follows: (1) 10 μL of microsome (20 mg/mL) was diluted with 330 μL 0.1 M phosphate buffer (3.3 mM MgCl₂); (2) about 3.3 mg of NADPH was dissolved in 200 μL of 0.1 M phosphate buffer (3.3 mM MgCl₂); (3) 40 μL of 10 μM ERD-3111 PBS solution, was added to microsome; (4) the master solution was pre-warmed at 37 °C for 5 min. NADPH (20 μL) was added to the abovementioned master solution to initiate the reaction. The final concentration of ERD-3111 in the reaction system was 1 μM. Aliquot of 40 μL was pipetted from the reaction solution and stopped by the addition of 160 μL cold MeCN containing 25 nM of CE302 as an internal standard at the designated time points (0, 5, 10, 15, 30, 45, and 60 min). The incubation solution was vortexed-mixed (800 rpm/10 min) and centrifuged at 3500 rpm for 10 min to precipitate proteins. The supernatant was collected and used for the LC/MS/MS analysis. The natural log peak area ratio (compound peak area/internal standard peak area) was plotted against time and the gradient of the line was determined.

hERG Channel Inhibition Assay. The hERG Channel Inhibition of ERD-3111 was evaluated in HEK293 cells that expressed hERG channel using IonWorks Barracuda system (Molecular Devices Corporation, Union City, CA) at Charles River, 14656 Neo Parkway, Cleveland, OH 44128, United State. HEPES-buffered intracellular solution (Charles River proprietary) for whole cell recordings was loaded into the intracellular compartment of the Population Patch Clamp planar electrode. Extracellular buffer (HB-PS) was loaded into PPC planar electrode plate wells (11 μL per well). The cell suspension was pipetted into the wells of the PPC planar electrode (9 μL per well). After establishment of a whole-cell configuration (the perforated patch), membrane currents were recorded using patch clamp amplifier in the IonWorks Barracuda system. The current recordings were performed one time before test article application to the cells (baseline)

and one time after application of the test article. Tested compound concentrations were applied to naive cells ($n = 4$, where $n =$ replicates/concentration). Each application consisted of addition of 20 μL of 2× concentrated test article solution to the total 40 μL of final volume of the extracellular well of the PPC plate. The duration of exposure to each compound concentration was 5 min hERG test voltage protocol: hERG current was measured using a pulse pattern with fixed amplitudes (the first conditioning pre-pulse to 10 mV for 60 s, the second conditioning pre-pulse: –90 mV for 20 ms; test pulse: +40 mV for 100 ms) from a holding potential of 0 mV (“zero holding” procedure). hERG current was measured as a difference between the peak current at 1 ms and at the end of the step to +40 mV. Data analysis: data acquisition and analyses were performed using the IonWorks Barracuda system operation software (version 2.0.2). The decrease in current amplitude after test article application was used to calculate the percent block relative to control. Results for each test article concentration ($n \geq 2$) were averaged; the mean and standard deviation values were calculated and used to generate dose–response curves. The block effect was calculated as: % block = $(1 - I_{TA}/I_{Baseline}) \times 100\%$, where $I_{Baseline}$ and I_{TA} were the currents measured before and after addition of a test article, respectively. The data were corrected for run-down: % block' = $100\% - ((\% \text{ block} - \% \text{ PC}) \times (100\% / (\% \text{ VC} - \% \text{ PC})))$, where % VC and % PC were the mean values of the current block with the vehicle and positive controls, respectively. Concentration–response data were fitted to an equation of the following form: % block = % VC + (% PC – % VC) / [1 + ([test]/IC₅₀)^N], where [test] was the concentration of test article, IC₅₀ was the concentration of the test article producing half-maximal block, N was the Hill coefficient, % VC was the mean current block at the vehicle control and % block was the percentage of ion channel current inhibited at each concentration of a test article. Nonlinear least squares fits were solved with the XLfit add-in for Excel (Microsoft, Redmond, WA).

Cytochrome P450 (CYP) Enzyme Inhibition Assay. The CYP inhibition of ERD-3111 was profiling in Shanghai Medicilon Inc. Shanghai, 201200, China. The protocol for the experiment is as follows. (1) Preheat 0.1 M K-Buffer with 5 mM MgCl₂ (K/Mg-buffer), pH 7.4; (2) prepare serial dilution for test compound and reference inhibitors in a 96-well plate: (a) transfer 8 μL of 10 mM test compounds to 12 μL of MeCN; (b) prepare individual inhibitor spiking solution for CYPs 1A2, 2C8, 2C19, 2C9, 2D6, and 3A4 from 8 μL of DMSO stock to 12 μL of MeCN; (c) perform 1:2 serial dilutions in DMSO/MeCN mixture (v/v: 40:60). (3) Prepare NADPH cofactor (66.7 mg NADPH in 10 mL 0.1 M K/Mg-buffer, pH 7.4). (4) Prepare the substrate (2 mL for each enzyme isoform) as indicated (add HLM where required on ice). (5) Prepare 0.2 mg/mL HLM solution (10 μL of 20 mg/mL to 990 μL of 0.1 M K/Mg-buffer). (6) Add 400 μL of 0.2 mg/mL HLM to the assay wells and then add 2 μL of test compound set (serially diluted, see step 2.1) into the designated wells. (7) Add 200 μL of 0.2 mg/mL HLM to the assay wells and then add 1 μL of serially diluted reference inhibitor solution (see step 2a and 2b) into the designated wells. (8) Add following solutions (in duplicate) in a 96-well assay plate on ice: (a) add 30 μL of test compound and reference compound in 0.2 mg/mL HLM solution (see step 6 and 7); (b) add 15 μL of substrate solution (see step 4). (9) Pre-incubate the 96-well assay plate and NADPH solution at 37 °C for 5 min. (10) Add 15 μL of pre-warmed 8 mM NADPH solution to into the assay plates to initiate the reaction (see step 3). (11) Incubate the assay plate at 37 °C. 5 min for CYP3A4, 10 min for CYP1A2 and CYP2C9, 20 min for CYP2D6 and CYP2C8, and 45 min for CYP2C19. (12) Stop the reaction by adding 180 μL of acetonitrile containing IS. (13) After quenching, shake the plates for 10 min (600 rpm/min) and then centrifuge at 6000 rpm for 15 min. (14) Transfer 80 μL of the supernatant from each well into a 96-well sample plate containing 120 μL of ultra-pure water for LC/MS analysis. The LC–MS analysis was conducted using LC–MS/MS-20(TQ-6500+) ACQUITY UPLC HSS T3 1.8 μm (50 mm × 2.10 mm) or LC–MS/MS-11(8050) ACQUITY UPLC BEH C18 1.7 μm (50 mm × 2.10 mm). Curve-fitting was performed to calculate IC₅₀ using a Sigmoidal (non-linear) dose–response model (GraphPad Prism 5.0 or Xlfit model 205) based on data calculation using the formula below: $Y = \text{bottom} + (\text{top} - \text{bottom}) / (1 + 10^{(\log EC_{50} - X) \times \text{HillSlope}})$,

where X is the logarithm of concentration and Y is the response starting from Bottom to Top in a sigmoid shape in response to inhibitor concentration from high to low. The results generated for the reference compounds were consistent with the historic values.

PK/PD and Efficacy Studies in Mice. All in vivo studies were performed under animal protocol (PRO00011174 and PRO00009463) approved by the Institutional Animal Care & Use Committee (IACUC) of the University of Michigan, in accordance with the recommendations in the Guide for the Care and Use of Laboratory Animals of the National Institutes of Health.

To develop wide-type MCF-7 breast cancer xenografts, CB17 SCID female mice (Charles River Laboratories) were given 4 $\mu\text{g}/\text{mL}$ 17 β -Estradiol in 0.05% EtOH drinking water for 1 week, followed with 8 $\mu\text{g}/\text{mL}$ 17 β -estradiol in 0.1% EtOH drinking water thereafter. For the development of *ESR1*^{Y537S} and *ESR1*^{G538D} mutant MCF-7 breast cancer xenografts, CB17 SCID female mice (Charles River Laboratories) were not treated with 17 β -Estradiol. Ten million cells suspended in 50% Matrigel were injected subcutaneously into mice.

For PK/PD studies, tumor-bearing SCID mice were once-daily administered with vehicle control, ARV-471 or ERD-3111 via oral gavage using 5% DMSO + 10% solutol + 85% saline as the dosing vehicle (dosing volume/mouse weight = 10 $\mu\text{L}/\text{g}$) when tumors reached 100–400 mm^3 . After continuous dosing for 3 days, 3 mice were sacrificed at indicated time points with 3 mice for each time point for each group, and blood samples and tumor tissues were harvested for analysis. At each time point, mice were euthanized with CO_2 , and 250–300 μL of blood were collected by cardiac puncture. The blood samples were put into 1.5 mL microfuge tubes containing Heparin sodium and stored on ice and then centrifuged at 15,000 rpm for 10 min. A minimum of 100 μL of blood plasma was collected from the upper layer, leaving the blood cells behind in the microfuge tube. The plasma was transferred into a fresh 1.5 mL microfuge tube and placed on wet ice at -80°C . The tumor samples from each mouse were divided into two parts. One part was immediately frozen in liquid nitrogen (LN_2), ground into fine powder, placed on dry ice, and stored in -80°C for Western blot analysis. Western blots were performed as detailed in the previous section. The other part of the tumor was placed in tared Precellys 2 mL Hard Tissue tubes with Homogenizing Ceramic Beads 16859 (Cayman Chem), weighed, snap-frozen in LN_2 , and stored at -80°C for drug concentration analysis.

To prepare tumor samples for LC–MS analysis, mixed ultrapure water and MeCN solution (4:1) were added to the defrosted tumor tissue samples 5:1, v/w in order to facilitate homogenization with a Precellys evolution homogenizer at 4°C . The homogenized tissues solution was denatured using cold MeCN (1:3, v/v) with vortex and centrifuged at 13,000 rpm 4°C for 10 min. Following protein precipitation, the final supernatants were collected for LC–MS analysis.

To determine drug concentrations in plasma and tumor samples, a LC–MS/MS method was developed and validated. The LC–MS/MS method consisted of a Shimadzu HPLC system, and chromatographic separation of a test compound was achieved using a Waters XBridge C18 column (5 cm \times 2.1 mm, 3.5 μm). An AB Sciex QTrap 5500 mass spectrometer equipped with an electrospray ionization source (Applied Biosystems, Toronto, Canada) in the positive-ion multiple reaction monitoring mode was used for detection. For example, the precursor/product ion transitions were monitored at m/z 855.3 for ERD-3111 and internal standard, respectively, in the positive electrospray ionization mode. The mobile phases used on HPLC were 0.1% formic acid in purified water (A) and 0.1% formic acid in MeCN (B). The gradient (B) was held at 10% (0–0.3 min), increased to 95% at 0.7 min, then kept at isocratic 95% B for 2.3 min, and then immediately stepped back down to 10% for 2 min re-equilibration. The flow rate was set at 0.4–0.5 mL/min and injection volume was 5–10 μL .

For the in vivo efficacy experiments, when tumors reached an average volume of 80–200 mm^3 , mice were tumor size-matched and randomly assigned to different experimental groups with 7–8 mice for each group. Drugs or vehicle control were administered via oral gavage at the dose schedule as indicated using 5% DMSO + 10% solutol + 85% saline as the dosing vehicle. Tumor sizes and animal weights were measured 2–3 times per week. Tumor volume (mm^3) = (length \times width²)/2. Tumor

growth inhibition was calculated as TGI (%) = $[1 - (V_t - V_0') / (V_c - V_0)] \times 100$, where V_c and V_t are the mean tumor volume of the vehicle control and treated group at the end of treatment (or the last monitored time point), respectively, and V_0 and V_0' are the mean tumor volume of the vehicle control and treated group at the start, respectively. Tumor regression was calculated as regression (%) = $(V_0' - V_t) / (V_0') \times 100$, where V_t is the mean of treated groups at the end of treatment (or the last monitored time point) and V_0' is that at the start. The tumor volumes at the end of treatment (or the last monitored time point) were statistically analyzed using a one-tailed, unpaired t -test with Welch's correction (GraphPad Prism 8.0).

■ ASSOCIATED CONTENT

Supporting Information

The Supporting Information is available free of charge at <https://pubs.acs.org/doi/10.1021/acs.jmedchem.3c01186>.

Tissue distribution profile for ERD-3111 in mice; metabolic stability data of ERD-3111 in rat and human liver microsomes; detailed PK data for ERD-3111 in rats, mice, and dogs; UPLC spectra for final compounds; NMR spectra for final compounds; NMR spectra for key intermediates; and HRMS spectra for compound 36 and compound 44 (ERD-3111) (PDF)

Molecular string file for all the final target compounds (CSV)

■ AUTHOR INFORMATION

Corresponding Author

Shaomeng Wang – Department of Internal Medicine, Division of Hematology/Oncology, University of Michigan, Ann Arbor, Michigan 48109, United States; Department of Pharmacology, Department of Medicinal Chemistry, College of Pharmacy, and The Rogel Cancer Center, University of Michigan, Ann Arbor, Michigan 48109, United States; orcid.org/0000-0002-8782-6950; Email: shaomeng@umich.edu

Authors

Zhixiang Chen – Department of Internal Medicine, Division of Hematology/Oncology, University of Michigan, Ann Arbor, Michigan 48109, United States

Biao Hu – Department of Internal Medicine, Division of Hematology/Oncology, University of Michigan, Ann Arbor, Michigan 48109, United States; orcid.org/0000-0002-4691-6490

Rohan Kalyan Rej – Department of Internal Medicine, Division of Hematology/Oncology, University of Michigan, Ann Arbor, Michigan 48109, United States; orcid.org/0000-0003-0904-9137

Dimin Wu – Department of Internal Medicine, Division of Hematology/Oncology, University of Michigan, Ann Arbor, Michigan 48109, United States

Ranjan Kumar Acharyya – Department of Internal Medicine, Division of Hematology/Oncology, University of Michigan, Ann Arbor, Michigan 48109, United States

Mingliang Wang – Department of Internal Medicine, Division of Hematology/Oncology, University of Michigan, Ann Arbor, Michigan 48109, United States

Tianfeng Xu – Department of Internal Medicine, Division of Hematology/Oncology, University of Michigan, Ann Arbor, Michigan 48109, United States; orcid.org/0000-0001-8996-4065

Jianfeng Lu – Department of Internal Medicine, Division of Hematology/Oncology, University of Michigan, Ann Arbor, Michigan 48109, United States

Hoda Metwally – Department of Internal Medicine, Division of Hematology/Oncology, University of Michigan, Ann Arbor, Michigan 48109, United States

Yu Wang – Department of Internal Medicine, Division of Hematology/Oncology, University of Michigan, Ann Arbor, Michigan 48109, United States

Donna McEachern – Department of Internal Medicine, Division of Hematology/Oncology, University of Michigan, Ann Arbor, Michigan 48109, United States

Longchuan Bai – Department of Internal Medicine, Division of Hematology/Oncology, University of Michigan, Ann Arbor, Michigan 48109, United States

Christina L. Gersch – Department of Internal Medicine, Division of Hematology/Oncology, University of Michigan, Ann Arbor, Michigan 48109, United States

Meilin Wang – Department of Pharmaceutical Sciences, College of Pharmacy, University of Michigan, Ann Arbor, Michigan 48109, United States

Wenjing Zhang – Department of Pharmaceutical Sciences, College of Pharmacy, University of Michigan, Ann Arbor, Michigan 48109, United States

Qixia Li – Department of Pharmaceutical Sciences, College of Pharmacy, University of Michigan, Ann Arbor, Michigan 48109, United States

Bo Wen – Department of Pharmaceutical Sciences, College of Pharmacy, University of Michigan, Ann Arbor, Michigan 48109, United States

Duxin Sun – Department of Pharmaceutical Sciences, College of Pharmacy, University of Michigan, Ann Arbor, Michigan 48109, United States; orcid.org/0000-0002-6406-2126

James M. Rae – Department of Internal Medicine, Division of Hematology/Oncology, University of Michigan, Ann Arbor, Michigan 48109, United States; Department of Pharmacology and The Rogel Cancer Center, University of Michigan, Ann Arbor, Michigan 48109, United States

Complete contact information is available at:

<https://pubs.acs.org/10.1021/acs.jmedchem.3c01186>

Author Contributions

[#]Z.C., B.H., R.K.R., D.W., R.K.A., M.W., and T.X., contributed equally.

Notes

The authors declare the following competing financial interest(s): The University of Michigan has filed patent applications on these ER degraders, which have been licensed to Proteovant Therapeutics and Oncopia Therapeutics. Z. Chen, B. Hu, R. K. Rej, D. Wu, R. K. Acharyya, M. Wang, J. Lu and S. Wang are co-inventors on one of more of these patent applications. S. Wang was a co-founder and served as a paid consultant to Oncopia. S. Wang and the University of Michigan also owned equity in Oncopia, which was acquired by Roivant Sciences and Proteovant Therapeutics, Inc. S. Wang is a paid consultant to Roivant Sciences and Proteovant Therapeutics, Inc. The University of Michigan has received a research contract from Oncopia (now part of Roivant Sciences and Proteovant Therapeutics, Inc.) for which S. Wang serves as the principal investigator. J. M. Rae and C. L. Gersch have no conflicts of interest to declare.

ACKNOWLEDGMENTS

This study was supported in part by funding from Oncopia Therapeutics, Inc., Proteovant Therapeutics, Inc., the University

of Michigan Rogel Cancer Center Core Grant from the National Cancer Institute, NIH (P30CA046592), and the generous support of Rogel Cancer Center philanthropic funds.

ABBREVIATIONS

ADME, absorption, distribution, metabolism, and excretion; AI, aromatase inhibitor; AUC, area-under-the-curve; CDK4/6, cyclin-dependent kinase 4 and 6; Cl, clearance; C_{max} , maximum drug concentration; CRBN, cereblon; CYP, cytochromes P450; DC_{50} , the concentration needed to reduce protein by 50%; D_{max} , maximal ER α degradation; DMPK, drug metabolism and pharmacokinetics; ER α , estrogen receptor α ; ESR1, estrogen receptor 1; ET, endocrine therapy; F, oral bioavailability; hERG, human ether-à-go-go-related gene; ICW, in-cell western; IV, intravenous administration; LBD, ligand binding domain; P_{app} , apparent permeability coefficient; PD, pharmacodynamic; PFS, progression-free survival; PK, pharmacokinetic; PO, oral administration; PROTAC, proteolysis-targeting chimera; SERD, selective estrogen receptor degrader; SERM, selective estrogen receptor modulator; UPS, ubiquitin–proteasome system; V_{ss} , volume of distribution at steady state; $T_{1/2}$, elimination half-life

REFERENCES

- (1) Sung, H.; Ferlay, J.; Siegel, R. L.; Laversanne, M.; Soerjomataram, I.; Jemal, A.; Bray, F. Global Cancer Statistics 2020: GLOBOCAN Estimates of Incidence and Mortality Worldwide for 36 Cancers in 185 Countries. *Ca-Cancer J. Clin.* **2021**, *71*, 209–249.
- (2) Siegel, R. L.; Miller, K. D.; Wagle, N. S.; Jemal, A. Cancer statistics, 2023. *Ca-Cancer J. Clin.* **2023**, *73*, 17–48.
- (3) DeSantis, C. E.; Ma, J.; Gaudet, M. M.; Newman, L. A.; Miller, K. D.; Goding Sauer, A.; Jemal, A.; Siegel, R. L. Breast cancer statistics, 2019. *Ca-Cancer J. Clin.* **2019**, *69*, 438–451.
- (4) Brzozowski, A. M.; Pike, A. C. W.; Dauter, Z.; Hubbard, R. E.; Bonn, T.; Engström, O.; Öhman, L.; Greene, G. L.; Gustafsson, J. Å.; Carlquist, M. Molecular basis of agonism and antagonism in the oestrogen receptor. *Nature* **1997**, *389*, 753–758.
- (5) Damodaran, S.; Hortobagyi, G. N. Estrogen Receptor: A Paradigm for Targeted Therapy. *Cancer Res.* **2021**, *81*, 5396–5398.
- (6) Howlader, N.; Altekruze, S. F.; Li, C. I.; Chen, V. W.; Clarke, C. A.; Ries, L. A. G.; Cronin, K. A. US Incidence of Breast Cancer Subtypes Defined by Joint Hormone Receptor and HER2 Status. *J. Natl. Cancer Inst.* **2014**, *106*, dju055.
- (7) Ferraro, E.; Walsh, E. M.; Tao, J. J.; Chandralapaty, S.; Jhaveri, K. Accelerating drug development in breast cancer: New frontiers for ER inhibition. *Cancer Treat Rev.* **2022**, *109*, 102432.
- (8) Rej, R. K.; Thomas, J. E.; Acharyya, R. K.; Rae, J. M.; Wang, S. Targeting the Estrogen Receptor for the Treatment of Breast Cancer: Recent Advances and Challenges. *J. Med. Chem.* **2023**, *66*, 8339–8381.
- (9) McDonnell, D. P.; Wardell, S. E.; Norris, J. D. Oral Selective Estrogen Receptor Downregulators (SERDs), a Breakthrough Endocrine Therapy for Breast Cancer. *J. Med. Chem.* **2015**, *58*, 4883–4887.
- (10) Grinshpun, A.; Chen, V.; Sandusky, Z. M.; Fanning, S. W.; Jeselsohn, R. ESR1 activating mutations: From structure to clinical application. *Biochim. Biophys. Acta, Rev. Cancer* **2023**, *1878*, 188830.
- (11) Herzog, S. K.; Fuqua, S. A. W. ESR1 mutations and therapeutic resistance in metastatic breast cancer: progress and remaining challenges. *Br. J. Cancer* **2021**, *126*, 174–186.
- (12) Jeselsohn, R.; Buchwalter, G.; De Angelis, C.; Brown, M.; Schiff, R. ESR1 mutations—a mechanism for acquired endocrine resistance in breast cancer. *Nat. Rev. Clin. Oncol.* **2015**, *12*, 573–583.
- (13) Schiavon, G.; Hrebien, S.; Garcia-Murillas, I.; Cutts, R. J.; Pearson, A.; Tarazona, N.; Fenwick, K.; Kozarewa, I.; Lopez-Knowles, E.; Ribas, R.; et al. Analysis of ESR1 mutation in circulating tumor DNA

- demonstrates evolution during therapy for metastatic breast cancer. *Sci. Transl. Med.* **2015**, *7*, 313ra182.
- (14) Nardone, A.; De Angelis, C.; Trivedi, M. V.; Osborne, C. K.; Schiff, R. The changing role of ER in endocrine resistance. *Breast* **2015**, *24*, S60–S66.
- (15) Howell, A.; DeFriend, D. J.; Blamey, R. W.; Robertson, J. F.; Walton, P. Response to a specific antioestrogen (ICI 182780) in tamoxifen-resistant breast cancer. *The Lancet* **1995**, *345*, 29–30.
- (16) Turner, N. C.; Swift, C.; Kilburn, L.; Fribbens, C.; Beaney, M.; Garcia-Murillas, I.; Budzar, A. U.; Robertson, J. F. R.; Gradishar, W.; Piccart, M.; et al. ESR1 Mutations and Overall Survival on Fulvestrant versus Exemestane in Advanced Hormone Receptor–Positive Breast Cancer: A Combined Analysis of the Phase III SoFEA and EFACT Trials. *Clin. Cancer Res.* **2020**, *26*, S172–S177.
- (17) Wang, L.; Sharma, A. SERDs: a case study in targeted protein degradation. *Chem. Soc. Rev.* **2022**, *51*, 8149–8159.
- (18) Scott, J. S.; Barlaam, B. Selective estrogen receptor degraders (SERDs) and covalent antagonists (SERCAs): a patent review (2015–present). *Expert Opin. Ther. Pat.* **2021**, *32*, 131–151.
- (19) Wang, L.; Sharma, A. The Quest for Orally Available Selective Estrogen Receptor Degraders (SERDs). *Chemmedchem* **2020**, *15*, 2072–2097.
- (20) Lu, Y.; Liu, W. Selective Estrogen Receptor Degraders (SERDs): A Promising Strategy for Estrogen Receptor Positive Endocrine-Resistant Breast Cancer. *J. Med. Chem.* **2020**, *63*, 15094–15114.
- (21) Scott, J. S.; Stead, D.; Barlaam, B.; Breed, J.; Carbajo, R. J.; Chiarparin, E.; Cureton, N.; Davey, P. R. J.; Fisher, D. I.; Gangl, E. T.; et al. Discovery of a Potent and Orally Bioavailable Zwitterionic Series of Selective Estrogen Receptor Degradation-Antagonists. *J. Med. Chem.* **2023**, *66*, 2918–2945.
- (22) Lu, Z.; Cao, Y.; Zhang, D.; Meng, X.; Guo, B.; Kong, D.; Yang, Y. Discovery of Thieno[2,3-*e*]indazole Derivatives as Novel Oral Selective Estrogen Receptor Degraders with Highly Improved Antitumor Effect and Favorable Druggability. *J. Med. Chem.* **2022**, *65*, 5724–5750.
- (23) Lu, J.; Chan, C. C.; Sun, D.; Hu, G.; He, H.; Li, J.; Dong, J.; Liu, K.; Shen, L.; Hu, L.; et al. Discovery and preclinical profile of LX-039, a novel indole-based oral selective estrogen receptor degrader (SERD). *Bioorg. Med. Chem. Lett.* **2022**, *66*, 128734.
- (24) Zhang, X.; Wang, Y.; Li, X.; Wu, J.; Zhao, L.; Li, W.; Liu, J. Dynamics-Based Discovery of Novel, Potent Benzoic Acid Derivatives as Orally Bioavailable Selective Estrogen Receptor Degraders for ER α + Breast Cancer. *J. Med. Chem.* **2021**, *64*, 7575–7595.
- (25) Zbieg, J. R.; Liang, J.; Li, J.; Blake, R. A.; Chang, J.; Friedman, L.; Goodacre, S.; Hartman, S. J.; Rei Ingalla, E.; Kiefer, J. R.; et al. Discovery of GNE-502 as an orally bioavailable and potent degrader for estrogen receptor positive breast cancer. *Bioorg. Med. Chem. Lett.* **2021**, *50*, 128335.
- (26) Liang, J.; Zbieg, J. R.; Blake, R. A.; Chang, J. H.; Daly, S.; DiPasquale, A. G.; Friedman, L. S.; Gelzleichter, T.; Gill, M.; Giltmane, J. M.; et al. GDC-9545 (Giredestrant): A Potent and Orally Bioavailable Selective Estrogen Receptor Antagonist and Degradation with an Exceptional Preclinical Profile for ER+ Breast Cancer. *J. Med. Chem.* **2021**, *64*, 11841–11856.
- (27) Scott, J. S.; Moss, T. A.; Balazs, A.; Barlaam, B.; Breed, J.; Carbajo, R. J.; Chiarparin, E.; Davey, P. R. J.; Delpuech, O.; Fawell, S.; et al. Discovery of AZD9833, a Potent and Orally Bioavailable Selective Estrogen Receptor Degradation and Antagonist. *J. Med. Chem.* **2020**, *63*, 14530–14559.
- (28) Liang, J.; Blake, R.; Chang, J.; Friedman, L. S.; Goodacre, S.; Hartman, S.; Ingalla, E. R.; Kiefer, J. R.; Kleinheinz, T.; Labadie, S.; et al. Discovery of GNE-149 as a Full Antagonist and Efficient Degradation of Estrogen Receptor α for ER+ Breast Cancer. *ACS Med. Chem. Lett.* **2020**, *11*, 1342–1347.
- (29) El-Ahmad, Y.; Tabart, M.; Halley, F.; Certal, V.; Thompson, F.; Filoche-Rommé, B.; Gruss-Leleu, F.; Muller, C.; Brollo, M.; Fabien, L.; et al. Discovery of 6-(2,4-Dichlorophenyl)-5-[4-[(3S)-1-(3-fluoropropyl)pyrrolidin-3-yl]oxyphenyl]-8,9-dihydro-7H-benzo[7]-annulene-2-carboxylic acid (SAR439859), a Potent and Selective Estrogen Receptor Degradation (SERD) for the Treatment of Estrogen-Receptor-Positive Breast Cancer. *J. Med. Chem.* **2020**, *63*, 512–528.
- (30) Scott, J. S.; Breed, J.; Carbajo, R. J.; Davey, P. R.; Greenwood, R.; Huynh, H. K.; Klinowska, T.; Morrow, C. J.; Moss, T. A.; Polanski, R.; et al. Building Bridges in a Series of Estrogen Receptor Degraders: An Application of Metathesis in Medicinal Chemistry. *ACS Med. Chem. Lett.* **2019**, *10*, 1492–1497.
- (31) Scott, J. S.; Bailey, A.; Buttar, D.; Carbajo, R. J.; Curwen, J.; Davey, P. R. J.; Davies, R. D. M.; Degorce, S. L.; Donald, C.; Gangl, E.; et al. Tricyclic Indazoles—A Novel Class of Selective Estrogen Receptor Degradation Antagonists. *J. Med. Chem.* **2019**, *62*, 1593–1608.
- (32) Lu, Y.; Gutgesell, L. M.; Xiong, R.; Zhao, J.; Li, Y.; Rosales, C. I.; Hollas, M.; Shen, Z.; Gordon-Blake, J.; Dye, K.; et al. Design and Synthesis of Basic Selective Estrogen Receptor Degraders for Endocrine Therapy Resistant Breast Cancer. *J. Med. Chem.* **2019**, *62*, 11301–11323.
- (33) Tria, G. S.; Abrams, T.; Baird, J.; Burks, H. E.; Firestone, B.; Gaither, L. A.; Hamann, L. G.; He, G.; Kirby, C. A.; Kim, S.; et al. Discovery of LSZ102, a potent, orally bioavailable selective estrogen receptor degrader (SERD) for the treatment of estrogen receptor positive breast cancer. *J. Med. Chem.* **2018**, *61*, 2837–2864.
- (34) Liu, J.; Zheng, S.; Guo, S.; Zhang, C.; Zhong, Q.; Zhang, Q.; Ma, P.; Skripnikova, E. V.; Bratton, M. R.; Wiese, T. E.; et al. Rational Design of a Boron-Modified Triphenylethylene (GLL398) as an Oral Selective Estrogen Receptor Downregulator. *ACS Med. Chem. Lett.* **2017**, *8*, 102–106.
- (35) Burks, H. E.; Abrams, T.; Kirby, C. A.; Baird, J.; Fekete, A.; Hamann, L. G.; Kim, S.; Lombardo, F.; Loo, A.; Lubicka, D.; et al. Discovery of an Acrylic Acid Based Tetrahydroisoquinoline as an Orally Bioavailable Selective Estrogen Receptor Degradation for ER α + Breast Cancer. *J. Med. Chem.* **2017**, *60*, 2790–2818.
- (36) Scott, J. S.; Bailey, A.; Davies, R. D. M.; Degorce, S. L.; MacFaul, P. A.; Gingell, H.; Moss, T.; Norman, R. A.; Pink, J. H.; Rabow, A. A.; et al. Tetrahydroisoquinoline Phenols: Selective Estrogen Receptor Downregulation Antagonists with Oral Bioavailability in Rat. *ACS Med. Chem. Lett.* **2016**, *7*, 94–99.
- (37) Lai, A.; Kahraman, M.; Govek, S.; Nagasawa, J.; Bonnefous, C.; Julien, J.; Douglas, K.; Sensintaffar, J.; Lu, N.; Lee, K.-j.; et al. Identification of GDC-0810 (ARN-810), an Orally Bioavailable Selective Estrogen Receptor Degradation (SERD) that Demonstrates Robust Activity in Tamoxifen-Resistant Breast Cancer Xenografts. *J. Med. Chem.* **2015**, *58*, 4888–4904.
- (38) Govek, S. P.; Nagasawa, J. Y.; Douglas, K. L.; Lai, A. G.; Kahraman, M.; Bonnefous, C.; Aparicio, A. M.; Darimont, B. D.; Grillot, K. L.; Joseph, J. D.; et al. Optimization of an indazole series of selective estrogen receptor degraders: Tumor regression in a tamoxifen-resistant breast cancer xenograft. *Bioorg. Med. Chem. Lett.* **2015**, *25*, 5163–5167.
- (39) De Savi, C.; Bradbury, R. H.; Rabow, A. A.; Norman, R. A.; de Almeida, C.; Andrews, D. M.; Ballard, P.; Buttar, D.; Callis, R. J.; Currie, G. S.; et al. Optimization of a Novel Binding Motif to (E)-3-(3,5-Difluoro-4-((1R,3R)-2-(2-fluoro-2-methylpropyl)-3-methyl-2,3,4,9-tetrahydro-1H-pyrido[3,4-b]indol-1-yl)phenyl)acrylic Acid (AZD9496), a Potent and Orally Bioavailable Selective Estrogen Receptor Downregulation and Antagonist. *J. Med. Chem.* **2015**, *58*, 8128–8140.
- (40) Lloyd, M. R.; Wander, S. A.; Hamilton, E.; Razavi, P.; Bardia, A. Next-generation selective estrogen receptor degraders and other novel endocrine therapies for management of metastatic hormone receptor-positive breast cancer: current and emerging role. *Ther. Adv. Med. Oncol.* **2022**, *14*, 175883592211136.
- (41) Garcia-Fructuoso, I.; Gomez-Bravo, R.; Schettini, F. Integrating new oral selective oestrogen receptor degraders in the breast cancer treatment. *Curr. Opin. Oncol.* **2022**, *34*, 635–642.
- (42) Downton, T.; Zhou, F. A.; Segara, D.; Jeselsohn, R.; Lim, E. Oral Selective Estrogen Receptor Degraders (SERDs) in Breast Cancer: Advances, Challenges, and Current Status. *Drug Des. Dev. Ther.* **2022**, *16*, 2933–2948.

- (43) Chen, Y.-C.; Yu, J.; Metcalfe, C.; De Bruyn, T.; Gelzleichter, T.; Malhi, V.; Perez-Moreno, P. D.; Wang, X. Latest generation estrogen receptor degraders for the treatment of hormone receptor-positive breast cancer. *Expert Opin. Invest. Drugs* **2022**, *31*, 515–529.
- (44) Lipsyc-Sharf, M.; Toloney, S. M. E. Who are optimal candidates for the first oral SERD? *Ann. Oncol.* **2023**, *34*, 449–451.
- (45) Antonio, S. Camizestrant May Be Superior to Fulvestrant in Patients With Hormone Receptor-positive, HER2-negative Breast Cancer. 2022, <https://www.aacr.org/about-the-aacr/newsroom/news-releases/camizestrant-may-be-superior-to-fulvestrant-in-patients-with-hormone-receptor-positive-her2-negative-breast-cancer/>.
- (46) Sakamoto, K. M.; Kim, K. B.; Kumagai, A.; Mercurio, F.; Crews, C. M.; Deshaies, R. J. Protacs: Chimeric molecules that target proteins to the Skp1–Cullin–F box complex for ubiquitination and degradation. *Proc. Natl. Acad. Sci. U.S.A.* **2001**, *98*, 8554–8559.
- (47) Li, K.; Crews, C. M. PROTACs: past, present and future. *Chem. Sci. Rev.* **2022**, *51*, 5214–5236.
- (48) Hu, Z. Y.; Crews, C. M. Recent Developments in PROTAC-Mediated Protein Degradation: From Bench to Clinic. *Chembiochem* **2022**, *23*, No. e202100270.
- (49) Bekes, M.; Langley, D. R.; Crews, C. M. PROTAC targeted protein degraders: the past is prologue. *Nat. Rev. Drug Discovery* **2022**, *21*, 181–200.
- (50) Li, X. Y.; Pu, W. C.; Zheng, Q. Q.; Ai, M.; Chen, S.; Peng, Y. Proteolysis-targeting chimeras (PROTACs) in cancer therapy. *Mol. Cancer* **2022**, *21*, 99.
- (51) Hanker, A. B.; Sudhan, D. R.; Arteaga, C. L. Overcoming Endocrine Resistance in Breast Cancer. *Cancer Cell* **2020**, *37*, 496–513.
- (52) Burke, M. R.; Smith, A. R.; Zheng, G. Overcoming Cancer Drug Resistance Utilizing PROTAC Technology. *Front. Cell Dev. Biol.* **2022**, *10*, 872729.
- (53) Lin, X.; Xiang, H.; Luo, G. Targeting estrogen receptor alpha for degradation with PROTACs: A promising approach to overcome endocrine resistance. *Eur. J. Med. Chem.* **2020**, *206*, 112689.
- (54) Guedeny, N.; Cornu, M.; Schwalen, F.; Kieffer, C.; Voisin-Chiret, A. S. PROTAC technology: A new drug design for chemical biology with many challenges in drug discovery. *Drug Discov. Today* **2023**, *28*, 103395.
- (55) Edmondson, S. D.; Yang, B.; Fallan, C. Proteolysis targeting chimeras (PROTACs) in 'beyond rule-of-five' chemical space: Recent progress and future challenges. *Bioorg. Med. Chem. Lett.* **2019**, *29*, 1555–1564.
- (56) Hu, J.; Hu, B.; Wang, M.; Xu, F.; Miao, B.; Yang, C. Y.; Wang, M.; Liu, Z.; Hayes, D. F.; Chinnaswamy, K.; et al. Discovery of ERD-308 as a Highly Potent Proteolysis Targeting Chimera (PROTAC) Degradator of Estrogen Receptor (ER). *J. Med. Chem.* **2019**, *62*, 1420–1442.
- (57) Disch, J. S.; Duffy, J. M.; Lee, E. C. Y.; Gikunju, D.; Chan, B.; Levin, B.; Monteiro, M. I.; Talcott, S. A.; Lau, A. C.; Zhou, F.; et al. Bispecific Estrogen Receptor α Degradators Incorporating Novel Binders Identified Using DNA-Encoded Chemical Library Screening. *J. Med. Chem.* **2021**, *64*, 5049–5066.
- (58) Loren, G.; Espuny, I.; Llorente, A.; Donoghue, C.; Verdager, X.; Gomis, R. R.; Riera, A. Design and optimization of oestrogen receptor PROTACs based on 4-hydroxytamoxifen. *Eur. J. Med. Chem.* **2022**, *243*, 114770.
- (59) Luo, G. S.; Li, X. Y.; Lin, X.; Lu, X.; Li, Z. B.; Xiang, H. Novel 11 beta-substituted estradiol conjugates: Transition from ER alpha agonists to effective PROTAC degraders. *J. Steroid Biochem. Mol. Biol.* **2022**, *223*, 106154.
- (60) Xie, B.; Yin, Z.; Hu, Z.; Lv, J.; Du, C.; Deng, X.; Huang, Y.; Li, Q.; Huang, J.; Liang, K.; et al. Discovery of a Novel Class of PROTACs as Potent and Selective Estrogen Receptor α Degradators to Overcome Endocrine-Resistant Breast Cancer In Vitro and In Vivo. *J. Med. Chem.* **2023**, *66*, 6631–6651.
- (61) Flanagan, J.; Qian, Y.; Gough, S.; Andreoli, M.; Bookbinder, M.; Cadelina, G.; Bradley, J.; Rousseau, E.; Willard, R.; Pizzano, J.; et al. Abstract P5-04-18: ARV-471, an oral estrogen receptor PROTAC degrader for breast cancer. *Cancer Res.* **2019**, *79*, P5-04-18.
- (62) Hamilton, E.; Vahdat, L.; Han, H. S.; Ranciato, J.; Gedrich, R.; Keung, C. F.; Chirnomas, D.; Hurvitz, S. Abstract PD13-08: First-in-human safety and activity of ARV-471, a novel PROTAC® estrogen receptor degrader, in ER+/HER2- locally advanced or metastatic breast cancer. *Cancer Res.* **2022**, *82*, PD13-08.
- (63) Wang, S.; Xu, T.; Wang, M.; Hu, J.; Han, X.; Xiang, W.; Rej, R. New substituted fused heterocyclic compounds cereblon ubiquitination inhibitors, useful for treating cancer including e.g. acute eosinophilic leukemia, acute erythroid leukemia, acute lymphoblastic leukemia and B-cell lymphoma. WO 2021041664 A1, 2021.
- (64) Wang, S.; Xu, T.; Wu, D.; Chen, Z.; Han, X.; Xiang, W.; Rej, R.; Aguilar, A.; Bai, L. New 3-aminopiperidine-2,6-dione derivatives are cereblon ubiquitination inhibitors used to treat e.g. cancer e.g. acute megakaryoblastic leukemia, adenoid cystic carcinoma, angiosarcoma, bladder cancer, head and neck cancer and carcinoma. WO 2022187423 A1, 2022.
- (65) O'Brien Laramy, M. N.; Luthra, S.; Brown, M. F.; Bartlett, D. W. Delivering on the promise of protein degraders. *Nat. Rev. Drug Discovery* **2023**, *22*, 410–427.
- (66) Hornberger, K. R.; Araujo, E. M. V. Physicochemical Property Determinants of Oral Absorption for PROTAC Protein Degradators. *J. Med. Chem.* **2023**, *66*, 8281–8287.
- (67) Han, X.; Zhao, L. J.; Xiang, W. G.; Qin, C.; Miao, B. K. Y.; McEachern, D.; Wang, Y.; Metwally, H.; Wang, L.; Matvekas, A.; et al. Strategies toward Discovery of Potent and Orally Bioavailable Proteolysis Targeting Chimera Degradators of Androgen Receptor for the Treatment of Prostate Cancer. *J. Med. Chem.* **2021**, *64*, 12831–12854.
- (68) Xiang, W. G.; Zhao, L. J.; Han, X.; Qin, C.; Miao, B. K. Y.; McEachern, D.; Wang, Y.; Metwally, H.; Kirchhoff, P. D.; Wang, L.; et al. Discovery of ARD-2585 as an Exceptionally Potent and Orally Active PROTAC Degradator of Androgen Receptor for the Treatment of Advanced Prostate Cancer. *J. Med. Chem.* **2021**, *64*, 13487–13509.
- (69) Han, X.; Zhao, L.; Xiang, W.; Miao, B.; Qin, C.; Wang, M.; Xu, T.; McEachern, D.; Lu, J.; Wang, Y.; et al. Discovery of ARD-2051 as a Potent and Orally Efficacious Proteolysis Targeting Chimera (PROTAC) Degradator of Androgen Receptor for the Treatment of Advanced Prostate Cancer. *J. Med. Chem.* **2023**, *66*, 8822–8843.
- (70) Gonzalez, T. L.; Hancock, M.; Sun, S.; Gersch, C. L.; Larios, J. M.; David, W.; Hu, J.; Hayes, D. F.; Wang, S.; Rae, J. M. Targeted degradation of activating estrogen receptor α ligand-binding domain mutations in human breast cancer. *Breast Cancer Res. Treat.* **2020**, *180*, 611–622.
- (71) Chen, X.; Crew, A. P.; Flanagan, J.; Gough, S. M.; Haskell, R. J.; Moore, M. D.; Qian, Y.; Taylor, I. C. A.; Wang, J.; Gough, C. M.; et al. Treating breast cancer by administering 3-(5-(4-(1-(4-((1R,2S)-6-hydroxy-2-phenyl-1,2,3,4-tetrahydro-naphthalen-1-yl)-phenyl)-piperidin-4-ylmethyl)-piperazin-1-yl)-1-oxo-1,3-dihydro-isoindol-2-yl)-piperidine-2,6-dione compound. WO 2021041348 A1, 2022.
- (72) Hu, B.; Wu, Z.; Bai, D.; Liu, T.; Ullenbruch, M. R.; Phan, S. H. Mesenchymal deficiency of Notch1 attenuates bleomycin-induced pulmonary fibrosis. *Am. J. Pathol.* **2015**, *185*, 3066–3075.